

The regulation of erythrocyte survival and suicidal cell death

**Die Regulation erythrozytären Überlebens und suizidalen
Zelltodes**

DISSERTATION

**der Fakultät für Chemie und Pharmazie
der Eberhard-Karls-Universität Tübingen**

zur Erlangung des Grades eines Doktors
der Naturwissenschaften

2008

vorgelegt von

Michael Föllner

Tag der mündlichen Prüfung: 27.06.2008
Dekan: Prof. Dr. Lars Wesemann
1. Berichterstatter: Prof. Dr. Florian Lang
2. Berichterstatter: Prof. Dr. Peter Ruth
3. Berichterstatter: Prof. Dr. Ingolf Bernhardt (Universität des Saarlandes)

Abbreviations

Akt	Protein kinase B
ANP	Atrial natriuretic peptide
ATP	Adenosine triphosphate
BNP	Brain natriuretic peptide
BSA	Bovine serum albumin
bw	body weight
c-Akt	Protein kinase B
CFSE	Carboxyfluorescein-diacetate-succinimidyl-ester
cGK	cGMP-dependent kinase
cGMP	Cyclic guanosine monophosphate
CNP	C type natriuretic peptide
Ctrl	Control
Da	Dalton
EDTA	ethylenediaminetetraacetic acid
EGTA	glycol-bis(2-aminoethylether)-N,N,N',N'-tetraacetic acid
FACS	Fluorescence-activated cell sorting
FCS	Fetal calf serum
FH	Forkhead
FITC	Fluorescein isothiocyanate
FL	Fluorescence channel
FSC	Forward scatter
G protein	GTP-dependent protein
GC	guanylate cyclase
GPI	Glycosyl phosphatidyl inositol
GSK	Glycogen synthase kinase
GTP	Guanosine triphosphate
Hb	Hemoglobin
HCT	Hematocrit
HEPES	32 N-2-hydroxyethylpiperazine-N-2-ethanesulfonic acid
HGB	Hemoglobin
HU	Hemolytic units
IFN	Interferon
Ig	Immunoglobuline
I-kB	Cytosolic inhibitor of NF-kB
IL	Interleukin
IONO	Ionomycin
i.v.	Intravenous
JAK	Janus kinase
KCC	K ⁺ /Cl ⁻ cotransporter
KO	Knockout
LPS	Lipopolysaccharide
MACS	Magnetic cell separation
MB	Methylene blue
MCH	Mean corpuscular hemoglobin

MCHC	Mean corpuscular hemoglobin concentration
MCV	Mean corpuscular volume
MDP	Muramyl dipeptide
MRI	Magnetic resonance imaging
NF	Nuclear factor
NO	Nitric oxide
NOS	Nitric oxide synthase
PAMP	Pathogen-associated molecular patterns
PBS	Phosphate-buffered saline
PDE	Phosphodiesterase
PDK1	3'-Phosphoinositide-dependent kinase-1
PE	Phycoerythrin
PGN	Peptidoglycan
PH	Pleckstrin homology
PI	Phosphoinositide
PI3K	Phosphoinositide 3-kinase
PKB	Protein kinase B
PMA	Paramethoxyamphetamine
Po	Open probability of an ion channel
PP	Protein phosphatase
PRR	Pattern recognition receptor
PS	Phosphatidylserine
RBC	Red blood cell
RDW	Red cell distribution width
RT	Room temperature
SDS	Sodium dodecyl sulfate
SDS-PAGE	SDS polyacrylamide gel electrophoresis
SEM	Standard error of the mean
sGC	Soluble guanylate cyclase
SM	Smooth muscle
Src	Sarcoma; a family of proto-oncogenic tyrosine kinases
SSC	Side scatter
S. aureus	Staphylococcus aureus
t-BHP	Tert-butylhydroperoxide
TFN	Tumor necrosis factor
TLR	Toll-like receptor
TSP	Thrombospondin
Tyr	Tyrosine

Contents

1	SUMMARY/ZUSAMMENFASSUNG	9
2	INTRODUCTION	13
2.1	The ionic composition of the erythrocytic cytosol	13
2.1.1	Preface	13
2.1.2	Transmembrane ionic distribution of erythrocytes	13
2.1.3	Regulation of the intracellular Ca^{2+} concentration of erythrocytes	15
2.1.4	Dehydration of erythrocytes	15
2.1.5	The erythrocytic Gardos channel	16
2.1.6	The erythrocytic KCl-cotransporter	19
2.1.7	The erythrocytic Na^+/K^+ pump	21
2.2	Eryptosis	22
2.2.1	Apoptosis of nucleated cells	22
2.2.2	Mechanisms of eryptosis	22
2.2.3	Induction of eryptosis	23
2.2.4	Significance of eryptosis	25
2.3	The cGMP-dependent protein kinase (G Kinase; cGK)	27
2.3.1	Characteristics	27
2.3.2	Guanylate cyclases	28
2.3.3	Significance of the NO/cGMP signaling for erythrocyte survival	28
2.4	PDK1	30
2.4.1	Phospholipids of biological membranes	30
2.4.2	Phosphoinositide 3-kinases (PI3K)	30
2.4.3	3'-Phosphoinositide-dependent kinase-1 (PDK1)	31
2.4.4	Protein kinase B (PKB)	32
2.4.5	Activation of PKB by PDK1	33
2.4.6	Proteins regulated by PKB	33
2.4.7	Significance of the PI3/PDK1 signaling pathway	33
2.5	Participation of erythrocytes in host pathogen interactions	34
2.5.1	Peptidoglycan	34
2.5.2	TLR-2	36
2.6	Objective of this study	37
3	METHODS AND MATERIALS	38
3.1	Investigation of the impact of the Gardos channel on the survival of erythrocytes	38
3.1.1	Mice	38
3.1.2	<i>In vitro</i> experiments	38
3.1.3	α -toxin from <i>Staph. Aureus</i>	41
3.1.4	<i>In vivo</i> experiments	44
3.2	Regulation of erythrocyte survival by cGKI signaling	45
3.2.1	Mice	45
3.2.2	Blood and plasma parameters	46
3.2.3	Analysis of spleens	46
3.2.4	Western blot analysis	47

3.2.5	Analysis of phosphatidylserine exposure and intracellular Ca ²⁺ in peripheral erythrocytes	48
3.2.6	Measurement of the clearance of fluorescence-labeled erythrocytes <i>in vivo</i>	48
3.2.7	Measurement of erythrocyte flexibility and osmotic resistance	49
3.2.8	Magnetic resonance imaging of spleen volume	49
3.3	Study of PDK1-mediated regulation of suicidal death of erythrocytes	50
3.3.1	Mice	50
3.3.2	Solutions	50
3.3.3	FACS analysis	51
3.3.4	Erythrocyte parameters	51
3.3.5	Measurement of intracellular Ca ²⁺	51
3.3.6	Measurement of the <i>in vivo</i> clearance of fluorescence-labeled erythrocytes	52
3.3.7	Statistics	52
3.4	Bacterial peptidoglycan induces cell death of erythrocytes	53
3.4.1	Erythrocytes, solutions, and chemicals	53
3.4.2	Light and fluorescence microscopy	54
3.4.3	FACS analysis of annexin V-binding and forward scatter	54
3.4.4	Measurement of intracellular Ca ²⁺	54
3.4.5	Measurement of hemolysis	54
3.4.6	Determination of ceramide formation	54
3.4.7	Determination of the intracellular ATP concentration	55
3.4.8	Measurement of the <i>in vivo</i> clearance of fluorescence-labeled erythrocytes	55
3.4.9	Statistics	55
4	RESULTS	57
4.1	Investigation of the impact of the Gardos channel on the survival of erythrocytes	57
4.2	Regulation of erythrocyte survival by cGKI signaling	65
4.3	Study of PDK1-mediated regulation of suicidal death of erythrocytes	76
4.4	Bacterial peptidoglycan induces cell death of erythrocytes	84
5	DISCUSSION	91
5.1	Investigation of the impact of the Gardos channel on the survival of erythrocytes	91
5.2	Regulation of erythrocyte survival by cGKI signaling	94
5.3	Study of PDK1-mediated regulation of suicidal death of erythrocytes	97
5.4	Bacterial peptidoglycan induces cell death of erythrocytes	99
6	REFERENCES	101
7	ACKNOWLEDGEMENT	133
8	COMPLETE LIST OF PUBLICATIONS	135
9	ACADEMIC TEACHERS	137

1 Summary/Zusammenfassung

The life span of erythrocytes is tightly regulated. Therefore, a mechanism is required to remove senescent or damaged erythrocytes without rupture of the cell membrane resulting in the release of hemoglobin which may impair kidney function. The mechanism of suicidal erythrocyte death is called eryptosis and shares similarities with apoptosis of nucleated cells such as exposure of phosphatidylserine at the cell surface, increase in cytosolic Ca^{2+} concentration, blebbing of the membrane, cell shrinkage and enzymatic degradation of the cytoskeleton. The cell shrinkage of eryptotic cells is mediated by a Ca^{2+} -dependent K^+ channel, the Gardos channel. Its activation by an increase in the intracellular Ca^{2+} concentration results in the efflux of K^+ , Cl^- and osmotically obliged water. Phosphatidylserine-exposing erythrocytes are rapidly engulfed by macrophages equipped with phosphatidylserine receptors and degraded. Excessive eryptosis may lead to anemia, the pathological lack of erythrocytes. The present study was performed to elucidate mechanisms regulating erythrocyte survival and suicidal cell death. First, the functional significance of the Gardos channel for suicidal erythrocyte death and erythrocyte clearance was studied. Furthermore, the protective role of Gardos channels during exposure to hemolytic toxins was elucidated. Both issues were addressed by experiments performed in mice lacking the Ca^{2+} -dependent K^+ channel $\text{K}_{\text{Ca}3.1}$, the Gardos channel, and their wildtype littermates. Using patch-clamp recording, flow cytometry, *in vitro* hemolysis and a mouse sepsis model, it is shown that Gardos channel activity and Gardos effect delay hemolysis of injured erythrocytes and, thus, prevent the disastrous filtration of released hemoglobin into the renal tubular system. In a further series of experiments, the role of the NO/cGMP pathway, a powerful regulator of the life span of a variety of cells, for erythrocyte survival is investigated. Flow cytometry, Western Blotting, hematological counts, and MRI imaging were used to illustrate by means of a cGKI-deficient mouse model that cGKI is a mediator of erythrocyte survival *in vitro* and *in vivo*. Moreover, the participation of the phosphoinositide-dependent kinase PDK1, a key element in the phosphoinositol-3-kinase signalling pathway, which is involved in the regulation of ion channels, transporters, cell volume and cell survival, in the regulation of suicidal

erythrocyte death was studied. Experiments performed in hypomorphic mice with some 20% of normal PDK1 activity and their wildtype littermates revealed that PDK1 deficiency is associated with decreased Ca^{2+} entry into erythrocytes and thus with blunted eryptotic effects of oxidative stress, osmotic shock and Cl^- removal. Finally, the functional significance of host pathogen interactions for suicidal erythrocyte death was investigated. Using flow cytometry, it could be shown that peptidoglycan, a main component of the bacterial cell wall, is a potent stimulus of eryptosis and thereby impairs erythrocyte survival. Peptidoglycan-induced eryptosis may therefore, at least in part, account for anemia observed in patients with bacterial infections.

Die Lebensdauer von Erythrozyten ist genau reguliert. Aus diesem Grund ist ein Mechanismus erforderlich, der es erlaubt, alte oder geschädigte Erythrozyten abzubauen, ohne daß die Zellmembran reißt und Hämoglobin freigesetzt wird, was zu akutem Nierenversagen führen könnte. Ein solcher Mechanismus ist der suizidale Erythrozytentod, der Eryptose genannt wird und Ähnlichkeiten zur Apoptose kernhaltiger Zellen aufweist wie zum Beispiel die Externalisierung von Phosphatidylserin auf der Zelloberfläche, die Zunahme der intrazellulären Calciumkonzentration, das Abknopsen von Membranteilen, Zellschrumpfung sowie der enzymatische Abbau des Zytoskeletts. Die Zellschrumpfung eryptotischer Zellen wird durch einen Ca^{2+} -abhängigen K^+ -Kanal, den Gardos-Kanal, vermittelt. Dessen Aktivierung durch die Erhöhung der intrazellulären Calciumkonzentration führt zum Verlust von K^+ , Cl^- und osmotisch folgendem Wasser. Phosphatidylserin-exponierende Erythrozyten werden zügig von Makrophagen, die über Phosphatidylserinrezeptoren verfügen, phagozytiert und abgebaut. Exzessiv gesteigerte Eryptose kann zu Anämie, dem krankhaften Mangel an roten Blutkörperchen, führen. Ziel der vorliegenden Arbeit war es, Mechanismen aufzuklären, die erythrozytäres Überleben sowie suizidales Sterben steuern. Zunächst wurde die funktionelle Bedeutung des Gardos-Kanals für den suizidalen Erythrozytentod und die Klärung der roten Blutkörperchen aus dem Blut untersucht. Ferner wurde die protektive Wirkung der Gardos-Kanäle bei Einwirkung hämolytischer Toxine studiert. Beide Fragestellungen wurden durch Experimente an Mäusen, die den Ca^{2+} -abhängigen K^+ -Kanal $\text{K}_{\text{Ca}3.1}$ nicht exprimierten, und ihren Wildtyp-Geschwistern angegangen. Durch Messungen mit der Membranfleckklemme, mit dem Durchflußzytometer, durch *in vitro* Hämolyse und mittels eines Maus-Sepsis-Modells wurde gezeigt, daß die Gardos-Kanal-Aktivität und der Gardos-Effekt die Hämolyse geschädigter Erythrozyten verzögern und dadurch die potentiell schädliche Filtration des hämolytisch freigesetzten Hämoglobins in das Nierentubulussystem unterbinden. In weiteren Experimenten wurde die Rolle des NO/cGMP-Signalweges, eines bedeutsamen Regulators der Lebensdauer verschiedener Zellen, für das erythrozytäre Überleben untersucht. Mittels Durchflußzytometrie, Western Blotting, Blutbildern sowie Kernspintomographie, wurde an einem cGKI-defizienten Maus-Modell gezeigt, daß die cGKI ein Mediator erythrozytären Überlebens *in vitro* und *in vivo* ist. Desweiteren wurde die Beteiligung der Phosphoinositid-abhängigen-Kinase

PDK1, eines Schlüsselenzyms des Phosphoinositol-3-kinase-Signalweges, der bei der Regulation von Ionenkanälen, Transportern, des Zellvolumens und –überlebens mitwirkt, an der Steuerung suizidalen Erythrozytentodes analysiert. Experimente an hypomorphen Mäusen mit lediglich 20%-iger PDK1-Aktivität und ihren Wildtyp-Geschwistern ergaben, daß PDK1-Defizienz mit vermindertem Calciumeinstrom in Erythrozyten und daher mit abgeschwächten eryptotischen Effekten von oxidativem Streß, osmotischem Schock und der Entfernung extrazellulären Chlorids verbunden ist. Schließlich wurde die funktionelle Signifikanz von Wirt-Erregerbeziehungen für suizidalen Erythrozytentod untersucht. Durchflußzytometrisch konnte gezeigt werden, daß Peptidoglykan, ein wesentlicher Bestandteil bakterieller Zellwände, ein potenter Auslöser von Eryptose ist und dadurch erythrozytäres Überleben beeinträchtigt. Zumindest theoretisch könnte daher Peptidoglykan-induzierte Eryptose zur Anämie von Patienten mit bakteriellen Infektionen beitragen.

2 Introduction

2.1 The ionic composition of the erythrocytic cytosol

2.1.1 Preface

Human erythrocytes have the highest soluble protein concentration of any cell of the human body. The major intracellular protein of erythrocytes is hemoglobin with an intracellular concentration of approximately 7.7 mM (Lew & Bookchin, 2005). Erythrocytes have a characteristic biconcave shape and an impressive mechanical flexibility. Both features are based on a two-dimensional, spectrin-actin-containing, meshlike cytoskeleton with highly structured links to integral membrane proteins embedded in the lipid bilayer (Branton *et al.*, 1981; Chasis & Mohandas, 1986; Chasis *et al.*, 1989; Lew & Bookchin, 2005; Lux, 1979; Palek & Liu, 1979; Palek & Lambert, 1990; Steck, 1974). Erythrocytes have a high water permeability ensuring their continued osmotic equilibrium in plasma so that they can shrink or swell only by the loss or gain of a fluid isosmotic with surrounding plasma resulting in mechanical flexibility (Lew & Bookchin, 2005). By comparison of the intracellular protein concentration of app. 7.7 mM with the plasma protein concentration of 1 mM, it becomes obvious that the resulting oncotic pressure challenges the mechanical stability of the erythrocyte with a powerful driving force of water into the cells. To avoid colloid-osmotic lysis and to remain osmotically stable over their 120-day circulatory life-span, erythrocytes require a strategy to regulate and maintain their cell volume (Lew & Bookchin, 2005). Since erythrocytes are devoid of all organelles, they depend on the exclusive generation of ATP by glycolysis. Therefore, their efforts to maintain their cell volume are restricted by a potential lack of energy. (Lew & Bookchin, 2005)

2.1.2 Transmembrane ionic distribution of erythrocytes

With regard to the main inorganic cations and anions, erythrocytes maintain high intracellular K^+ and Cl^- concentrations while the intracellular Na^+ and Ca^{2+} concentrations are low (Maher & Kuchel, 2003). This ionic distribution is accomplished

by various pumps, transporters and cation channels. The cation gradients across the erythrocyte membrane are set up by the two ATP-dependent pumps Na^+/K^+ ATPase and the Ca^{2+} ATPase (Maher & Kuchel, 2003). The following list contains the transport pathways participating in the determination of the ionic distribution of potassium (Maher & Kuchel, 2003):

- (1) Ca^{2+} ATPase
- (2) Na^+/K^+ ATPase
- (3) the Gardos channel
- (4) K^+/Cl^- cotransport
- (5) Band 3 anion exchanger
- (6) $\text{Na}^+/\text{K}^+/2\text{Cl}^-$ cotransporter
- (7) glucose transporter

In general, the permeabilities of erythrocytes for Na^+ and K^+ are extremely low (Lew & Bookchin, 2005). The unidirectional fluxes of Na^+ or K^+ in mature normal erythrocytes are 2–3 $\text{mmol} \cdot \text{l}^{-1}$ original cells $\cdot \text{h}^{-1}$, whereas in reticulocytes they may be 10- to 30-fold higher (Lew & Bookchin, 2005; Johnstone & Ahn, 1990; Johnstone *et al.*, 1989; Johnstone *et al.*, 1987; Johnstone *et al.*, 1991; Wiley, 1981). As a consequence, a small number of ATP-driven Na^+/K^+ pumps is sufficient to counteract the basal cation leak (Lew & Bookchin, 2005). Furthermore, the anion permeability of erythrocytes can serve another purpose: the transport of CO_2 between the periphery and the lungs. This transport is based on the presence of the $\text{Cl}^-/\text{HCO}_3^-$ exchanger. The complete cycle is also referred to as the Jacobs-Stewart cycle (Lew & Bookchin, 2005). Due to the high permeability for anions, the membrane potential of the erythrocyte is close to the equilibrium potentials of Cl^- and HCO_3^- which is about -10 mV (Freedman & Hoffman, 1979; Hoffman & Laris, 1974; Hoffman & Laris, 1984; Laris & Hoffman, 1986). The above described processes are impaired in erythrocytes from patients with a certain mutation of a single nucleotide, the reason for sickle cell trait, resulting in malfunction of the ion fluxes, ion content regulation, and hydration state (Lew & Bookchin, 2005).

2.1.3 Regulation of the intracellular Ca²⁺ concentration of erythrocytes

Since mature erythrocytes lack specialized Ca²⁺-accumulating organelles such as the endoplasmatic reticulum or mitochondria, they only have a cytoplasmic Ca²⁺-buffering capacity (Ferreira & Lew, 1976;Tiffert & Lew, 1997;Tiffert *et al.*, 1993) which is, compared to other cell types, low. The total calcium content of erythrocytes is estimated to <5 mol/l original cells (Bookchin & Lew, 1980;Engelmann & Duhm, 1987;Harrison & Long, 1968). For determination of the intracellular calcium concentration, the following equation may be applied (Lew & Bookchin, 2005):

$$[Ca^{2+}]_i = a [Ca^{2+}_T]_i$$

where $[Ca^{2+}]_i$ represents the free cellular calcium concentration and is expressed in $\mu\text{mol/l}$ cell water, $a = 0.2 - 0.3$ over a wide range of experimentally induced $[Ca_T]_i$ values, and $[Ca^{2+}_T]_i$ represents the total calcium content of erythrocytes and is also expressed in units of $\mu\text{mol/l}$ original cells.

The free intracellular calcium concentration $[Ca^{2+}]_i$ reflects the balance of passive influx (passive or through a non-selective cation channel) and active efflux through the P type ATP-dependent Ca²⁺ ATPase whose V_{max} is $5\text{-}25 \text{ mmol} \cdot \text{l}^{-1}$ original cells $\cdot \text{h}^{-1}$ (Lew *et al.*, 2003) compared to a pump-leak turnover rate of $50 \mu\text{mol} \cdot \text{l}^{-1}$ original cells $\cdot \text{h}^{-1}$ (Desai *et al.*, 1991;Lew *et al.*, 1982b). The marked variation of different erythrocytes in the V_{max} values of their Ca²⁺ pumps may explain different dehydration or shrinkage responses upon equal permeabilization of the membrane for Ca²⁺ since in some erythrocytes the activation threshold of the Gardos channel may be exceeded while in others not (Lew & Bookchin, 2005).

2.1.4 Dehydration of erythrocytes

Erythrocyte dehydration (loss of water) *in vivo* may result from the activation of one or more of three transporters expressed in their plasma membranes (Lew & Bookchin, 2005):

1) the Ca^{2+} -sensitive, small-conductance, K^+ -selective channel (Gardos channel, IK1, $\text{K}_{\text{Ca}3.1}$, or hSK4; (Lew & Bookchin, 2005; Gardos, 1959; Hoffman *et al.*, 2003; Vandorpe *et al.*, 1998)). This channel is not exclusively expressed in erythrocytes. It can be found in many other eukaryotic cell types (Lew & Bookchin, 2005; Petersen & Maruyama, 1984)

2) a K^+/Cl^- cotransporter (KCC). This transporter is regulated by the internal pH and, most importantly, by cell volume (Brugnara *et al.*, 1986; Franco *et al.*, 1995; Gillen *et al.*, 1996; Lauf *et al.*, 1992; Lauf & Theg, 1980). It is functionally active in reticulocytes and, to a smaller extent, in mature erythrocytes.

3) the Na^+/K^+ pump (Post, 1974; Glynn & Karlish, 1975; Skou & Esmann, 1992).

The three transporters differ considerably in their dehydrating modalities, potencies, and distributions among erythrocytes (Lew & Bookchin, 2005).

2.1.5 The erythrocytic Gardos channel:

2.1.5.1 General characteristics

The following characteristics are typical of the Gardos channel (Maher & Kuchel, 2003):

- dependence on Ca^{2+} at the intracellular face of the channel ($(\text{Ca}^{2+})_i$)
- a single channel conductance of 10-20 pS (at 0 mV)
- high selectivity of K^+ over Na^+ ($P_{\text{K}}/P_{\text{Na}} > 100$)
- evidence of open channel inward rectification
- gating independence of membrane potential
- inhibition by more or less specific drugs such as clotrimazole, Tram34 and charybdotoxin
- inhibition upon pre-incubation of cells in the absence of external potassium ($(\text{K}^+)_o$).

- protein kinase A reportedly induces a dramatic enhancement of Gardos channel activity possibly by modulating the Ca^{2+} sensitivity (Romero & Rojas, 1992; Pellegrino & Pellegrini, 1998)

2.1.5.2 Structure of the Gardos channel

The Gardos channel is thought to be a homo-tetramer of six-transmembrane-domain polypeptides (Maher & Kuchel, 2003). The region between the s5 and s6 membrane domains contains the pore ('p') region, analogous to that in the K^+ channel of *Streptomyces lividans*, the structure of which is known (Maher & Kuchel, 2003; Doyle *et al.*, 1998). The K^+ selectivity is mediated by the carbonyl oxygen atoms within the selectivity filter protruding from the backbone of the polypeptides from each of the four identical subunits (Maher & Kuchel, 2003).

2.1.5.3 Abundance and activation of Gardos channels in erythrocytes

Every erythrocyte is thought to have approximately 100-200 Gardos channels in its membrane (Alvarez & Garcia-Sancho, 1987; Brugnara *et al.*, 1993; Grygorczyk *et al.*, 1984; Hoffman *et al.*, 2003; Lew *et al.*, 1982a) which are believed to be generated by the $\text{K}_{\text{Ca}3.1}$ (hSK4, IK, KCNN4) subtype of the small/intermediate conductance Ca^{2+} -activated K^+ channel family (Hoffman *et al.*, 2003; Lang *et al.*, 2003d). The normal intracellular Ca^{2+} concentration of human erythrocytes is 20-50 nM (Lew & Bookchin, 2005). At this concentration, Gardos channels are closed. However, they are activated, if the intracellular Ca^{2+} concentration is increased (Lew & Bookchin, 2005). A wide range of values of intracellular Ca^{2+} concentration required for activation of the Gardos channel is reported. According to some studies, 150 nM Ca^{2+} (Simons, 1976; Tiffert *et al.*, 1988) are sufficient while others suggest 2-4 μM (Grygorczyk *et al.*, 1984; Yingst & Hoffman, 1984; Leinders *et al.*, 1992). Also, the number of Ca^{2+} ions per channel required for opening the channel is a matter of controversy. It is reported to be either 1 (Grygorczyk & Schwarz, 1983) or 2 (Leinders *et al.*, 1992). Ca^{2+} acts via binding to

calmodulin which is constitutively associated with the Gardos channels (Maher & Kuchel, 2003).

2.1.5.4 Physical characteristics

The single Gardos channel conductance is 10 pS under physiological conditions (Grygorczyk & Schwarz, 1983). Unlike erythrocytes from other mammals losing Gardos channel activity during maturation, human erythrocytes have functional Gardos channels (Brown *et al.*, 1978). In addition to intracellular Ca^{2+} , Gardos channel activity critically depends on temperature: Even at saturating Ca^{2+} levels, the open-state probability of the Gardos channels is low (between 0.01 and 0.1) at 35°C increasing sharply at 25°C and then falling slowly with decreasing temperature (Grygorczyk, 1987; Hoffman *et al.*, 2003). On the other hand, marked Gardos channel-mediated dehydration is seen at low temperatures since the Ca^{2+} pump lowering the intracellular Ca^{2+} concentration is inhibited at low temperatures (Lew *et al.*, 1997; Garcia-Sancho & Lew, 1988).

2.1.5.5 Cellular effects of Gardos channel activation

Intracellular Na^+ is known to inhibit Gardos channel-mediated K^+ fluxes by interaction with several intracellular sites of the channel (Stampe & Vestergaard-Bogind, 1989). K^+ and H^+ ions also modify the activation state of the Gardos channel at both sides of the membrane since lack of extracellular K^+ and decrease of pH render the Gardos channel inactive (Grygorczyk *et al.*, 1984; Heinz & Passow, 1980; Heinz & Hoffman, 1990). Upon activation, the erythrocyte is hyperpolarized due to efflux of potassium ions (Lew & Bookchin, 2005). This creates a driving force for the loss of anions such as chloride or bicarbonate via parallel voltage-sensitive pathways. The resulting net loss of KCl and KHCO_3 is coupled to osmotic-driven water loss, leading to cell dehydration and shrinkage. Once the Gardos channels are fully activated by a high intracellular Ca^{2+} level, the cellular loss of the anions becomes rate-limiting for shrinkage and dehydration (Lew & Bookchin, 2005): K^+ fluxes through the Gardos channel may reach mean values

of $1 \text{ mol} \cdot \text{l}^{-1}$ original cells $\cdot \text{h}^{-1}$ (Lew & Ferreira, 1976) reflecting a mean permeability value of $2 \cdot 10^{-7} \text{ cm/s}$ (Freeman *et al.*, 1987) while the rate-limiting anion permeability is approximately $2 \cdot 10^{-8} \text{ cm/s}$. This means that the anion permeability is an order of magnitude lower than that through fully activated Gardos channels. Thus, full dehydration or shrinkage requires 1 h provided that the Gardos channels are completely activated (Lew & Bookchin, 2005).

2.1.5.6 Pharmacological inhibition

Gardos channels may be pharmacologically inhibited by charybdotoxin (IC_{50} : 1.2 nM) or clotrimazole (IC_{50} : 51 nM), a drug in therapeutical use against fungal infections (Brugnara *et al.*, 1993). Furthermore, volatile anaesthetics can inhibit the Gardos effect in resealed erythrocytes *in vitro* (Caldwell & Harris, 1985) and IK currents in *Xenopus* oocytes expressing the channel protein (Namba *et al.*, 2000). Halothane has also been shown to inhibit the Gardos channel in intact erythrocytes (Scharff & Foder, 1989). Recently, Tram34 (1-((2-chlorophenyl)diphenylmethyl)-1H-pyrazole) has been shown to have similar inhibitory potency but much higher specificity than clotrimazole (Maher & Kuchel, 2003). Besides direct inhibition of the channel, Gardos-mediated shrinkage or dehydration can also be prevented by inhibition of the anion permeabilities (Bennekou *et al.*, 2001; Bennekou *et al.*, 2000).

2.1.5.7 Significance of the Gardos channel

By delaying colloid osmotic hemolysis and fostering phosphatidylserine exposure, the Gardos effect is thought to play a pivotal role for the appropriate clearance of injured erythrocytes. This might be particularly important during infections with hemolytic bacteria. This hypothesis is tested in the present study.

2.1.6 The erythrocytic KCl cotransporter

The KCl cotransporter mediates a strictly coupled electroneutral transport of K^+ and Cl^- independent of the membrane potential (Jennings & Adame, 2001). They are abundant in many eukaryotic cells including erythroid precursors (Lauf *et al.*, 1992; Gillen *et al.*, 1996). While mature erythrocytes have reduced KCl cotransporter activity (Lew & Bookchin, 2005), most of the passive K^+ fluxes of reticulocytes are mediated by the KCl-cotransporter (Hall & Ellory, 1986). Similar to the loss of cell volume via the Gardos channel, the driving force for RBC dehydration via the KCl cotransporter occurs by K^+ permeabilization based on an outward electrochemical gradient of K^+ . An important side effect of isotonic dehydration by KCl and $KHCO_3$ loss is cell acidification (Lew & Bookchin, 1986), a phenomenon described by the Lew Bookchin red cell model (Lew & Bookchin, 1986): The positive charges within an erythrocyte are due to sodium, potassium, magnesium, and calcium and amount to 150 meq/l cell water, while the negative charges base on hemoglobin (50 meq/l cell water), chloride, and bicarbonate (together 100 meq/l cell water). If the erythrocytes lose water isototically due to efflux of 150 meq/l KCl and $KHCO_3$, the concentrations of Cl^- and HCO_3^- are higher in the effluent as compared to the cell. Thus, with proceeding efflux, the intracellular concentrations of chloride and bicarbonate decrease while the extracellular concentrations approximately remain the same (Lew & Bookchin, 2005). The bicarbonate/chloride exchanger of the erythrocyte membrane together with the CO_2 shunt, however, equilibrate immediately according to the Jacobs-Stewart mechanism (Jacobs & Craig, 1935) by increasing the intracellular H^+ concentration as a consequence of the decreased intracellular bicarbonate concentration.

The KCl cotransporter is regulated by the oxidation state of hemoglobin (Joiner *et al.*, 1998), by decreased intracellular pH, by increase in cell volume, and by low intracellular Mg^{2+} concentrations (Brugnara & Tosteson, 1987; Jennings, 1999; Jennings & al Rohil, 1990; Lauf, 1985). Phosphorylation and dephosphorylation of serine/threonine and tyrosine residues of the cotransporter change the activation state. It has been shown (Jennings, 1999; Jennings & al Rohil, 1990) that swelling of rabbit erythrocytes leads to inactivation of a serine/threonine kinase. Another study suggests that hypotonic swelling of erythrocytes is associated with increased activities of protein phosphatases (PP1 and PP2A), that PP1 increased in erythrocytes whose ionic strength was lowered at constant volume, and that PP1 appears to mediate parts of urea-

stimulated KCC activity. For the present study, it is important that KCl cotransporter activity is further enhanced by the cGMP-dependent protein kinase (cGKI, G Kinase) (Adragna *et al.*, 2006;Adragna *et al.*, 2004;Adragna *et al.*, 2002;Adragna *et al.*, 2000).

2.1.7 The erythrocytic Na⁺/K⁺ pump

The Na⁺/K⁺ pumping-process depends on ATP and is therefore an active energy-requiring process. The stoichiometry of the Na⁺/K⁺ pump is 3:2 (Garrahan & Glynn, 1967;Post *et al.*, 1967). Due to the high anion permeability of erythrocytes and reticulocytes, electroneutrality is mainly maintained by anion efflux balancing the extra Na⁺ efflux. If the Na⁺/K⁺ pump is stimulated by an elevated internal Na⁺/K⁺ concentration ratio, the resulting increased NaCl efflux, if not compensated by changes in passive fluxes, would induce cell dehydration (Clark *et al.*, 1981;Glader & Nathan, 1978;Joiner *et al.*, 1986). Since every erythrocyte has only approximately 400 molecules of the Na⁺/K⁺ pump protein per cell (Dunham & Hoffman, 1970;Glynn & Karlsh, 1975;Joiner & Lauf, 1978), the effect is bound to be rather slow, as confirmed by model simulations (Lew & Bookchin, 2005).

2.2 Eryptosis

2.2.1 Apoptosis of nucleated cells

Apoptosis is one of the major forms of programmed cell death. It is a physiological mechanism to eliminate abundant cells without inflammation reaction (Green & Reed, 1998; Gulbins *et al.*, 2000). As the term programmed cell death suggests, apoptosis involves a defined program of cellular mechanisms leading to suicidal death of the cell. This program includes nuclear condensation, DNA fragmentation, mitochondrial depolarization, cell shrinkage, and breakdown of the phosphatidylserine asymmetry of the plasma membrane (Green & Reed, 1998; Gulbins *et al.*, 2000). An inflammation reaction is prevented by the rapid engulfment of the dying cell by phagocytes equipped with special receptors (Gulbins *et al.*, 2000; Eda & Sherman, 2002). Apoptosis affects the activity of a variety of cellular transporters such as K⁺ channels (Gulbins *et al.*, 1997; Lang *et al.*, 2003d; Maeno *et al.*, 2000), anion channels (Maeno *et al.*, 2000; Szabo *et al.*, 1998), Ca²⁺ channels (Lepple-Wienhues *et al.*, 1999), taurine release channels (Lang *et al.*, 1998b; Lang *et al.*, 2000; Moran *et al.*, 2000) and Na⁺/H⁺ exchangers (Lang *et al.*, 2000).

2.2.2 Mechanisms of eryptosis

Erythrocytes are the most abundant cells in the blood of mammals. They have a regular life span of 120 days (Bratosin *et al.*, 2001). Every second, 2 million erythrocytes are newly formed in the human body. Erythrocytes lack organelles and therefore do not have a nucleus or mitochondria, which play a major role in apoptosis. Therefore, erythrocytes cannot undergo the same type of suicidal cell death as nucleated cells. However, it has been shown that erythrocytes exposed to the Ca²⁺ ionophore ionomycin undergo shrinkage, membrane blebbing, and break down of cell membrane phosphatidylserine asymmetry, all typical features of apoptosis in nucleated cells (Daugas *et al.*, 2001; Berg *et al.*, 2001; Bratosin *et al.*, 2001). To illustrate the similarity of this type of suicidal cell death of erythrocytes with apoptosis of nucleated cell, the process has been given the name eryptosis (Lang *et al.*, 2005a). Intracellular calcium

plays a major role for eryptosis (Lang *et al.*, 2005a): Either, an increase in intracellular calcium induces eryptosis or the cellular machinery involved in eryptosis downstream of calcium is sensitized to the effects of calcium by ceramide (Lang *et al.*, 2005a). Of course, both mechanisms can also be operative together. Increased intracellular calcium has various effects in erythrocytes: It stimulates the erythrocyte scramblase (Woon *et al.*, 1999), thus leading to the breakdown of the phosphatidylserine asymmetry (Lang *et al.*, 2003b). The consequence is the exposure of phosphatidylserine at the erythrocyte surface. Moreover, calcium activates the Ca^{2+} -dependent cysteine endopeptidase calpain (Lang *et al.*, 2005a). However, calpain activity appears not to be required for stimulation of phosphatidylserine exposure (Lang *et al.*, 2005a). Calpain leads to cell membrane blebbing (Berg *et al.*, 2001). Elevated intracellular calcium levels, in addition, stimulate the above described Ca^{2+} -sensitive Gardos K^+ channels in erythrocytes (Franco *et al.*, 1996;Brugnara *et al.*, 1993). The significance of this channel for eryptosis is investigated in this study. As described above, the activation of the channels leads to hyperpolarization of the cell membrane driving Cl^- in parallel to K^+ into the extracellular space. The cellular loss of KCl favours cell shrinkage. It is even likely that the cellular loss of K^+ itself participates in the triggering of “eryptosis” (Schneider *et al.*, 2007).

2.2.3 Induction of eryptosis

Erythrocytes under resting conditions show low permeabilities of their membranes to ions, especially to cations. They are predominantly permeable to chloride (Schneider *et al.*, 2007;Lang *et al.*, 2005a). All effects of calcium described above can therefore be the result of ionophore (ionomycin)-induced increase in intracellular calcium. However, erythrocytes have non-selective cation channels that, upon activation, allow the influx of calcium ions (Duranton *et al.*, 2002;Huber *et al.*, 2001;Kaestner *et al.*, 2000). TRPC6 has been shown to be part of the non-selective cation conductance of erythrocytes (Foller *et al.*, 2008). A variety of conditions, pharmacological activators, and diseases have been characterized to increase the activity of the non-selective cation channel resulting in calcium influx and triggering of eryptosis. Among those are metal ions such as aluminium (Niemoeller *et al.*, 2006c), gold (Sopjani *et al.*, 2007), or copper (Lang *et al.*

al., 2007), pharmaceutical products (e.g. amantadine (Foller *et al.*, 2007a), cyclosporine (Niemoeller *et al.*, 2006a), paclitaxel (Lang *et al.*, 2006c)) or diseases (e.g. sepsis (Kempe *et al.*, 2007), Wilson's disease (Lang *et al.*, 2007), and Hemolytic Uremic Syndrome (Lang *et al.*, 2006b). All these stimuli induce eryptosis.

Besides activation of the non-selective cation channel, eryptosis may also be induced by activation of an erythrocyte sphingomyelinase leading to the release of ceramide (Lang *et al.*, 2003c). Ceramide then potentiates the effect of calcium on phosphatidylserine exposure (Lang *et al.*, 2003c). Similar to activators of the non-selective cation channel, certain triggers of ceramide release have been identified, which trigger eryptosis. Among those are again metal ions (e.g. copper (Lang *et al.*, 2007), lead (Kempe *et al.*, 2005)), drugs (e.g. methyl dopa (unpublished observations)), certain diseases (e.g. Wilson's disease (Lang *et al.*, 2007), sepsis (Kempe *et al.*, 2007)) or stress stimuli (e.g. hyperosmotic shock (Lang *et al.*, 2004a)). Figure 1_{Intro} summarizes the mechanisms involved in eryptosis.

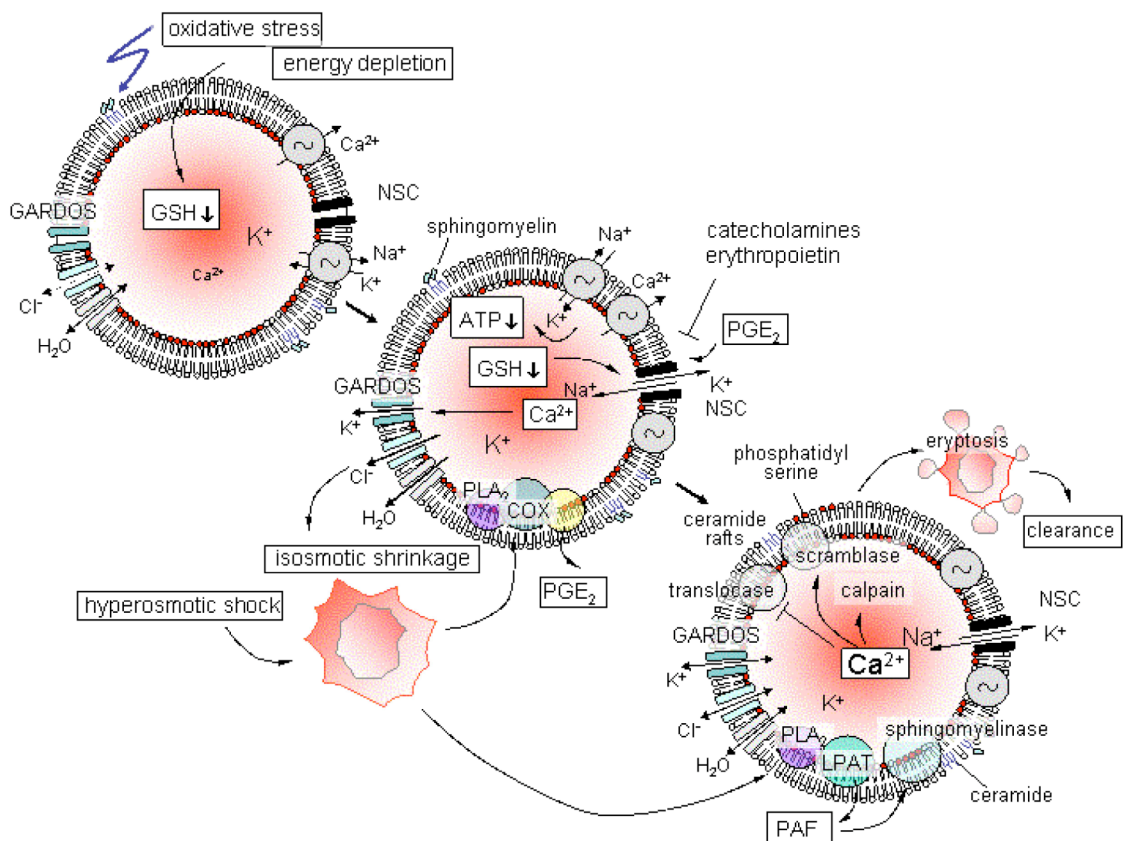


Figure 1_{Intro}. Synopsis of the mechanisms involved in eryptosis.

2.2.4 Significance of eryptosis

As described above, both pathways, i.e. an increase in the intracellular calcium concentration or the formation of ceramide, lead to exposure of phosphatidylserine on the surface of erythrocytes. Phosphatidylserine-exposing erythrocytes are rapidly engulfed and degraded by macrophages (Boas *et al.*, 1998; Kempe *et al.*, 2006) which are equipped with phosphatidylserine receptors. Enhanced clearance of phosphatidylserine-exposing erythrocytes from circulating blood, i.e. the removal of erythrocytes from the blood stream, thus, should lead to a lack of erythrocytes, i. e. anemia. The above described stimuli of either an increase in the intracellular calcium concentration or the release of ceramide are indeed all associated with the development of anemia. Excessive triggering of eryptosis may, thus, lead to anemia (Lang *et al.*, 2005a).

Furthermore, natural ageing of erythrocytes is associated with an increase in the intracellular calcium concentration (Kiefer & Snyder, 2000; Romero & Romero, 1999). Therefore, triggering of eryptosis and engulfment of phosphatidylserine-exposing erythrocytes by macrophages may contribute to the physiological limitation of erythrocyte survival (Lang *et al.*, 2005a).

Excessive death of erythrocytes can also result in hemolysis. Triggers such as antibodies (hemolytic anemia), mechanical stress (damaged heart valves) or toxins may either damage the plasma membrane of erythrocytes mechanically or, in the case of certain bacterial toxins (hemolysin (Lang *et al.*, 2004b), listeriolysin (Foller *et al.*, 2007b)), permeabilize the membrane by insertion of proteins. The result of both mechanisms is hemolysis, the loss of cellular proteins and hemoglobin. The lack of ATP (energy depletion), impaired function of the cellular Na^+/K^+ ATPase or other leakiness of the cell membrane lead to the accumulation of Na^+ , Cl^- , and osmotically obliged water with subsequent cell swelling (Lang *et al.*, 1998a). Initially, the entry of Na^+ may be compensated by cellular loss of K^+ , the decrease of the K^+ equilibrium potential will, however, eventually lead to depolarisation, which will favour the entry of Cl^- . Thus, finally, the increase in cell volume causes the rupture of the cell membrane with cellular release of hemoglobin, i.e. again hemolysis (Lang *et al.*, 2005a).

Regardless of its origin, excessive hemolysis might lead to acute renal failure since glomerularly-filtrated hemoglobin precipitates within the acid lumen of the renal tubular system thereby impairing kidney function (Lang *et al.*, 2005a; Sillix & McDonald, 1987). To prevent those consequences, the erythrocytes might become eryptotic and are therefore degraded by macrophages prior to rupture of the cell membrane and the release of hemoglobin (Lang *et al.*, 2005a). As a matter of fact, many conditions that are associated with hemolysis also induce eryptosis (e.g. Hemolytic Uremic Syndrome (Lang *et al.*, 2006b), energy depletion (Klarl *et al.*, 2006), hemolysin (Lang *et al.*, 2004b), or listeriolysin (Foller *et al.*, 2007b)). Therefore, eryptosis might protect the organism from excessive hemolysis (Lang *et al.*, 2005a).

2.3 The cGMP-dependent protein kinase (G Kinase, cGK)

2.3.1 Characteristics

The cGMP-dependent protein kinase (G-kinase, cGK) is a homodimer serine/threonine kinase activated by submicro- to micromolar concentrations of cGMP (Gamm *et al.*, 1995; Feil *et al.*, 2003; Ruth *et al.*, 1997; Hofmann, 2005). This kinase is expressed in many eukaryotes ranging from the unicellular organism *Paramecium* to *Homo sapiens* (Pfeifer *et al.*, 1999). In mammals, two isoforms are distinguished: soluble cGKI and membrane-bound cGKII with the corresponding genes *prkg1* and *prkg2*. cGKI itself also exists as two isoforms, cGKI α and cGKI β . They are encoded by two splicing variants of the exon of the N-terminus (Hofmann, 2005). cGK is expressed in smooth muscles cells, platelets, cerebellum, hippocampus, dorsal root ganglia, neuromuscular endplate, kidney cells, cardiac muscle cells, vascular endothelium, granulocytes, chondrocytes, and osteoclasts (Hofmann, 2005). Heart, lung, cerebellum and dorsal root glia mainly contain the I α isoform whereas the I β isoform is found in platelets, hippocampus and olfactory bulb neurons (Hofmann, 2005). cKII is found in several brain nuclei, intestinal mucosa, kidney, adrenal cortex, chondrocytes and in the lung (El Husseini *et al.*, 1995; Werner *et al.*, 2004).

cGK contains three domains, an N-terminal (A) domain with an autoinhibitory/pseudosubstrate and autophosphorylation site inhibiting the catalytic center as well as a leucine zipper motif for homodimerization, a regulatory (R) domain with two tandem cGMP-binding sites interacting allosterically and binding cGMP with high and low affinity and a catalytic (C) domain with MgATP- and peptide-binding pockets (Hofmann, 2005). Upon binding of cGMP at both binding sites of the R-domain, the conformation of the enzyme changes (Wall *et al.*, 2003; Zhao *et al.*, 1997), and the catalytic center of the enzyme is released from inhibition by the A-domain. Then, the enzyme can phosphorylate target proteins and, at low cGMP levels, its A-domain (autophosphorylation) resulting in higher activity (Hofmann *et al.*, 1985; Vaandrager *et al.*, 2003).

2.3.2 Guanylate cyclases

cGMP required for the activation of cGK is generated by guanylate cyclases, a family of enzymes catalyzing the conversion of GTP to cGMP (Domek-Lopacinska & Strosznajder, 2005). Two forms of guanylate cyclases can be distinguished: membrane-bound and soluble isoforms (Domek-Lopacinska & Strosznajder, 2005). Membrane-bound guanylate cyclase are activated by natriuretic peptides such as atrial (ANP), B-type (BNP), and C-type (CNP) (Munzel *et al.*, 2003). ANP and BNP are synthesized in the heart as response to increased atrial pressure whereas CNP is released by endothelial cells (Feil *et al.*, 2003;Munzel *et al.*, 2003). All three lead via activation of the membrane-bound guanylate cyclase to relaxation of smooth muscle cells and vasodilation (Feil *et al.*, 2003;Munzel *et al.*, 2003). Moreover, ANP, as a functional antagonist of the renin-angiotensin-aldosterone-system, increases vascular permeability and glomerular filtration rate, and inhibits the sympathetic nerve system resulting in natriuresis and diuresis (Munzel *et al.*, 2003;Venugopal, 2001).

The soluble isoform (sGC) is activated by nitric oxide (NO) (Domek-Lopacinska & Strosznajder, 2005) which is formed by nitric oxide synthases (NOS) thereby inhibiting constriction, proliferation, and migration of the vascular smooth muscle cells and reducing adhesion and activation of platelets as well as vascular inflammation (El Husseini *et al.*, 1999).

sGC, a heterodimeric protein consisting of α - and β -subunits, is found in the cytoplasm of many mammalian cells. Each subunit consists of a N-terminal regulatory and heme-binding domain required for activation of sGC by NO and a C-terminal catalytic domain (Domek-Lopacinska & Strosznajder, 2005). It is important to note for the present study that sGC can pharmacologically be inhibited by methylene blue (MB) (Evora & Viaro, 2006).

2.3.3 Significance of NO/cGMP signaling for erythrocyte survival

NO is known to induce or inhibit apoptosis of nucleated cells depending on the source or concentration of NO and on the influence of additional regulators (Brune, 2003). It may either influence apoptosis by S-nitrosylation of target proteins or by activation of

the sGC generating cGMP and subsequently of the cGMP-dependent protein kinase type I (cGKI), a well-known signaling cascade downstream of NO (Hofmann *et al.*, 2006;Friebe & Koesling, 2003). Cells of erythroid differentiation are known to have functional NO/cGMP signaling (Chen & Mehta, 1998;Ikuta *et al.*, 2001;Kleinbongard *et al.*, 2006).

2.4 PDK1

2.4.1 Phospholipids of biological membranes

Cell membranes have, among others, phospholipids containing inositol. Those lipids have a glycerol-backbone which is esterified with fatty acids at position 1 and 2 and with inositol-1-phosphate at position 3. If this lipid does not contain further phosphate residues at positions of the ring except positions 2 and 6, it is a phosphatidylinositol (Figure 2_{Intro}).

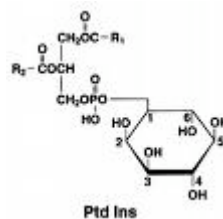


Figure 2_{Intro}. Chemical structure of phosphatidylinositol.

If phosphorylated, it is called a phosphoinositide (PI).

2.4.2 Phosphoinositide 3-kinases (PI3K)

Phosphoinositide 3-kinases (PI3K) phosphorylate the 3'-OH position of the inositol ring in inositol phospholipids, generating 3'-PIs. In vivo, three products may be the result of PI3K-dependent phosphorylation:

- phosphatidylinositol (3,4,5)-trisphosphate
- phosphatidylinositol (3,4)-bisphosphate
- phosphatidylinositol 3-phosphate.

As discussed below, activation of protein kinase B (PKB) requires the first two lipids. In mammalian cells under basal conditions, phosphatidylinositol 3-phosphate is found at

an appreciable concentration, however, phosphatidylinositol (3,4,5)-trisphosphate and phosphatidylinositol (3,4)-bisphosphate are absent under those conditions. Almost all stimuli depending on tyrosine kinase activity for their signaling lead to the generation of phosphatidylinositol (3,4,5)-trisphosphate and phosphatidylinositol (3,4)-bisphosphate (Vanhaesebroeck & Alessi, 2000; Stephens *et al.*, 1993). Tyrosine kinase activity may result from receptors with intrinsic Tyr kinase activity or from non-receptor tyrosine kinases [such as kinases of the Src or JAK (Janus kinase) family] (Vanhaesebroeck & Alessi, 2000).

Three classes of PI3Ks can be divided. Only class I PI3Ks have been shown to activate PKB in cells (Vanhaesebroeck & Waterfield, 1999; Vanhaesebroeck & Alessi, 2000; Wymann & Pirola, 1998). The preferred substrate of class I PI3Ks appears to be phosphatidylinositol (4,5)-bisphosphate. The resulting phosphatidylinositol (3,4,5)-trisphosphate is then converted by a 5'-inositol phosphatase to phosphatidylinositol (3,4)-bisphosphate (Woscholski & Parker, 1997). Class I PI3Ks are heterodimers consisting of a 110 kDa catalytic subunit (p110) and an adaptor/regulatory subunit. Class I PI3Ks linked to Tyr kinases and heterotrimeric G protein-coupled receptors are referred to as class IA and class IB PI3Ks respectively (Vanhaesebroeck & Alessi, 2000).

2.4.3 3'-Phosphoinositide-dependent kinase-1 (PDK1)

The 3'-phosphoinositide 3-kinase (PDK1) is a serine-threonine kinase ubiquitously expressed in human tissues. The enzyme is mainly localized in the cytosol (Anderson *et al.*, 1998; Currie *et al.*, 1999). It consists of an N-terminal kinase domain and a C-terminal PH (pleckstrin homology) domain. PH domains comprise about 120 amino acid residues and are abundant in proteins involved in intracellular signaling. This domain binds phosphatidylinositol lipids contained in cell membranes. The PH domain of PDK1 binds phosphatidylinositol (3,4,5)-trisphosphate and phosphatidylinositol (3,4)-bisphosphate with higher affinity than other phosphatidylinositol derivatives such as phosphatidylinositol (4,5)-bisphosphate (Vanhaesebroeck & Alessi, 2000). Partly, PDK1 is associated with the cell membrane, a process dependent on the PH domain (Currie *et al.*, 1999). The molecular mass of PDK1 is about 63 kDa. The first protein

found to be phosphorylated by PDK1 was PKB α (Alessi *et al.*, 1997b;Currie *et al.*, 1999;Stephens *et al.*, 1998). Since this reaction was only observed in the presence of phosphatidylinositol (3,4,5)-trisphosphate and phosphatidylinositol (3,4)-bisphosphate, this kinase was given the name 3'-phosphoinositide-dependent kinase-1 (Alessi *et al.*, 1997b). Even under basal cell conditions, PDK1 is phosphorylated and therefore active. Thus, upon cell stimulation with agonists of PI3K, no further activation of PDK1 is neither required nor possible (Alessi *et al.*, 1997a;Pullen *et al.*, 1998). The main task of PDK1 is the phosphorylation of PKB.

2.4.4 Protein kinase B (PKB)

Once, the protein kinases A and C had already been known, PKB was identified as a protein kinase with high homology with these kinases and was therefore termed PKB (Vanhaesebroeck & Alessi, 2000). Since it is the cellular homologue of the viral oncoprotein v-Akt, it is therefore also referred to as c-Akt or Akt. Similar to PDK1, PKB is a serine-threonine kinase with a PH domain abundant in many tissues of the human body. PKB consists of a N-terminal PH domain, a kinase domain and a C-terminal regulatory-tail. PDK1 and PKB also share the similarity to preferentially bind phosphatidylinositol (3,4,5)-trisphosphate and phosphatidylinositol (3,4)-bisphosphate with higher affinity than other phosphatidylinositol derivatives (Stephens *et al.*, 1998;James *et al.*, 1996). The molecular mass of PKB is about 57 kDa. In mammals, three closely related PKB genes were found, encoding the isoforms PKB α , PKB β and PKB γ . The latter two show 81% and 83% amino acid identity with PKB α respectively. Unlike PDK1, full activation of PKB requires the phosphorylation of two specific sites by PDK1, one in the kinase domain (Thr308) and the other one in the C-terminal regulatory region (Ser473) (Vanhaesebroeck & Alessi, 2000). In unstimulated cells, PKB is found in the cytosol. PKB partly translocates to the plasma membrane upon activation of PI3K. There, it becomes activated (Andjelkovic *et al.*, 1997;Welch *et al.*, 1998). Active PKB then appears to detach from the plasma membrane and to translocate through the cytosol to the nucleus (Vanhaesebroeck & Alessi, 2000;Andjelkovic *et al.*, 1997).

2.4.5 Activation of PKB by PDK1

PKB exists in a low-activity conformation in the cytosol of unstimulated cells. Upon activation of PI3K, phosphatidylinositol (3,4,5)-trisphosphate and phosphatidylinositol (3,4)-bisphosphate are synthesized at the plasma membrane and PKB interacts through its PH domain with these lipids. This interaction leads to the translocation of PKB from the cytosol to the cell membrane and to a conformational change converting PKB into a substrate for PDK1, perhaps by exposing the threonine308 and serine473 phosphorylation sites. PDK1 then phosphorylates and activates PKB (Vanhaesebroeck & Alessi, 2000).

2.4.6 Proteins regulated by PKB

PKB has a large variety of substrates. Among those are proteins inactivated by PKB-dependent phosphorylation such as Bad and caspase-9, FH transcription factors, GSK3, or Raf. Other proteins such as I κ B kinase, PDE-3B, or eNOS are activated by PKB (Vanhaesebroeck & Alessi, 2000).

2.4.7 Significance of the PI3/PDK1 signaling pathway

The PI3/PDK1 signaling pathway regulates ion channels, transporters, cell volume, and cell survival (Lang *et al.*, 2006a). The significance of PDK1-dependent regulation of cellular function is illustrated by the fact that the PDK1 knockout mouse is not viable (Lawlor *et al.*, 2002). PDK1 hypomorphic mice (*pdk1^{hm}*) expressing only some 20% of PDK1 activity, are smaller than their wild type littermates (*pdk1^{wt}*), a difference largely attributed to reduced cell size (Lawlor *et al.*, 2002). Moreover, PDK1 hypomorphic mice suffer from decreased intestinal and renal transport (Artunc *et al.*, 2006; Rexhepaj *et al.*, 2006; Sandu *et al.*, 2006).

2.5 Participation of erythrocytes in host pathogen interactions

2.5.1 Peptidoglycan

Peptidoglycan (PGN) is a component of the cell walls of nearly all bacteria (Dziarski, 2003; Schleifer & Kandler, 1972). It is a polysaccharide consisting of $\beta(1-4)$ -linked N-acetylglucosamine and N-acetylmuramic acid, crosslinked by short peptides. While the glycan chain (usually N-acetylated and sometimes O-acetylated) does not differ much between different bacteria, the crosslinking peptides differ between gram-negative and gram-positive bacteria: The former all have the same order of L and D amino acid residues (Dziarski, 2003). Their PGN layer is relatively thin and surrounds the cytoplasmic membrane underneath the lipopolysaccharide (LPS)-containing outer membrane (Dziarski, 2003; Rosenthal & Dziarski, 1994a). Figure 3_{Intro} shows the structure of *Staphylococcus aureus* PGN.

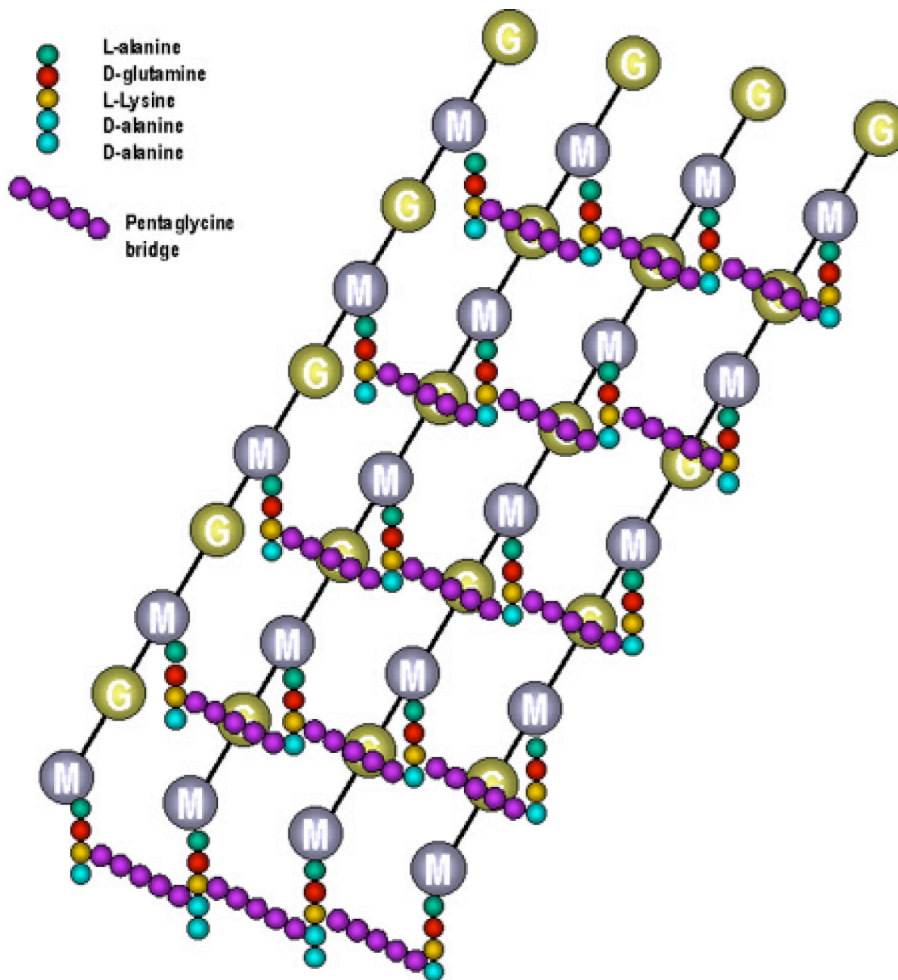


Figure 3_{intro}. Structure of *Staphylococcus aureus* PGN.

In gram-positive bacteria, almost 50% of the mass of the cell wall consists of PGN to which proteins and other polysaccharides are bound. Their PGN also varies in length and amino-acid composition. Especially in the case of gram-positive bacteria, PGN is a suitable target for antibiotics that inhibit bacterial cell wall synthesis (Dziarski, 2003) since PGN is not found in eukaryotic cells. Therefore, PGN is also a target of the innate immune system and belongs to the group of “Pathogen-Associated Molecular Patterns” (PAMP) (Kepler & Chan, 2007). Different “Pattern Recognition Receptors” (PRRs) of the host cell recognize PGN. Among those are CD14, a cell surface lysosylphosphatidylinositol (GPI)-linked 55-kDa glycoprotein highly expressed predominantly on myelomonocytic cells, PGN recognition proteins (PGRPs) (Kang *et al.*, 1998; Liu *et al.*, 2001), Nods, a family of cytoplasmic proteins (Inohara *et al.*, 2002), and TLR-2 (Dziarski, 2003). Cellular effects of PGN exposure include host cell

apoptosis (Bluml *et al.*, 2005;Chen *et al.*, 2005;Colino & Snapper, 2003;Haslinger-Loffler *et al.*, 2005;Haslinger-Loffler *et al.*, 2006;Simons *et al.*, 2007) and anemia (Coccia *et al.*, 2001).

2.5.2 TLR-2

TLR2 functions as a cell-activating receptor not only for Gram-positive bacteria, PGN and LTA, but also for lipoproteins, lipopeptides, mycobacterial lipoarabinomannan and fungal cell walls (zymosan) (Dziarski, 2003;Medzhitov, 2001;Underhill *et al.*, 1999;Verstak *et al.*, 2007). TLR2-mediated responses to PGN and other bacterial components usually do not require CD14, but are often enhanced by CD14 (Dziarski *et al.*, 2001;Dziarski, 2003;Schwandner *et al.*, 1999). PGN has been shown to directly bind to TLR-2 (Iwaki *et al.*, 2002) whose 25 amino acids (Ser40–Ile64) in the extracellular domain are required for cell activation (Mitsuzawa *et al.*, 2001). Thus, this sequence might be the binding site of PGN. The stimulation of TLR-2 by PGN then leads to activation of the NF κ B pathway resulting in the release of chemokines, cytokines, and other mediators of inflammation (Mitsuzawa *et al.*, 2001;Medzhitov, 2001;Janeway, Jr. & Medzhitov, 2002;Dziarski, 2003;Aderem & Ulevitch, 2000).

2.6 Objective of this study

This study aimed at elucidating erythrocytic mechanisms, which regulate and control erythrocyte survival, and, in addition, at defining the impact of host pathogen interactions on suicidal death of erythrocytes. As described above, an increase in the intracellular Ca^{2+} concentration of erythrocytes results in cell shrinkage due to the efflux of K^+ , Cl^- , and osmotically obliged water (Gardos effect). In this study, the functional significance of this effect for suicidal erythrocyte death and erythrocyte clearance was studied. Furthermore, the protective role of Gardos channels during exposure to hemolytic toxins was elucidated. Both issues were addressed by experiments performed in mice lacking the Ca^{2+} -dependent K^+ channel $\text{K}_{\text{Ca}3.1}$, the Gardos channel, and their wildtype littermates. Using patch-clamp recording, flow cytometry, *in vitro* hemolysis and a mouse sepsis model, it is shown that Gardos channel activity and Gardos effect delay hemolysis of injured erythrocytes and, thus, prevent disastrous filtration of released hemoglobin into the renal tubular system. In a further series of experiments, the role of the NO/cGMP signaling pathway, a powerful regulator of the life span of a variety of cells (Dimmeler *et al.*, 2002; Liu & Stamler, 1999), for erythrocyte survival is investigated. Flow cytometry, Western Blotting, hematological counts, and MRI imaging were used to illustrate by means of a cGKI-deficient mouse model that cGKI is a mediator of erythrocyte survival *in vitro* and *in vivo*. Moreover, the participation of PDK1, a key element in the PI3 signaling pathway, which is involved in the regulation of ion channels, transporters, cell volume and cell survival, in the regulation of suicidal erythrocyte death was studied. Experiments performed in hypomorphic mice with some 20% of normal PDK1 activity and their wildtype littermates revealed that PDK1 deficiency is associated with decreased Ca^{2+} entry into erythrocytes and thus with blunted eryptotic effects of oxidative stress, osmotic shock, and Cl^- removal. Finally, the functional significance of host pathogen interactions for suicidal erythrocyte death was investigated. Using flow cytometry, it could be shown that PGN, a main component of the bacterial cell wall, is a potent stimulus of eryptosis and thereby impairs erythrocyte survival.

3 Methods and Materials

3.1 Investigation of the impact of the Gardos channel on survival of erythrocytes

3.1.1 Mice

$K_{Ca3.1}$ -deficient mice ($K_{Ca3.1}^{-/-}$) were generated as described (Sausbier *et al.*, 2006) and maintained at the animal facility of the Pharmaceutical Institute, Department of Pharmacology & Toxicology, University of Tübingen. Either litter- or age-matched wildtype and $K_{Ca3.1}^{-/-}$ mice of both gender with hybrid SV129/C57BL6 background (always F2 generation) were randomly assigned to the experimental procedures with respect to the German legislation on animal protection. The mice have kindly been provided by Peter Ruth and Matthias Sausbier, Pharmaceutical Institute, Department of Pharmacology & Toxicology, University of Tübingen.

3.1.2 *In vitro* experiments

Erythrocytes and solutions. Blood from $K_{Ca3.1}^{-/-}$ mice and their wild type littermates was drawn by retroorbital puncture and collected in heparin-coated tubes. After 3 times of washing in NaCl solution (containing in mM: 125 NaCl, 5 KCl, 1 MgSO₄, 32 N-2-hydroxyethylpiperazine-N-2-ethanesulfonic acid, HEPES/NaOH, 5 glucose, 1 CaCl₂; pH 7.4), cells were suspended in NaCl solution. Ca²⁺ permeabilization of the erythrocyte membrane (patch-clamp and flow cytometry experiments of Figures 1 and 3) was accomplished by addition of 10 μM and 1 μM Ca²⁺ ionophore ionomycin to the NaCl solution, respectively. The effects of oxidative stress on the cytosolic free Ca²⁺ concentration ($[Ca^{2+}]_i$) and on phospholipid scrambling (Figure 4) were assessed by incubating the cells (0.4% hematocrit) for 45 min at 37°C in the absence or presence of *tert*-butylhydroperoxide (0.1 mM; t-BHP) in NaCl solution or KCl solution (containing in mM: 130 KCl, 32 HEPES/KOH, 5 glucose, 1 MgSO₄, 1 CaCl₂; pH 7.4). To test for sensitivity against *Staphylococcus aureus* α-toxin (Sigma, Schnellendorf, Germany), cells

were incubated for 90 min at 37°C in NaCl solution (0.4% hematocrit) in the absence or presence of α -toxin (10 hemolytic units/ml, HU/ml).

Patch-Clamp Experiments. The bath was grounded via a bridge filled with NaCl bath solution (see above). Borosilicate glass pipettes (8-14 M Ω pipette resistance; GC150 TF-10, Clark Medical Instruments, Pangbourne, UK) manufactured by a microprocessor-driven DMZ puller (Zeitz, Augsburg, Germany) were used in combination with a STM electrical micromanipulator (Lang GmbH and Co KG, Germany). Currents were recorded in fast whole-cell, voltage-clamp mode, and 3-kHz low-pass-filtered by an EPC-9 amplifier (Heka, Lambrecht, Germany) using Pulse software (Heka) and an ITC-16 Interface (Instrutech, Port Washington, NY, USA). After giga-Ohm seal formation, the membrane was ruptured by additional suction.

The liquid junction potentials ΔE between the pipette and the bath solutions and between the salt bridge and the bath solutions were estimated as described earlier (Barry & Lynch, 1991). Data were corrected for the estimated ΔE values. Whole-cell currents were evoked by 10 voltage pulses (400 ms each) from -30 mV holding potential to voltages between -100 mV and +80 mV. Applied voltages refer to the cytoplasmic face of the membrane with respect to the extracellular space. Inward currents, defined as flow of positive charge from the extracellular to the cytoplasmic membrane face, are negative currents and depicted as downward deflections of the original current traces. Current values were analyzed by averaging the whole-cell currents between 350 and 375 ms of each square pulse.

Cells were recorded with a pipette solution containing (in mM) 80 KCl, 60 K-D-gluconate, 10 HEPES/KOH, 1 ethylene glycol-bis(β -aminoethyl ether)-N,N,N',N'-tetraacetic acid (EGTA), 1 Mg-ATP, 1 MgCl₂ (pH 7.2) and NaCl bath solution. The open probability (nPo) of K⁺ channels was determined at 0 min voltage by subtracting the averaged current value under control condition from that recorded thereafter in the presence of ionomycin (10 μ M). The ionomycin-stimulated current fraction was then divided by the single channel current amplitude (for K_{Ca}3.1^{-/-} erythrocytes, the ionomycin-stimulated current fraction was divided by the mean single channel current amplitude determined in wildtype erythrocytes).

Forward scatter. To assess Gardos K⁺ channel-mediated changes in erythrocyte size/volume, K_{Ca}3.1^{-/-} and wildtype erythrocytes were suspended in NaCl solution and

forward scatter was recorded and analyzed by flow cytometry using a FACS-Calibur (Becton and Dickinson, Heidelberg, Germany).

Cytosolic free Ca^{2+} -concentration. For measurement of $[Ca^{2+}]_i$, control and oxidized $K_{Ca3.1}^{-/-}$ and wildtype erythrocytes were washed in NaCl solution and then loaded with Fluo3/AM (2 μ M; Calbiochem; Bad Soden, Germany) in NaCl solution for 15 min at 37°C. Thereafter, cells were washed twice and resuspended in NaCl solution and the Ca^{2+} -dependent Fluo3 fluorescence intensity was measured in fluorescence channel FL-1 (excitation at 488 nm, emission at 530 nm) and analyzed by geometrical mean.

Break-down of the phospholipid asymmetry of the erythrocyte membrane. Phosphatidylserine appearance in the outer membrane leaflet was determined by annexin V-binding in flow cytometry. Control and oxidized $K_{Ca3.1}^{-/-}$ and wildtype erythrocytes were washed and loaded for 20 min at 37°C with annexin V-fluos (1:500 dilution; Roche Diagnostics, Mannheim, Germany) in $CaCl_2$ (5 mM)-containing NaCl solution. After washing, annexin V fluorescence was determined by flow cytometry in FL-1, and the percentage of annexinV-binding cells was determined.

Hemolysis. After incubation with α -toxin (10 HU/ml, for 90 min at 37°C), cells were centrifuged at 400 g for 3 min and the supernatants were harvested. The hemoglobin (Hb) concentration of the supernatant was determined photometrically at 405 nm. Erythrocyte lysis in distilled water was defined as 100% hemolysis.

Blood parameters. Erythrocyte number, packed cell volume, mean corpuscular volume and blood hemoglobin concentration were determined using an electronic hematology particle counter (type MDM 905 from Medical Diagnostics Marx; Butzbach, Germany) equipped with a photometric unit for hemoglobin determination. The gating was adjusted for the application on mouse erythrocytes.

Reticulocyte count. Whole blood (5 μ l) was added to 1 ml Retic-COUNT (Thiazole orange) reagent from Becton Dickinson. Samples were stained for 30 min at room temperature and flow cytometry was performed according to the manufacturer's instructions. Forward scatter (FSC), side scatter (SSC), and thiazole orange-fluorescence intensity (in FL-1) of the blood cells were determined. The number of Retic-COUNT positive reticulocytes was expressed as the percentage of the total gated

erythrocyte populations. Gating of erythrocytes was achieved by analysis of FSC vs. SSC dot plots using CellQuest software.

Measurement of the osmotic resistance of erythrocytes. In a 96 well plate, 2 μ l erythrocyte pellets were exposed (2 min) to phosphate-buffered saline (PBS) solutions of decreasing osmolality as prepared by mixing PBS solution with a defined volume of distilled water. After centrifugation (500 g for 5 min), the Hb concentration of the supernatants was determined photometrically (at 405 nm) in an ELISA reader.

3.1.3 α -toxin from *Staph. aureus*

The gram-positive bacterium *Staphylococcus aureus* is a pathogen responsible for community-acquired and nosocomial infections (Fournier & Philpott, 2005). *S. aureus* often causes minor skin and wound infections after skin damages. However, it can also cause severe diseases and thereby infect all organs. Among those are quite frequent infections of the bones (osteomyelitis), the heart (endocarditis), and the lung (pneumonia). In the worst case, the immune system cannot confine a *S. aureus* infection to its focus so that bacteria spread. The consequence is a sepsis (septicemia) which can lead to multi-organ failure and death (Fournier & Philpott, 2005). Definitely, *S. aureus* is among the most common causes of bacterial infections in humans, producing a broad spectrum of diseases. Along with *Escherichia coli*, it also heads the list of agents that are responsible for hospital-acquired infections (Bhakdi & Tranum-Jensen, 1991). *S. aureus* often colonizes hosts asymptotically and lives as a commensal of the human nose. The anterior nares are the major reservoir of *S. aureus*: 20% of persons are persistently colonized and 60% are intermittent carriers, whereas 20% never carry *S. aureus* (Kluytmans *et al.*, 1997). *S. aureus*' pathogenicity is due to the interaction of toxins, exoenzymes, adhesins, and immune-modulating proteins (Fournier & Philpott, 2005). Besides enterotoxins causing gut infections and a typical self-limiting food poisoning, four hemolytic toxins produced by *Staph. aureus* are known: α -, β -, γ - and δ -toxin (Bhakdi & Tranum-Jensen, 1991).

The hemolysins were differentiated on the basis of their lytic activity for different species of erythrocytes. Since they do not only act on erythrocytes but partly preferably on other cells, the term "cytolytic toxin" defined as bacterial products

capable of causing physical dissolution of a variety of cells *in vitro* (Rogolsky, 1979;Bernheimer & Rudy, 1986) was suggested. However, also this term does not reflect the entire mechanism of action of all the toxins as, at least at low concentrations, some toxins do not induce cell lysis but permeabilize the otherwise intact cells (Thelestam & Mollby, 1975). Therefore, the term “membrane-damaging toxin” (Rogolsky, 1979) seems to be more appropriate to describe α -, β -, γ - and δ -toxin.

α -toxin, a protein of defined amino acid composition (Wiseman, 1975), is most intensely studied (Rogolsky, 1979). The α -toxin gene is located on the chromosome (Brown & Pattee, 1980;Pattee, 1986). α -toxin abundance in *S. aureus* strains seems to dependent on the coagulase-status of the strain which is used in clinical practise to differentiate different strains (Bhakdi & Tranum-Jensen, 1991): While 20 coagulase-positive strains had the α -toxin gene, it was not detected in 30 coagulase-negative strains (Bhakdi & Tranum-Jensen, 1991). Furthermore, many *S. aureus* isolates produce only small amounts of α -toxin. Each toxin molecule contains two domains (α and β) having affinity for each other (Bhakdi & Tranum-Jensen, 1991). During infection, tissue damage is attributed to α -toxin. In clinical relevant situations, three target cells were found: platelets (Siegel & COHEN, 1964), monocytes (Bhakdi *et al.*, 1989), and endothelial cells (Bhakdi & Tranum-Jensen, 1991). Especially the deleterious effect on platelets is clinically relevant since they have an procoagulatory effect favouring thrombosis (Bhakdi & Tranum-Jensen, 1991). Furthermore, α -toxin is hemolytic, however the activity is 100 times higher on rabbit erythrocytes compared to human erythrocytes (Bernheimer & Rudy, 1986;Rogolsky, 1979). Mouse erythrocytes display intermediate sensitivity towards α -toxin, probably due to the presence of binding sites of lower affinity (Bhakdi & Tranum-Jensen, 1991). The different sensitivity to α -toxin might be explained by a lack of specific receptors for α -toxin or by a different composition of membrane proteins and lipids compared to rabbit erythrocytes. In line with this, a correlation of hemolytic activity and binding to the membrane is described in an earlier study (Cassidy & Harshman, 1976b). Also, the rate of hemolysis is proportional to the concentration of α -toxin (Bhakdi & Tranum-Jensen, 1991;Cassidy & Harshman, 1976a). In some earlier studies, α -toxin is thought to function as an protease hydrolyzing membrane proteins (Wiseman & Caird, 1972;Wiseman & Caird, 1970). According to this theory, *S. aureus* secretes α -toxin as a proenzyme which needs to be

activated by a membrane-bound enzyme. The different availability of this activating enzyme in erythrocytes from different species might explain the different sensitivity to α -toxin. In line with the “proteolysis” hypothesis, trypsin could also induce α -toxin-based proteolytic activity according to one study (Wiseman *et al.*, 1975). Today, the proteolytic mode of action is denied (Rogolsky, 1979; Freer *et al.*, 1968). It is now established that α -toxin is a pore-forming agent (Bhakdi & Trantum-Jensen, 1991; Belmonte *et al.*, 1987; Forti & Menestrina, 1989). According to this model, α -toxin binds in monomer form to membranes. Upon their subsequent collision during lateral diffusion in the bilayer (Reichwein *et al.*, 1987), α -toxin molecules oligomerize to form noncovalently associated, stable hexameric protein complexes. This process is associated with an exposure of lipid-binding domains, presumably resulting from conformational changes (e.g., unfolding), that enable the hexamer to spontaneously insert into the membrane. The hollow interior of the hexamer generates a hydrophilic channel across the lipid bilayer (Bhakdi & Trantum-Jensen, 1991).

α -toxin initially binds to the erythrocyte membrane at specific sites (Cassidy & Harshman, 1976b; Cassidy & Harshman, 1976a) leading to the release of K^+ followed by the release of hemoglobin and lysis (Bernheimer & Rudy, 1986). While binding to the erythrocyte membrane, the membrane is segmentally separated (Klainer *et al.*, 1972). The chemical nature of the binding site and the kinetics of binding are still questionable. In addition to specific binding at the membrane, α -toxin can absorb in a nonspecific fashion to lipid bilayers (Bhakdi & Trantum-Jensen, 1991). Furthermore, it is cytotoxic and cytolytic to a wide variety of cell types, also dermonecrotic and neurotoxic (Rogolsky, 1979). The molecular mass varies from 26 to 39 kDa depending on the method used for purification (Rogolsky, 1979). Toxin preparations can be transferred to 50 mM ammonium acetate and lyophilized. In this form, the protein is stable for years at -20°C and for weeks at room temperature (Bhakdi & Trantum-Jensen, 1991).

The mean lethal dose of the toxin is approximately 30 $\mu\text{g}/\text{kg}$ of body weight for adult mice injected intraperitoneally (Rogolsky, 1979). Rabbits injected intravenously with a minimal lethal dose die after a few days (Watanabe & Kato, 1974). The major pathological finding was kidney necrosis usually accompanied by flaccid paralysis of the hind legs. Larger doses produced respiratory difficulty, intermittent muscular spasms, intravascular hemolysis, and death within minutes (Rogolsky, 1979).

Due to its properties, α -toxin is an excellent tool for controlled permeabilization of cell membranes. It is stable over a wide pH range and water-soluble. The permeabilizing does not require special conditions (e.g. defined ionic composition). Therefore, α -toxin is widely used as a biological tool (Ahnert-Hilger *et al.*, 1985;Bader *et al.*, 1986;Bhakdi & Trantum-Jensen, 1991;Grant *et al.*, 1987;Hohman *et al.*, 1990).

3.1.4 *In vivo* experiments

For the evaluation of the kidney function, wildtype and $K_{Ca}3.1^{-/-}$ mice were placed individually in metabolic cages (Techniplast, Hohenpeissenberg, Germany). They were allowed to adapt to the metabolic cages for three days prior to the experiment. During this time period, food and water intake, urinary flow rate, urinary excretion of salt, and body weight were monitored every day to ascertain that the mice were adapted to the new environment. Subsequently, 24 h urine and blood specimens (by retroorbital puncture) were collected before and 48 h after a single i.v. injection of α - toxin (1,300 HU/kg body weight in PBS). To assure quantitative urine collection, metabolic cages were siliconized and urine was collected under water-saturated oil as described previously (Vallon, 2003). Plasma and urinary concentrations of Na^+ and K^+ were measured by flame photometry (AFM 5051, Eppendorf, Germany). Plasma and urinary creatinine concentrations were measured using an enzymatic colorimetric method (Labor + Technik, Berlin, Germany).

3.2 Regulation of erythrocyte survival by cGKI signaling

3.2.1 Mice

Experiments were performed with 3- to 10-week-old conventional cGKI knockout mice (Wegener *et al.*, 2002) carrying the L-null allele (cGKI ko mice, genotype: cGKI^{L-/L-}) and with 4- to 45-week-old cGKI smooth muscle rescue mice (Weber *et al.*, 2007), in which the expression of the cGKI α or cGKI β isozyme was selectively restored in smooth muscle but not in other cell types of cGKI^{L-/L-} mice (SM-I α or SM-I β rescue mice, genotype: cGKI^{L-/L-};SM-I α ^{+/-} or cGKI^{L-/L-};SM-I β ^{+/-}). As controls, litter- and gender-matched mice with the following genotypes were used: For cGKI ko mice, wild-type (cGKI^{+/+}) mice and heterozygous cGKI (cGKI^{+/-}) mutants were used, collectively referred to as “ctr” in the text. For SM rescue mice, mice expressing endogenous cGKI as well as the respective SM-I α or SM-I β transgene (SM-I α or SM-I β control mice, genotype: cGKI^{+/-};SM-I α ^{+/-} or cGKI^{+/-};SM-I β ^{+/-}) were used as controls, collectively referred to as “ctr SM rescue” in the text. The results did not significantly differ between male and female mice of the same genotype, between SM-I α and SM-I β rescue mice, between cGKI^{+/+} and cGKI^{+/-} control mice, and between SM-I α and SM-I β control mice. Therefore, data were pooled from both sexes, from SM-I α and SM-I β rescue mice, from cGKI^{+/+} and cGKI^{+/-} control mice, and from SM-I α and SM-I β control mice. All mice were on a 129/Sv genetic background. The targeted alleles were established in the R1 embryonic stem cell line (Nagy *et al.*, 1993), which was derived from a (129X1/SvJ x 129S1) F1 3.5-day blastocyst. The mice have kindly been provided by Susanne and Robert Feil, Interfakultäres Institut für Biochemie, University of Tübingen.

Blood was retrieved either by puncture of the retroorbital venous plexus or, in the case of sacrificed mice, by puncture of the heart, and collected in heparin- or EDTA-coated tubes. Bone marrow was obtained by rinsing the femur and the tibia with PBS. Cells from the bone marrow and spleen were separated with Netwells (Corning) prior to further analysis.

3.2.2 Blood and plasma parameters

RBC number, HCT, MCV and hemoglobin concentration were determined using an electronic hematology particle counter (type MDM 905 from Medical Diagnostics Marx; Butzbach, Germany). These measurements were confirmed by the measurement of the hematocrit by centrifugation at 15,000 g for 3 minutes, measuring the hemoglobin concentration photometrically at 546 nm after adding 20 µl blood to 3 ml of a hemoglobin transformation solution (Dr. Lange AG, Hegnau, Switzerland) and by counting the RBCs manually after a 1:400 dilution with Heyem's solution (Fluka, Buchs, Switzerland) in a Neubauer chamber. Using the hematocrit, hemoglobin and RBC count obtained this way, the MCV, MCH and MCHC were calculated. The RDW was determined from images of blood smears taken with a CCD camera (AxioCam, Zeiss, Deisenhofen, Germany) at a magnification of 400x (Axioskop, Zeiss). From 1829 to 3444 individual erythrocytes of each animal (n=3 to 4), the size was determined using an image analyzing system (MCID, Ontario, Canada). The obtained standard deviations and the means of the erythrocyte size were used to calculate the coefficient of variation as a measure for the RDW. Relative reticulocyte numbers were determined using the Retic-COUNT reagent (BD, Germany) according to the manufacturer's instructions.

The plasma concentration of erythropoietin, haptoglobin, and transferrin were determined using immunoassay kits according to the manufacturer's instructions (erythropoietin: R&D systems, Wiesbaden-Nordenstadt, Germany; others: Kamiya, Seattle, USA). Vitamin B12 and folate were determined by competitive immunoassays according to clinical standards by Prof. Dr. Erwin Schleicher and Dr. Frank Baumgartner, University of Tübingen.

3.2.3 Analysis of spleens

Single cell suspensions of freshly isolated spleens were stained for surface markers and intracellular cytokines and analyzed by flow cytometry according to standard

procedures. Antibodies to Ter119, CD41, CD3, CD4, CD8, B220, IL-2, IL-4, IL-10, IL-17, IFN- γ , TNF, and appropriate isotype controls labeled with FITC or PE were obtained from BD, Germany. Annexin V-FITC staining was performed using an Apoptosis Detection Kit (BD). For intracellular cytokine staining, isolated splenocytes were stimulated with PMA (15 ng/ml) and ionomycin (1.5 μ g/ml) (both Sigma, Germany) for 4 hours in the presence of Brefeldin A (Golgi Plug, BD). Cells were fixed in 2% formaldehyde, washed and permeabilized with 0.5% Saponin/0.5% BSA and incubated with the indicated antibodies. After washing, 50,000 or 100,000 events were counted on a FACS Calibur (BD). For the investigation of the proliferative capacity of splenocytes, 1×10^5 cells per well were cultured in medium or stimulated with LPS (1 μ g/ml). Cell proliferation was examined by measuring DNA synthesis using [3 H]thymidine incorporation (1.25 μ Ci/ml) for 12 hours before harvesting and counting using a MicroBeta device (Perkin Elmer, Germany). Except for the analysis of Ter119, CD41, and annexin V, cells were treated with ammonium chloride to lyse the RBCs before further experiments. The analysis of the spleens was performed by Susanne Feil and Kamran Ghoreschi, University of Tübingen.

3.2.4 Western blot analysis

Erythroid cells were isolated from the bone marrow and peripheral blood by immunomagnetic selection using magnetically-labeled anti-Ter119 MicroBeads and magnetic cell sorting (MACS, Miltenyi Biotec) (Kina *et al.*, 2000). Proteins were separated on a SDS gel, transferred to a PVDF membrane and stained with a polyclonal rabbit antiserum to cGKI (Feil *et al.*, 2005b) or with an antibody against thrombospondin-1 (TSP-1) (Lab Vision). As a positive control for both cGKI as well as TSP-1 expression, platelet-rich plasma was also loaded. Western blot analysis was performed by Susanne Feil, Interfakultäres Institut für Biochemie, University of Tübingen.

3.2.5 Analysis of phosphatidylserine exposure and intracellular Ca²⁺ in peripheral erythrocytes

Erythrocytes were washed two times in Ringer solution (in mM: 125 NaCl, 5 KCl, 1 MgSO₄, 32 HEPES, 5 glucose, 1 CaCl₂, pH = 7.4). Then, erythrocytes at a final hematocrit of 0.4% were incubated in Ringer solution at 37°C in the absence or presence of drugs as indicated. After incubation, FACS analysis was performed essentially as described (Lang *et al.*, 2003b). Cells were stained with annexin V fluos (Roche, Mannheim, Germany) in Ringer containing 5 mM Ca²⁺ at a 1:500 dilution. After 20 min, samples were measured by flow cytometry (FACS-Calibur). Annexin V fluorescence intensity was measured in fluorescence channel FL-1. For intracellular Ca²⁺ measurements, erythrocytes were loaded with fluo-3/AM in Ringer solution containing 5 mM CaCl₂ and 2 μM fluo-3/AM. The cells were incubated at 37°C for 20 min under shaking and washed twice. The fluo-3/AM-loaded erythrocytes were resuspended in 200 μl Ringer solution. Then, Ca²⁺-dependent fluorescence intensity was measured in FL-1.

3.2.6 Measurement of the clearance of fluorescence-labeled erythrocytes *in vivo*

Erythrocytes (obtained from 200 μl blood) were fluorescence-labeled by staining the cells with 5 μM carboxyfluorescein-diacetate-succinimidyl-ester (CFSE) (Molecular Probes, Leiden, Netherlands) in PBS and incubated for 30 min at 37°C. After washing twice in PBS containing 1% FCS, the pellet was resuspended in Ringer solution (37°C), and 100 μl of the CFSE-labeled erythrocytes were injected into the tail vein of the recipient mouse. After two days, blood was retrieved from the tail veins of the mice and CFSE-dependent fluorescence intensity of the erythrocytes was measured in FL-1 as described above. The percentage of CFSE-positive erythrocytes was calculated in % of the total labeled fraction determined 5 min after injection.

3.2.7 Measurement of erythrocyte flexibility and osmotic resistance

Freshly drawn blood (20 μ l) was suspended in 2 ml PBS containing Dextran (MW 60000, Serva, Wallisellen, Switzerland) in amounts yielding a viscosity of 24.4 or 10.4 mPa*s (measured with a cone-plate viscosimeter, DVIII+ Rheometer, Brookfield Engineering Laboratories INC, Middlebrow, MA, USA). The osmolarity of these solutions was adjusted to 310 mosm/L. The red cell / test solution suspension was transferred into a laser defractometer (Myrenne, Röttgen, Germany) and the percent elongation of the erythrocytes was recorded at shear stresses between 0.31 and 61 s^{-1} (24.4 mPa*s solution) or 0.13 and 26 s^{-1} (10.4 mPa*s solution). For determination of the osmotic resistance of erythrocytes, 1 μ l blood was added to 200 μ l of PBS solutions of decreasing osmolarity. After centrifugation for 5 min at 500 g, the supernatant was transferred to a 96 well plate and the absorption at 405 nm was determined as a measure of hemolysis. Absorption in isoosmolar PBS was defined as 0% hemolysis and absorption in pure distilled water was defined as 100% hemolysis. The measurements using a laser defractometer were performed by Beat Schuler and Johannes Vogel, University of Zürich, Switzerland.

3.2.8 Magnetic resonance imaging of spleen volume

Longitudinal magnetic resonance imaging (MRI) was performed with a dedicated 7 Tesla *in vivo* animal MRI system Clinscan (Bruker BioSpin, Ettlingen, Germany), equipped with a 300 mT/m gradient system and operated by the software platform Syngo (Siemens, Erlangen, Germany). After blood withdrawal via tail veins, mice were anesthetized with 1.5-2% isoflurane (in 0.8 l/min oxygen) and placed inside the MR scanner containing a 35 mm quadrature whole body mouse transmitter/receiver coil. Respiration was recorded by an animal monitoring and gating system (SA Instruments, Stony Brook, NY) to trigger MR image acquisition. A full 3D T_2 weighted sequence (T_R : 3500 ms; T_E : 355 ms; 3 averages) was acquired within 15-18 min, leading to an image dataset with a field of view of 56 mm x 42 mm x 23 mm and a voxel size of 0.22 mm x 0.22 mm x 0.22 mm (matrix size: 256 x 192 x 104). Image analysis was

performed with PMOD (PMOD Technologies Ltd., Zurich, Switzerland). Spleen volumes were determined by following the spleen boundaries visible in transversal sections of the MR images. To account for variations in spleen volume estimation, every dataset was evaluated in triplicate, and averaged spleen volumes were used for further calculations. MRI was performed by Martin Thunemann, Interfakultäres Institut für Biochemie, University of Tübingen.

3.3 Study of PDK1-mediated regulation of suicidal death of erythrocytes

3.3.1 Mice

Erythrocytes were drawn from the tail vein of PDK1 hypomorphic mice (*pdk1^{hm}*) and their wild type littermates (*pdk1^{wt}*). The mice have kindly been provided by Dario Alessi, Department of Biochemistry, University of Dundee, United Kingdom. The blood was collected in PBS containing 2 mM EDTA. Generation and basic properties of those mice have been described previously (Lawlor *et al.*, 2002). Genotyping was made by PCR on tail DNA using PDK1- and neo-R-specific primers. Mice had free access to standard mouse diet (C1310, Altromin, Langen, Germany) and tap water.

3.3.2 Solutions

Erythrocytes were washed two times in Ringer solution. Then, erythrocytes were incubated in Ringer solution at 37°C for different periods of time as indicated. Where indicated, the cells were exposed to osmotic shock (addition of 300 mM sucrose on top of isotonic Ringer), oxidative stress (addition of 100 µM *tert*-Butyl hydroperoxide [t-BOOH]), Cl⁻ removal (isosmotic replacement by gluconate), or 1 µM Ca²⁺ ionophore ionomycin (all from SIGMA, Taufkirchen, Germany).

3.3.3 FACS analysis

FACS analysis was performed essentially as described above. After incubation, cells were washed in Ringer solution + 4 mM CaCl_2 . Erythrocytes were stained with annexin V fluos (Roche, Mannheim, Germany) at a 1:500 dilution. After 15 min, samples were measured by flow cytometric analysis. The relative reticulocyte numbers were also determined as described above using Retic-COUNT (Thiazole orange) reagent from Becton Dickinson.

3.3.4 Erythrocyte parameters

RBC number, hematocrit, hemoglobin concentration, MCV, MCHC, and MCH of *pdkl^{hm}* and *pdkl^{wt}* mice were determined in 20 μl of full blood collected in EDTA-containing tubes on a scil Vet abc animal blood counter (scil animal care company GmbH, Viernheim, Germany) suitable for analysis of mice blood according to the manufacturer's instructions. The blood counter was kindly provided by Ulf Scheurlen, Tierärztlicher Dienst, University of Tübingen.

3.3.5 Measurement of intracellular Ca^{2+}

For intracellular Ca^{2+} measurements of erythrocytes, fluo-3/AM was utilized as described above. For the quantification of the intracellular Ca^{2+} concentration, erythrocytes were stained with fluo-3/AM in Ca^{2+} -free Ringer solution containing 4 mM EGTA, 2 μM fluo-3/AM, and 1 mM of the Ca^{2+} -ATPase inhibitor sodium orthovanadate (Sigma, Taufkirchen, Germany) at a hematocrit of 0.2% for 20 minutes at 37°C. After incubation, 100 μl of the suspensions were added to 2 ml of EGTA (4 mM)-buffered and 1 mM sodium orthovanadate-containing Ringer solutions of defined free Ca^{2+} concentrations (ranging from 1 nM to 300 μM) adjusted according to the calculations by WEBMAXC Standard programme. Then, fluo3 fluorescence was measured before and after a 10 min incubation with 10 μM of ionomycin in FL-1.

Linear fitting was made in the range from 3 nM to 100 nM of the linear dependence of fluo3 fluorescence on intracellular Ca^{2+} concentration.

3.3.6 Measurement of the *in vivo* clearance of fluorescence-labeled erythrocytes

Erythrocytes from *pdkl^{hm}* and *pdkl^{wt}* mice were either left untreated or exposed to oxidative stress (addition of 400 μM t-BOOH to Ringer solution and incubation for 30 min at 37°C). After incubation, erythrocytes were washed twice and then fluorescence-labeled by staining the cells with CFSE. The labeling solution was prepared by addition of adequate amounts of a CFSE stock solution (10 mM in DMSO) to PBS to yield a final concentration of 5 μM . Then, the cells were incubated with labeling solution for 30 min at 37°C under light protection. The cells were pelleted at 400 g for 5 min, washed twice in PBS containing 1% FCS, and pelleted at 400 g for 5 min. The pellet was then resuspended in fresh, prewarmed Ringer solution. The fluorescence-labeled erythrocytes were injected in a volume of 100 μl intravenously into the same mice. After the respective time periods, blood was taken from the injected mice and CFSE-dependent fluorescence intensity of the erythrocytes was measured in FL-1 as described above. The percentage of CFSE-positive erythrocytes was calculated in % of the total erythrocyte number.

3.3.7 Statistics

Data are expressed as arithmetic means \pm SEM, and statistical analysis was made by ANOVA using Tukey's test as post hoc test or unpaired t-test, as appropriate.

3.4 Bacterial peptidoglycan induces cell death of erythrocytes

3.4.1 Erythrocytes, solutions, and chemicals

Experiments were performed at 37°C with isolated erythrocytes drawn from healthy volunteers. The volunteers provided informed consent. The study has been approved by the ethics committee of the University of Tübingen (184/2003V). In Ca²⁺-free Ringer, 1 mM CaCl₂ was substituted for 1 mM EGTA.

Ultrapure (according to the manufacturer) soluble PGN from *Staphylococcus aureus* (Invivogen, Toulouse, France) was used at concentrations ranging from 5 to 100 µg/ml. The preparation was made as previously described (Rosenthal & Dziarski, 1994b). Briefly, gram-positive bacteria grown in the presence of β-lactam antibiotics secrete soluble polymeric PGN fragments (Barrett & Shockman, 1984; Fischer & Tomasz, 1984; Keglevic *et al.*, 1974; Mirelman *et al.*, 1974). Isolation of this soluble PGN includes (i) obtaining exponentially growing cells in enriched medium; (ii) harvesting the cells and transferring them into synthetic medium; (iii) growing the cells in the synthetic medium in the presence of penicillin; (iv) obtaining and concentrating the PGN-containing supernatant; and (v) isolating and purifying soluble PGN from the supernatant. The latter can be done by ion-exchange chromatography (Tynecka & Ward, 1975), Sephadex gel filtration (Zeiger *et al.*, 1982), or vancomycin affinity chromatography (Dziarski, 1991). To test for purity, soluble PGN was analysed in 10% SDS-PAGE after dissolving in water at a concentration of 1 mg/ml. Bovine serum albumin (BSA; Carl Roth, Karlsruhe, Germany) was used as a positive control. The samples (50 µg soluble PGN and 2 µg or 4 µg BSA) were mixed with 5X SDS gel loading dye, heated at 95°C for 5 min and loaded onto the gel. The gel was stained with Coomassie blue (Biorad, München, Germany) for 1 h and destained with 10% acetic acid overnight. Fig 25A shows the purity of the preparation used in this study. Ionomycin was used at a concentration of 1 µM. The final concentration of the solvent DMSO was 0.1%.

3.4.2 Light and fluorescence microscopy

After incubation, cells were washed in Ringer solution + 4 mM CaCl₂. Erythrocytes were stained with annexin V fluos at a 1:80 dilution. After 15 min, 10 µl of the cell suspension were analysed under a Zeiss fluorescence microscope (IM35 Zeiss, Oberkochen, Germany), and digital pictures were taken using a digital imaging system.

3.4.3 FACS analysis of annexin V-binding and forward scatter

Annexin V-binding of erythrocytes was quantified in FACS analysis as described above.

3.4.4 Measurement of intracellular Ca²⁺

Intracellular Ca²⁺ measurements were performed as described above. As a positive control for enhanced Ca²⁺ activity, fluo-3-labeled erythrocytes were incubated in Ringer containing 5 mM CaCl₂ and 1 µM ionomycin for 2 min.

3.4.5 Measurement of hemolysis

After 48 hours of incubation of PGN-treated (50 µg/ml and 100 µg/ml) and non-treated erythrocytes at 37°C, the samples were centrifuged (3 min at 400 g, RT) and the supernatants were harvested. As a measure of hemolysis, the hemoglobin (Hb) concentrations of the supernatants were determined photometrically at 405 nm (n=4).

3.4.6 Determination of ceramide formation

To determine ceramide, a monoclonal antibody-based assay was used that had been validated by other groups before (Bieberich *et al.*, 2003;Grassme *et al.*, 2002). After

incubation, cells were stained for 1 hour at 37°C with 1 µg/ml anti-ceramide antibody (clone MID 15B4; Alexis, Grünberg, Germany) in PBS containing 0.1% BSA at a dilution of 1:5. After two washing steps with PBS-BSA, cells were stained for 30 minutes with polyclonal FITC-conjugated goat anti-mouse IgG and IgM specific antibody (Pharmingen, Hamburg, Germany) diluted 1:50 in PBS-BSA. Unbound secondary antibody was removed by repeated washing with PBS-BSA. Samples were then analysed by flow cytometric analysis on a FACS-Calibur in FL-1.

3.4.7 Determination of the intracellular ATP concentration

90 µl of erythrocyte pellet were incubated for 48 h at 37 °C in Ringer solution with or without 100 µg/ml PGN (final hematocrit 5%). All manipulations were then performed at 4°C to avoid ATP degradation. Cells were lysed in distilled water, and proteins were precipitated by addition of HClO₄ (5%). After centrifugation, an aliquot of the supernatant (400 µl) was adjusted to pH 7.7 by addition of saturated KHCO₃ solution. After dilution of the supernatant, the ATP concentration of the aliquots was determined utilizing the luciferin–luciferase assay kit (Roche Diagnostics) on a luminometer (Berthold Biolumat LB9500, Bad Wildbad, Germany) according to the manufacturer's protocol. ATP concentrations are expressed as mmol/l packed erythrocyte volume.

3.4.8 Measurement of the *in vivo* clearance of fluorescence-labeled erythrocytes

Erythrocytes from wildtype mice were either left untreated or exposed to 100 µg/ml PGN for 24 hours at 37°C. After incubation, erythrocytes were washed, fluorescence-labeled twice by staining the cells with CFSE and measured on a FACS Calibur as described above. The percentage of CFSE-positive erythrocytes was calculated in % of the total erythrocyte number.

3.4.9 Statistics

Data are expressed as arithmetic means \pm SEM, and statistical analysis was made by unpaired t-test or ANOVA using Tukey's test as post hoc test, as appropriate.

4 Results

4.1 Investigation of the impact of the Gardos channel on survival of erythrocytes

Erythrocytic Gardos channels are thought to be encoded by the *KCNN4* gene. To directly test this assumption, whole-cell currents were recorded in erythrocytes from $K_{Ca3.1}^{-/-}$ and wildtype mice with KCl/K-gluconate solution in the pipette and NaCl Ringer solution in the bath. Records were obtained before and after Ca^{2+} -permeabilizing of the erythrocyte membrane by addition of ionomycin (10 μ M) to the bath solution. In wildtype but not in $K_{Ca3.1}^{-/-}$ erythrocytes, ionomycin stimulated sparse channel-mediated current transitions (Figure 1A) that superimposed the very low resting erythrocyte whole-cell currents (Figure 1A, insert). The ionomycin-stimulated channels generated outward current transitions, which were apparent at voltages of ≥ -40 mV (Figure 1B). Extrapolation of the mean current-voltage (I-V) relationship of the unitary channel transitions (Figure 1C) indicated a reversal potential at K^+ electrochemical equilibrium and, thus, a K^+ selectivity of the channels. The slope of the I-V curve (as calculated by linear regression between -20 mV and +50 mV) suggested a small unitary conductance of 10 ± 3 pS of the K^+ channels ($n = 4$; Figure 1C).

The ionomycin-stimulated channel activity of the wildtype erythrocytes was very variable between the individual cells but significantly different from 0 ($p = 0.03$; two-tailed one-sample t-test; Figure 1D, open circles). The observed low mean open probability (nPo ; $n =$ number of active channels and $Po =$ mean open probability of the individual channels) in the range of 3 ($n = 10$; Fig 1D) of the Ca^{2+} -permeabilized wildtype erythrocytes hinted to a low number of functional channels per cell. In $K_{Ca3.1}^{-/-}$ erythrocytes ($n = 8$), in contrast, ionomycin did not increase outward currents which were significantly different from zero ($p = 0.8$; two-tailed one-sample t-test; Figure 1D, closed triangles) indicative of absent K^+ channel activity. Taken together, the data suggest that *KCNN4* encodes the intermediate conductance Ca^{2+} -activated K^+ channel $K_{Ca3.1}$ in mouse erythrocytes. In addition, the data further suggest that $K_{Ca3.1}$ is the only Ca^{2+} -activated K^+ channel subtype expressed by murine erythrocytes.

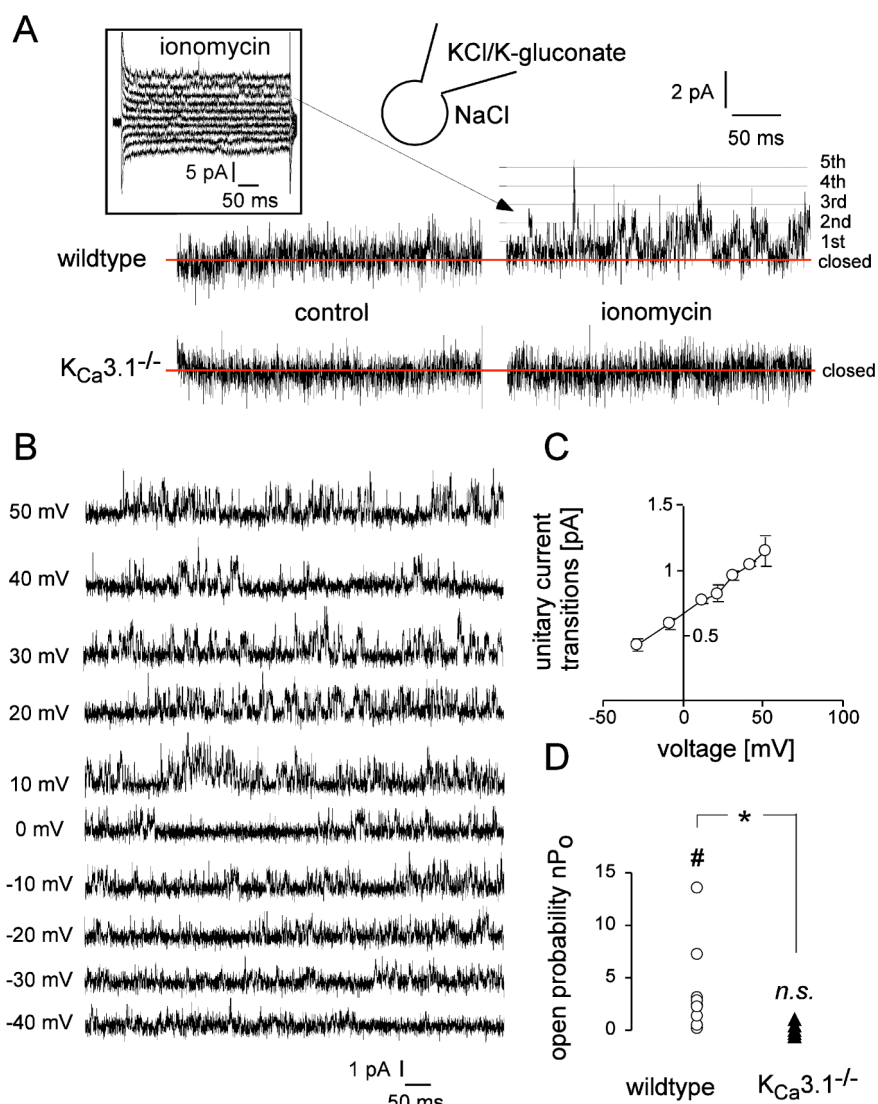


Figure 1. Erythrocytes from $K_{Ca3.1}^{-/-}$ mice lack Gardos K^+ channels. (A) Whole-cell current tracings recorded with KCl/K-gluconate pipette and NaCl bath solution from a wildtype (upper line) and a $K_{Ca3.1}^{-/-}$ erythrocyte (lower line) during voltage square pulses from -30 mV holding potential to +60 mV. Records were obtained prior to (left) and upon stimulation with Ca^{2+} ionophore (10 μ M ionomycin; right). The insert shows the whole-cell currents of the ionomycin-stimulated wildtype cell at 10 different test voltages between -100 mV and +80 mV in lower magnification. Note the outward current transitions, which overlay the whole-cell current and which reflect the activity of individual channels (closed channel state is indicated by red line; the states of increasing number of simultaneously open channels by black lines). (B) Dependence of the single channel currents on voltage. Whole-cell current tracings recorded as in (A, upper line) from an ionomycin-stimulated wildtype cell at different voltages (as indicated). (C) Mean current voltage relationship (\pm SE; $n=4$) of single channels recorded as in (A, B) in wildtype erythrocytes. (D) Open probability (nPo; with P_o = mean open probability and n = unknown number of active channels) as recorded in (A) in wildtype erythrocytes (open circles; $n=10$) and $K_{Ca3.1}^{-/-}$ erythrocytes (closed triangles; $n=8$): #: significant ($p \leq 0.05$) and n.s.: not significantly different from 0, two-tailed one-sample t-test; *: $p \leq 0.05$; two-tailed Welch-corrected t-test.

Blood parameters, such as erythrocyte number, Hb, HCT, MCV, MCH, MCHC, reticulocyte number, or the osmotic resistance of erythrocytes were not significantly different between wildtype and $K_{Ca3.1}^{-/-}$ mice (Fig 2). Thus, Gardos K^+ channel

deficiency *per se* does not appear to influence hematopoiesis nor to shorten mouse erythrocyte lifetime under normal, i.e., non-pathophysiological conditions.

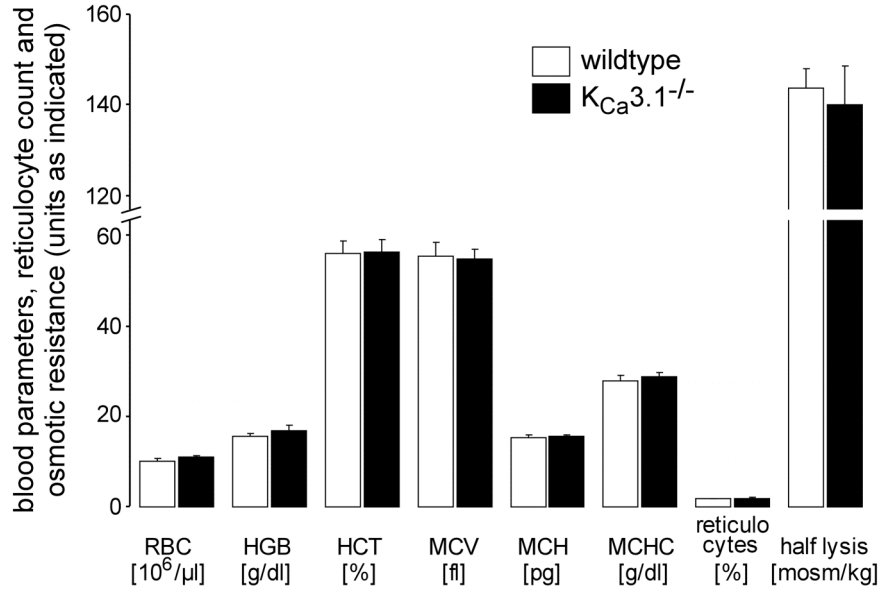


Figure 2. Blood parameters, reticulocyte number and the osmotic resistance of erythrocytes are similar in wildtype and K_{Ca}3.1^{-/-} mice. Blood parameters, reticulocyte number and the osmotic resistance of erythrocytes of wild type (open bars) and K_{Ca}3.1^{-/-} mice (closed bars). Data are means ± SE (n = 5-8).

To estimate the functional relevance of the Ca²⁺-stimulated small conductance K⁺ channels for Ca²⁺-induced erythrocyte shrinkage, the forward scatter of wildtype and K_{Ca}3.1^{-/-} erythrocytes as a measure of erythrocyte size were recorded by flow cytometry. Ionomycin (1 μM) stimulated a decrease of forward scatter in wildtype but not in K_{Ca}3.1^{-/-} erythrocytes incubated in NaCl solution (Figure 3A,B). The slope of forward scatter decline as calculated for the first 5 min of ionomycin stimulation by linear regression was significantly higher in wildtype than in K_{Ca}3.1^{-/-} erythrocytes. Moreover, the slope of K_{Ca}3.1^{-/-} erythrocytes was not different from zero indicating that K_{Ca}3.1^{-/-} cells completely lack Ca²⁺-stimulated K⁺ channels and the Gardos effect (Figure 3C).

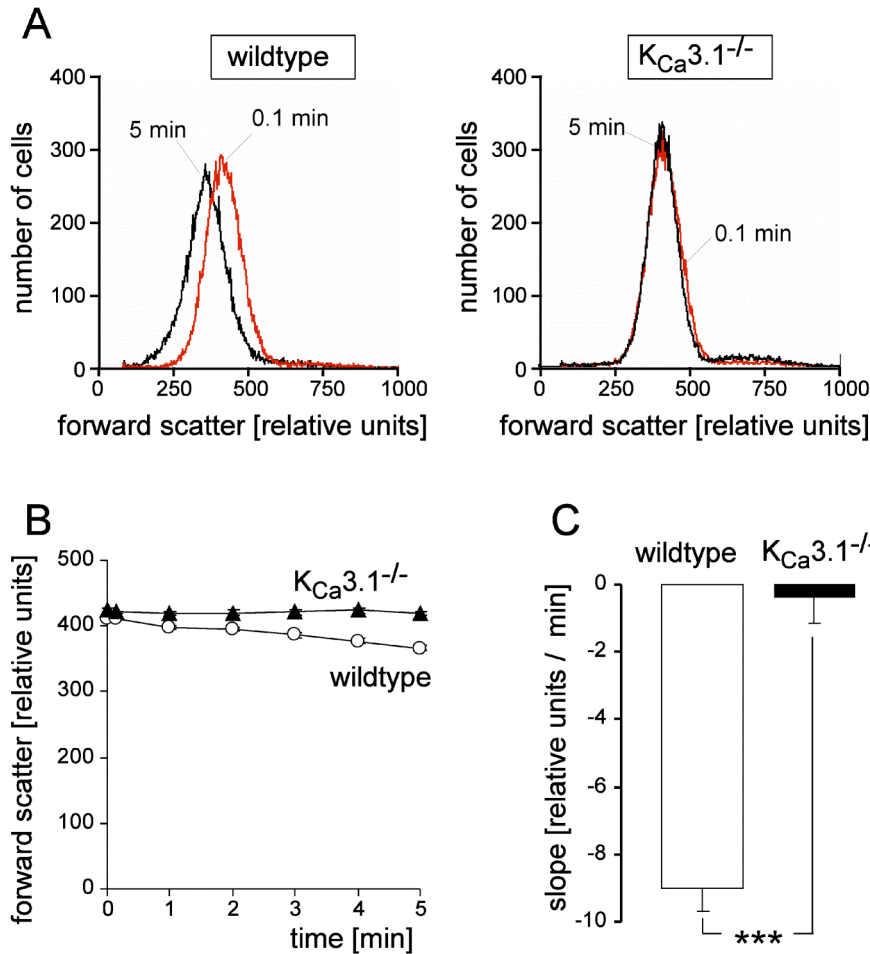


Figure 3. $K_{Ca3.1}^{-/-}$ erythrocytes lack the Gardos effect. (A) Histograms showing the forward scatter in flow cytometry 0.1 min (red line) and 5 min (black line) after addition of ionomycin (1 μ M) to wildtype (left) and $K_{Ca3.1}^{-/-}$ erythrocytes (right) suspended in NaCl solution. (B) Time course of ionomycin (1 μ M)-stimulated changes in mean forward scatter (\pm SE; $n = 4$ mice) of wildtype (open circles) and $K_{Ca3.1}^{-/-}$ erythrocytes (closed triangles). The forward scatter was determined as in (A), ionomycin was added at time 0 min. (C) Mean slope (\pm SE; $n = 4$) of ionomycin-induced forward scatter decline in wildtype (open bar) and $K_{Ca3.1}^{-/-}$ erythrocytes (closed bar; ***: $p \leq 0.001$, two-tailed Welch-corrected t-test).

The suicidal death program of erythrocytes, eryptosis, is thought to prevent colloid osmotic hemolysis of injured erythrocytes. Erythrocyte shrinkage extends the survival of the dying erythrocyte and breakdown of the phospholipid asymmetry fosters its recognition and clearance by phagocytes (Lang *et al.*, 2005a). To define the $K_{Ca3.1}$ channel function for the Ca^{2+} -induced suicidal death program, wildtype and $K_{Ca3.1}^{-/-}$ erythrocytes were subjected to oxidative stress which reportedly activates Ca^{2+} -permeable cation channels in erythrocytes (Duranton *et al.*, 2002). To assess suicidal erythrocyte death, the cytosolic free Ca^{2+} ($[Ca^{2+}]_i$) concentration and breakdown of the phospholipid asymmetry were assessed in flow cytometry by the use of the Ca^{2+} -

sensitive dye fluo3, and phosphatidylserine-binding of a fluorescent annexin V protein, respectively. In non-oxidized wildtype erythrocytes, the fluo3 fluorescence intensity was not significantly higher than in non-oxidized $K_{Ca}3.1^{-/-}$ cells (Figure 4A, top and Figure 4B, 1st and 2nd bars) suggesting similar steady state $[Ca^{2+}]_i$ in both genotypes. Oxidative stress was followed by an almost tripling of the fluo3 fluorescence in wildtype erythrocytes (Figure 4A, bottom and Figure 4B, open bars) but had a significantly smaller effect in $K_{Ca}3.1^{-/-}$ cells (Figure 4B, closed bars).

Annexin V-binding in flow cytometry demonstrated break-down of the membrane phospholipid asymmetry in only about 1% of non-oxidized wildtype and $K_{Ca}3.1^{-/-}$ erythrocytes incubated in NaCl solution (Figure 4D, 1st and 2nd bar). Oxidation in NaCl solution stimulated a dramatic increase in the percentage of annexin V-binding cells in wildtype erythrocytes (Figure 4C, top and Figure 4D, 1st and 3rd bar) while having far less effect in $K_{Ca}3.1^{-/-}$ cells (Figure 4D, 2nd and 4th bar). To test whether this difference is due to Gardos-mediated membrane hyperpolarization and subsequent erythrocyte shrinkage, cells were oxidized in KCl solution. This condition sets the K^+ electrochemical equilibrium to 0 mV and, thus, prevents Gardos K^+ channel-mediated membrane hyperpolarization. As compared to NaCl solution, oxidation in KCl solution decreased the percentage of annexin V-binding wildtype and increased the percentage of annexin-binding $K_{Ca}3.1^{-/-}$ erythrocytes, respectively, and, most importantly, abolished the difference in oxidation-stimulated annexin V-binding between the genotypes (Figure 4C, bottom and Figure 4D, 5th and 6th bar). Taken together, the data suggest that Gardos K^+ channel-mediated membrane hyperpolarization and/or erythrocyte shrinkage facilitate oxidative stress-induced Ca^{2+} entry and subsequent break-down of the phospholipid asymmetry and, thus, contribute to the oxidative stress-triggered suicidal death program. As a consequence, suicidal erythrocyte death was impaired in $K_{Ca}3.1^{-/-}$ erythrocytes.

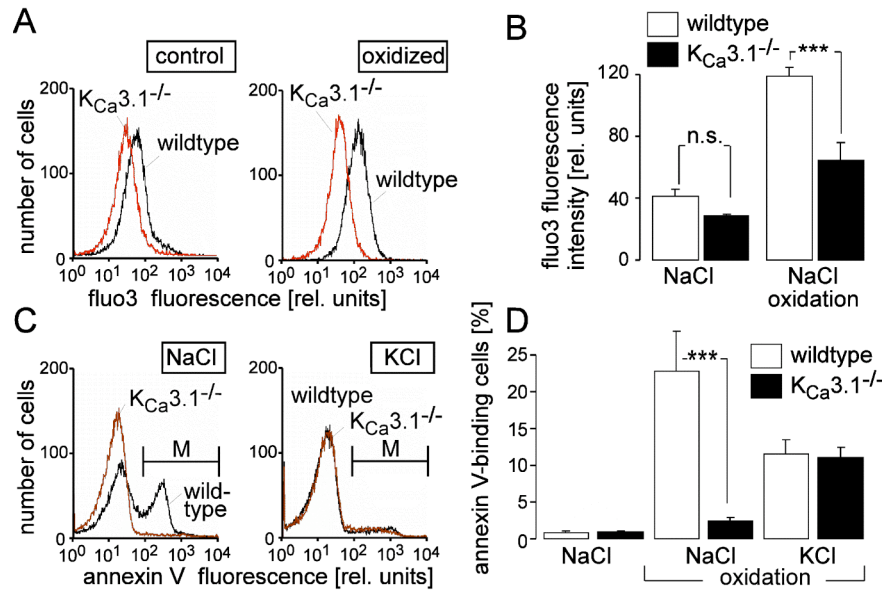


Figure 4. $K_{Ca}3.1^{-/-}$ erythrocytes execute an incomplete suicidal death program. (A). Histograms showing Ca^{2+} -specific fluo3 fluorescence intensity of wildtype (black line) and $K_{Ca}3.1^{-/-}$ erythrocytes (red line) as recorded by flow cytometry in the absence (left) and presence of oxidative stress (0.1 mM tert-butylhydroperoxide, t-BHP, for 45 min; right). (B) Mean fluo3 fluorescence intensity (\pm SE; n = 8) of wildtype (open bars) and $K_{Ca}3.1^{-/-}$ erythrocytes (closed bars) incubated as in (A) under control conditions (1st and 2nd bar) or after oxidative stress (3rd and 4th bar). (C) Histogram of annexin V-binding to oxidized (0.1 mM t-BHP for 45 min) wildtype (black line) and $K_{Ca}3.1^{-/-}$ erythrocytes (red line) incubated in NaCl (left) or KCl solution (right). (D) Mean percentage (\pm SE; n = 5-9) of annexin V-binding wildtype (open bars) and $K_{Ca}3.1^{-/-}$ erythrocytes (closed bars) incubated (45 min at 37°C) in the absence (1st and 2nd bar) or presence of oxidative stress (3rd to 6th bar) in NaCl (1st to 4th bar) or KCl solution (5th and 6th bar; ***, $p \leq 0.001$, n.s.: not significantly different, ANOVA).

To test whether this impairment promotes colloid osmotic hemolysis *in vitro*, wildtype and $K_{Ca}3.1^{-/-}$ erythrocytes were treated with α -toxin from *Staphylococcus aureus* forming a beta barrel pore in the erythrocyte membrane (Song *et al.*, 1996). The results were highly variable between the individual experiments. On average, α -toxin (10 HU/ml in NaCl solution) hemolyzed 40% of the wildtype cells but more than 70% of the $K_{Ca}3.1^{-/-}$ erythrocytes within 90 min of incubation at 37°C (Figure 5A). Normalization of the α -toxin effect to the hemolysis of the $K_{Ca}3.1^{-/-}$ erythrocytes indicated a significantly higher hemolysis of $K_{Ca}3.1^{-/-}$ than wildtype erythrocytes (Figure 5B) indicating that the Gardos effect indeed delays hemolysis *in vitro*.

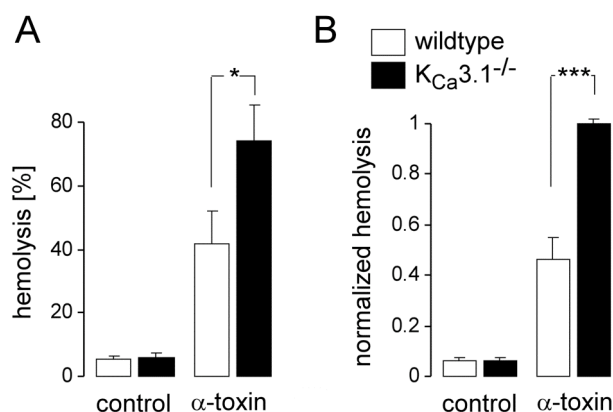


Figure 5. $K_{Ca}3.1^{-/-}$ erythrocytes are prone to hemolyse *in vitro* upon challenge with *S. aureus* α -toxin. Mean percentage of hemolyzed cells (A) and (B) mean normalized hemolysis (\pm SE; n = 12) of wildtype (open bars) and $K_{Ca}3.1^{-/-}$ erythrocytes (closed bars) incubated for 90 min in the absence (1st and 2nd bar) and presence (3rd and 4th bar) of α -toxin (10 HU/ml; ***: p \leq 0.001, ANOVA).

To identify a potential functional significance of the Gardos effect for *S. aureus* infections *in vivo*, food and water intake, body weight, urinary flow rate, plasma Na^+ and K^+ concentrations, urinary Na^+ and K^+ excretion, and creatinin clearance were determined in wildtype and $K_{Ca}3.1^{-/-}$ mice before and 48h after a single i.v. injection of α -toxin (1,300 HU/kg body weight). As shown in Table 1, α -toxin significantly increased plasma K^+ concentrations most probably due to hemolysis-mediated release of erythrocytic K^+ into the plasma. This was accompanied by a significant decrease of the creatinine clearance in $K_{Ca}3.1^{-/-}$ but not in wildtype mice. Moreover, α -toxin-treated $K_{Ca}3.1^{-/-}$ mice exhibited a significant lower urinary output and urinary K^+ excretion than α -toxin-treated wildtype mice (Table 1). Taken together, the data indicate that α -toxin induced acute renal failure in $K_{Ca}3.1^{-/-}$ but not in wildtype mice.

Table 1. Metabolic parameters prior to and following α -toxin treatment. Means \pm SE (n=4-6) of body weight, food and fluid intake, hematocrit, plasma Na^+ and K^+ concentrations, renal excretion of Na^+ , K^+ , and creatinin clearance in $K_{Ca}3.1^{-/-}$ mice and their wild type littermates prior to and after 48 hours of α -toxin treatment (single i.v. injection of 1,300 HU/kg body weight; * indicates significant difference (p \leq 0.05, two-tailed t-test) from wild type mice, # indicates significant difference (p \leq 0.05, paired two-tailed t-test) between control and treatment with α -toxin.

	<i>wild type</i>		$K_{Ca}3.1^{-/-}$	
	control	treatment	control	treatment
Body weight (g)	25.11 \pm 1.5	21.1 \pm 1.3	25.76 \pm 2.0	25.3 \pm 1.6

Food intake (g/24h)	4.11 ± 0.3	3.64 ± 0.3	4.40 ± 0.2	4.3 ± 0.3
Fluid intake (ml/24h)	5.73 ± 0.4	5.26 ± 0.3	5.82 ± 0.3	5.15 ± 0.3
urinary output (ml/24 h)	0.87 ± 0.3	1.17 ± 0.3	0.63 ± 0.1	0.36 ± 0.1 [*]
[Na⁺]_{plasma} (mM)	125.8 ± 3	132 ± 3	127.6 ± 2	133.2 ± 2
[K⁺]_{plasma} (mM)	3.64 ± 0.1	5.35 ± 0.7 [#]	3.56 ± 0.2	4.84 ± 0.5 [#]
24h-creatinine clearance (µl/min)	253.7 ± 101	218.2 ± 18	284.7 ± 75	99 ± 34 ^{*#}
urinary Na⁺ excretion (µmol/24h)	28.55 ± 13	30.3 ± 11	30.8 ± 8.7	32.6 ± 13
urinary K⁺ excretion (µmol/24h)	341.7 ± 74	520 ± 79	396.7 ± 61	269 ± 74 [*]

4.2 Regulation of erythrocyte survival by cGKI signaling

The analysis of peripheral blood showed significant erythrocyte abnormalities in conventional cGKI knockout (ko) mice as compared to litter-matched control (ctr) mice. The RBC counts, HCT, and Hb concentration were significantly smaller in 10-week-old cGKI ko than in ctr mice (Figure 6A). The difference was larger for the erythrocyte number ($\approx 52\%$) than for packed cell volume ($\approx 33\%$) and hemoglobin ($\approx 31\%$). Accordingly, MCV and MCH of erythrocytes were higher in 10-week-old cGKI ko than in ctr mice, whereas MCHC was not altered.

In theory, the anemia could have resulted from decreased erythrocyte formation, which should be reflected by a decreased number of reticulocytes. However, the reticulocyte number was higher in cGKI ko than in ctr mice (Figure 6B). Consistent with reticulocytosis, RDW was increased in cGKI ko mice (Figure 6A). Thus, the anemia could not be explained by decreased formation of erythrocytes. The increased reticulocyte number in cGKI ko mice could have resulted from enhanced stimulation of erythropoiesis by erythropoietin. As illustrated in Figure 6C, the plasma erythropoietin concentration was indeed about twofold higher in cGKI ko than in ctr mice. Increased reticulocyte and erythropoietin levels could be indicative of hemolytic anemia in cGKI ko mice. To explore this possibility, the plasma concentration of haptoglobin was determined. The haptoglobin concentration in anemic cGKI ko mice was similar to control mice (in mg/ml, cGKI ko 0.11 ± 0.02 , n=8; ctr 0.12 ± 0.03 , n=11) excluding a hemolytic anemia. Moreover, iron deficiency due to chronic bleeding or impaired iron absorption are unlikely, since plasma transferrin levels were not significantly different between genotypes (in mg/ml, cGKI ko 1.17 ± 0.05 , n=8; ctr 1.37 ± 0.08 , n=7) and the erythrocytes of cGKI ko mice were not microcytic (Figure 6A).

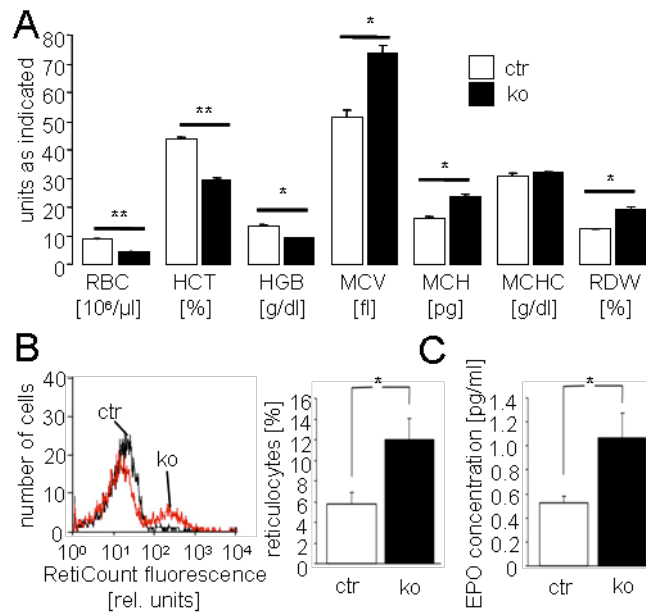


Figure 6. Anemia in cGKI-deficient mice. Circulating blood of 10-week-old control (ctr, open bars) and cGKI ko (ko, black bars) mice was analysed. (A) Counts of RBC, HCT, Hb concentration, MCV, MCH, MCHC, and RDW. The data shown were obtained from a litter-matched group of mice (n=3-4) and are representative for at least three experiments with independent groups of animals. (B) Representative histogram of Retic count fluorescence (left panel) and reticulocyte number (right panel, n=8). The first and the second peak correspond to cell populations with low and high staining intensity, respectively. (C) Plasma erythropoietin concentration (n=4). * and ** indicate significant differences between genotypes with p<0.05 and p<0.01, respectively. The genotypes of the ctr mice were cGKI^{+/+} or cGKI^{+/-}.

Anemia of cGKI-deficient mice was associated with severe splenomegaly. Based on the organ/body weight ratio, 10-week-old cGKI ko mice had ≈3-fold larger spleens than control mice, whereas the size of the heart and kidneys was normal (Figure 7A,B). Analysis of individual animals revealed that splenomegaly was evident in most cGKI ko mice aged 8 to 10 weeks (Figure 7C). It is important to note that conventional cGKI ko mice have a severe smooth muscle (SM) phenotype, which causes premature death of ≈50% of the mutant animals by 6 weeks of age, presumably due to gastrointestinal dysfunction (Wegener *et al.*, 2002; Pfeifer *et al.*, 1998). In line with their increased MCV (Figure 6A), 10-week-old cGKI ko animals tended to have lower plasma levels of vitamin B12 (in ng/dl, cGKI ko 1770 ± 318, n=3; ctr 2718 ± 252, n=5, P=0.08) and folic acid (in ng/dl, cGKI ko 6981 ± 1001, n=3; ctr 9373 ± 848, n=5, P=0.13), but the differences did not reach statistical significance. Vitamin B12 and folic acid deficiency of conventional cGKI ko mice could be due to gastrointestinal malabsorption. To estimate the potential contribution of SM dysfunction and poor health status to anemia and splenomegaly of

cGKI ko mice, another cGKI-deficient mouse model, the so-called cGKI SM rescue mouse (Weber *et al.*, 2007), was analysed. In cGKI SM rescue mice, expression of cGKI has been restored selectively in SM cells but not in other cell types resulting in the rescue of SM dysfunction and a dramatic extension of life span to more than one year (Weber *et al.*, 2007). Thus, cGKI SM rescue mice are a useful genetic model to study the role of cGKI in non-SM cells of relatively “healthy” mice.

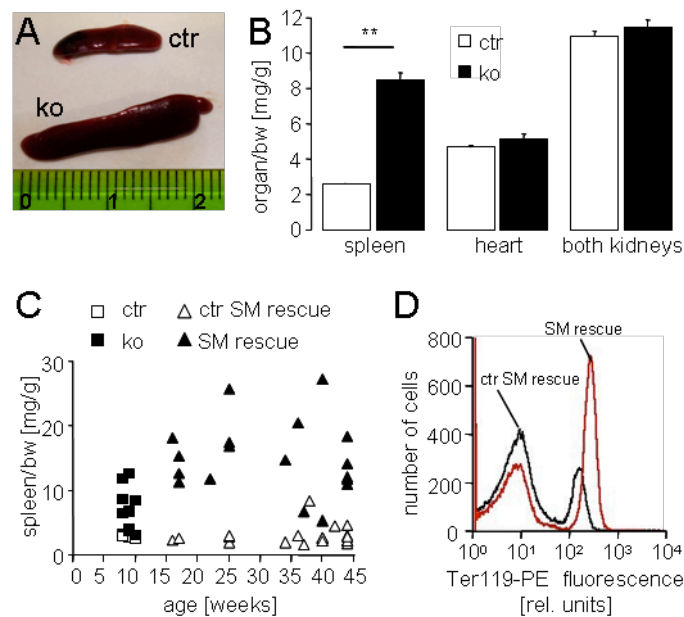


Figure 7. Splenomegaly associated with increased erythroid cell mass in cGKI-deficient mice. (A) Spleens and (B) organ/body weight (bw) ratios of 10-week-old ctr (open bars) and ko (black bars) mice (**, $P < 0.01$). The data shown were obtained from a litter-matched group of mice ($n = 3-4$) and are representative for at least three experiments with independent groups of animals. (C) Spleen/bw ratios of individual mice at various ages. The diagram includes conventional ko mice (black boxes) and their ctr littermates (open boxes) as well as cGKI SM rescue mice (black triangles) and their controls (ctr SM rescue, open triangles). (D) Representative flow-cytometric quantification of Ter119⁺ spleen cells isolated from a 42-week-old cGKI SM rescue mouse and a litter-matched control mouse. The first and the second peak correspond to cell populations with low and high staining intensity, respectively. The genotypes of ctr mice were cGKI^{+/+} or cGKI^{+/-}. The genotypes of ctr SM rescue mice were cGKI^{+/-};SM-1 α ^{+/-} or cGKI^{+/-};SM-1 β ^{+/-}. The experiments presented in this figure have been performed by members of Robert Feil’s group, Interfakultäres Institut für Biochemie, University of Tübingen.

Similar to conventional cGKI ko mice, 10-week-old cGKI SM rescue mice suffered from anemia and splenomegaly (Figure 8). Their hematological phenotype was similar to that of the conventional cGKI ko mice. However, as compared to litter-matched control mice (referred to as “ctr SM rescue”) their MCV and MCH was only moderately increased and their RDW was not altered (Figure 8).

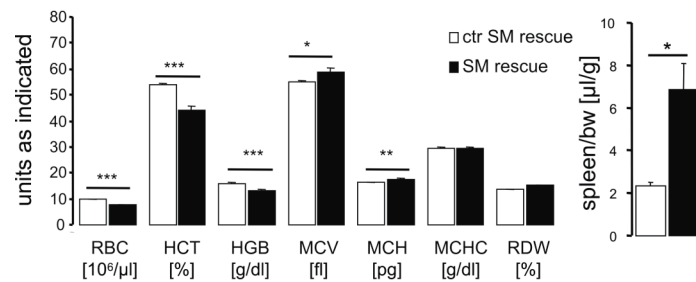


Figure 8. Anemia and splenomegaly in 10-week-old cGKI SM rescue mice (SM rescue, black bars) as compared to their control littermates (ctr SM rescue, open bars). Left diagram, counts of RBC, HCT, HGB concentration, MCV, MCH, MCHC, and RDW. Right diagram, spleen/body weight (bw) ratios. The data were obtained from a litter-matched group of mice (n=4-5). *, ** and *** indicate significant differences between genotypes with $p < 0.05$, $p < 0.01$ and $p < 0.001$, respectively. The genotypes of the ctr SM rescue mice were $\text{cGKI}^{+/L-}; \text{SM-}\alpha^{+/-}$ or $\text{cGKI}^{+/L-}; \text{SM-}\beta^{+/-}$. The experiments presented in this figure have been performed by members of Robert Feil's group, Interfakultäres Institut für Biochemie, University of Tübingen.

“Older” cGKI SM rescue mice (16- to 45-week-old) were also anemic (RBC in $10^6/\mu\text{l}$, SM rescue 7.3 ± 0.3 , n=19; ctr SM rescue 9.8 ± 0.2 , n=29; $P < 0.001$) and showed massive splenomegaly at all ages analysed (Figure 7C). Their plasma levels of vitamin B12 (in ng/dl, SM rescue 2215 ± 244 , n=4; ctr SM rescue 2573 ± 101 , n=6) and folic acid (in ng/dl, SM rescue 15826 ± 2477 , n=4; ctr SM rescue 15620 ± 1341 , n=6), however, were not decreased. Thus, anemia and splenomegaly of the SM rescue mice were not due to SM dysfunction, potential malabsorption, or poor health.

Further experiments were performed to elucidate characteristics of the cells that apparently accumulated in the enlarged spleens of cGKI-deficient mice. Freshly prepared splenocytes were stained with an antibody against Ter119, a marker of late-stage murine erythroid cells and mature erythrocytes (Kina *et al.*, 2000) and with annexin V to examine the externalization of PS indicative of suicidal cell death. Flow-cytometric analysis showed that cGKI SM rescue mice had, proportionally, $\approx 96\%$ more Ter119⁺ splenocytes than ctr SM rescue mice (Figure 7D, Table 2). When corrected for the increased spleen size in cGKI mutants, this reflects a ≈ 6 -fold increase in spleen erythroid cell mass. Annexin V-binding indicated that Ter119⁺ splenocytes of cGKI-deficient animals contained, proportionally, twice as much PS-exposing cells than control mice (percentage of PS-exposing / total erythroid cells, SM rescue $\approx 20\%$, ctr SM rescue $\approx 9\%$), whereas

nonerythroid cells showed no significant difference in the level of annexin V-labeled cells between genotypes (Table 2). Immunophenotyping for marker proteins revealed that the relative proportion of splenic CD41⁺ megakaryocytes (Tiedt *et al.*, 2007), CD4⁺ T cells, CD8⁺ T cells, and B220⁺ B cells as well as the proliferative activity of the splenocytes in the absence and presence of lipopolysaccharide (LPS) were similar in control and cGKI SM rescue animals (Table 2). Moreover, the analysis of splenocytes for intracellular and secreted cytokines did not reveal altered levels of pro-inflammatory (IL-2, IL-17, IFN- γ , TNF) or anti-inflammatory (IL-4, IL-10) mediators in the spleens of cGKI mutants compared to controls (data not shown). Similar results were obtained with spleens of 10-week-old conventional cGKI ko mice; they contained about twice as many eryptotic erythroid cells as their litter-matched controls (percentage of PS-exposing / total erythroid cells, ko $20 \pm 3\%$, n=3; ctr $8 \pm 2\%$, n=4; $P < 0.05$), whereas the nonerythroid cells of cGKI ko mice showed no significant abnormalities according to the parameters listed in Table 2 (data not shown). Thus, increased spleen size of the cGKI-deficient mice was not due to an increase in nonerythroid cells including lymphocytes, but was caused, at least in large part, by an increased number of eryptotic erythrocytes.

Table 2. Analysis of the cell populations derived from the spleens of cGKI SM rescue mice. The experiments presented in this table have been performed by members of Robert Feil's group, Interfakultäres Institut für Biochemie, University of Tübingen.

	Ctrl	SM rescue
Erythroid cells, % (Ter119 ⁺ / total splenocytes)	28 \pm 3.6	55 \pm 6.5*
Apoptotic erythroid cells, % (Ter119 ⁺ & annexin V ⁺ / total splenocytes)	2.5 \pm 0.4	11 \pm 0.7*
Apoptotic nonerythroid cells, % (Ter119 ⁻ & annexin V ⁺ / total splenocytes)	27 \pm 6.5	20 \pm 3.5
CD41 ⁺ megakaryocytes, %	10 \pm 4.0	7.9 \pm 2.0
CD4 ⁺ T cells, %	31 \pm 5.8	24 \pm 4.9
CD8 ⁺ T cells, %	9.1 \pm 1.4	6.1 \pm 1.4
B220 ⁺ B cells, %	35 \pm 4.1	30 \pm 6.1
³ H-thymidine incorporation		
basal, cpm	448 \pm 95	377 \pm 109
LPS (1 μ g/ml), cpm	6563 \pm 1688	4781 \pm 1854

All data are means \pm SEM (n = 3-5 mice). 34- to 45-week-old cGKI SM rescue mice and their control littermates (genotype: cGKI^{+L-}; SM-I α ^{+/-} or cGKI^{+L-};SM-I β ^{+/-}) were analysed. Statistical test results are reported as *P* value by *t* test. *, *p*<0.05 vs. ctr SM rescue.

The accumulation of erythrocytes in the spleens of cGKI-deficient animals could be linked to their higher sensitivity to eryptosis. Therefore, it was explored whether cGKI signaling plays a role in eryptosis. Western blot analysis showed that cGKI protein is present in both erythroid cells from the bone marrow as well as in peripheral erythrocytes (Figure 9). To exclude a potential contamination of the erythroid cells with platelets containing high levels of cGKI (Feil *et al.*, 2003;Hofmann *et al.*, 2006), the same membranes were stained for the platelet marker thrombospondin-1 (TSP-1). While TSP-1 was readily detected in platelet-rich plasma, it was not present in erythroid cell preparations used for Western analysis, thus, excluding a contamination with platelets (Figure 9).

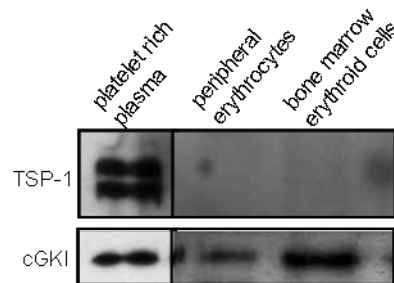


Figure 9. Expression of cGKI in murine erythroid cells. Western blot analysis of cGKI expression in erythroid cells from a 26-week-old wild-type mouse. Protein extracts of platelet-rich plasma (5 μ g) and of Ter119⁺ erythroid cells isolated from peripheral blood (30 μ g) or bone marrow (30 μ g) were stained with an antiserum raised against cGKI (lower panel) or thrombospondin-1 (TSP-1, upper panel). The experiments presented in this figure have been performed by members of Robert Feil's group, Interfakultäres Institut für Biochemie, University of Tübingen.

Further evidence for cGKI activity in erythrocytes came from the functional analysis of erythrocytes retrieved from ctr and cGKI ko mice. Eryptosis was monitored by flow cytometry utilizing annexin V-binding to PS-exposing cells. The membrane-permeable cGMP analog, 8-Br-cGMP, suppressed ionomycin-induced eryptosis in ctr but not in cGKI ko erythrocytes indicating that activation of the cGMP/cGKI signaling

pathway protects from erythrocyte death (Figure 10A). Accordingly, erythrocytes from cGKI ko mice showed a significantly higher percentage of PS-exposing erythrocytes than ctr mice following a 48 hours incubation in Ringer solution at 37°C (Figure 10B). Externalization of PS is stimulated by increased cytosolic Ca²⁺ concentration (Lang *et al.*, 2003b). The determination of the intracellular Ca²⁺ concentrations using fluo3 showed that the cytosolic Ca²⁺ concentration was indeed significantly higher in cGKI ko erythrocytes than in ctr cells (Figure 10C).

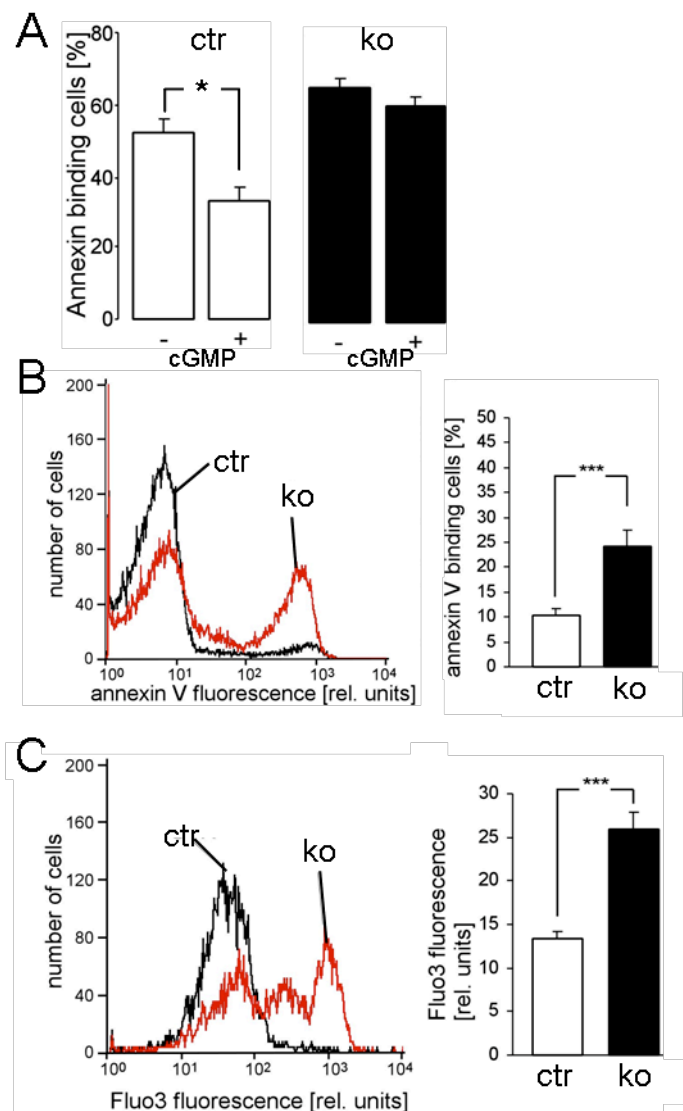


Figure 10. Increased eryptosis and intracellular Ca²⁺ level in cGKI-deficient (ko, black bars) erythrocytes compared to control (ctr, open bars) erythrocytes. (A) Effect of cGMP on eryptosis. PS exposure of ctr and ko erythrocytes was determined by annexin V-binding after a 30 min incubation with the Ca²⁺ ionophore ionomycin (0.1 μM) at 37°C. Before addition of ionomycin, cells were preincubated for 30 min with the guanylyl cyclase inhibitor methylene blue (20 μM) followed by additional 60 min in the absence (-) or presence (+) of 1 mM 8-bromo-cGMP

(n=11-12; *, $P < 0.05$). (B) Surface exposure of PS as determined by annexin V-binding and (C) measurement of intracellular Ca^{2+} by fluo3 fluorescence in ctr and ko erythrocytes after incubation in Ringer solution at 37°C for 48 hours. The respective left panel shows a representative flow cytometric histogram and the right panel shows the statistical analysis (n=12; ***, $p < 0.001$). The first and the second peak correspond to cell populations with low and high staining intensity, respectively. Erythrocytes were isolated from 10-week-old cGKI knockout mice and their litter-matched controls. The genotypes of the ctr mice were cGKI^{+/+} or cGKI^{+/-}.

Similar results were obtained with erythrocytes isolated from cGKI SM rescue mice, *i.e.* these erythrocytes displayed significantly enhanced cytosolic Ca^{2+} and eryptosis as compared to the respective control erythrocytes (Figure 11).

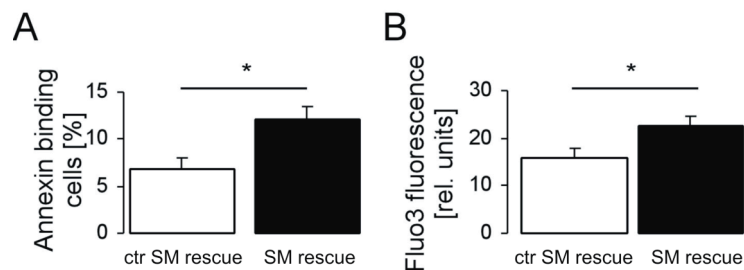


Figure 11. Increased eryptosis and intracellular Ca^{2+} level in erythrocytes isolated from 10-week-old cGKI SM rescue mice (SM rescue) as compared to their control littermates (ctr SM rescue). (A) Surface exposure of PS as determined by annexin V-binding and (B) measurement of intracellular Ca^{2+} by fluo3 fluorescence after incubation in Ringer solution at 37°C for 48 hours (n=5-6; *, $p < 0.05$). The genotypes of the ctr SM rescue mice were cGKI^{+/-};SM-I α ^{+/-} or cGKI^{+/-};SM-I β ^{+/-}.

These data suggested that cGKI inhibits erythrocyte death *in vitro* by reducing the cytosolic Ca^{2+} concentration, which in turn limits the exposure of PS at the cell surface. To investigate whether cGKI deficiency also affected mechanical properties of the erythrocytes, cGKI ko and ctr erythrocytes were exposed to shear stress and the resulting cell elongation as a measure of erythrocyte flexibility was determined using laser-defractometry. cGKI ko erythrocytes were slightly but significantly more flexible than ctr cells. For instance, the % elongation at a shear stress of 3.1 Pa in a high viscosity solution (24.4 mPa*s) were 24 ± 0.4 in cGKI ko and 19 ± 0.3 in ctr erythrocytes ($p < 0.05$), and the % elongation at a shear stress of 2.6 Pa in a low viscosity solution (10.4 mPa*s) were 17 ± 0.2 in cGKI ko and 14 ± 0.4 in ctr erythrocytes ($p < 0.05$). Since deformability of cGKI-deficient erythrocytes was slightly improved, their mechanical properties could not

account for their accumulation in the spleens of cGKI mutant mice. Furthermore, the osmotic resistance of cGKI-deficient erythrocytes was not altered (Figure 12).

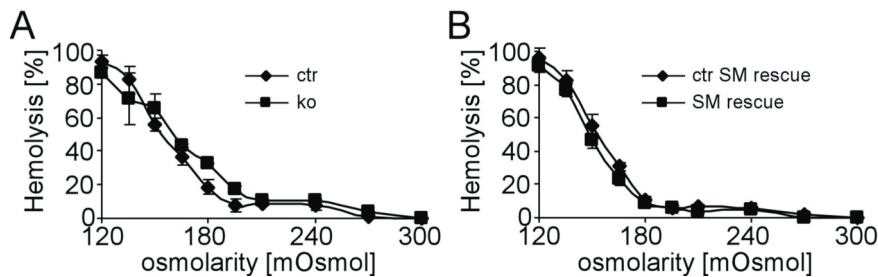


Figure 12. Osmotic resistance of cGKI-deficient erythrocytes. Erythrocytes were isolated from (A) conventional cGKI knockout mice (ko, boxes) and their controls (ctr, diamonds) or (B) cGKI SM rescue mice (SM rescue, boxes) and their controls (ctr SM rescue, diamonds). Mice were 10 weeks old. The genotypes of the ctr mice were cGKI^{+/+} or cGKI^{+/-}. The genotypes of the ctr SM rescue mice were cGKI^{+/-};SM-1 α ^{+/-} or cGKI^{+/-};SM-1 β ^{+/-}.

The above experiments suggested that cGKI deficiency promotes the death of erythrocytes, which might accumulate in the spleens of the mutant animals, thus leading to splenomegaly. To determine their *in vivo* survival, erythrocytes were isolated from ctr or cGKI ko donor mice, labeled with CFSE, and subsequently injected into the tail vein of ctr or cGKI ko mice. The clearance of CFSE-labeled erythrocytes from the circulation, an indirect indicator of erythrocyte death, was determined two days after reinjection. In line with the accelerated *in vitro* eryptosis of cGKI-deficient erythrocytes, $\approx 14\%$ of cGKI-deficient erythrocytes disappeared from peripheral blood of ctr mice as compared to only $\approx 5\%$ of ctr erythrocytes (Figure 13). CFSE-labeled ctr erythrocytes were cleared more rapidly in ko mice than in ctr mice, most likely due to their retention in the enlarged spleens of the recipient mice ($\approx 34\%$ of the initial cells were cleared two days after injection). Clearance of erythrocytes was even faster, when ko cells were injected into cGKI ko mice ($\approx 53\%$ of the initial cells were cleared two days after injection; Figure 13).

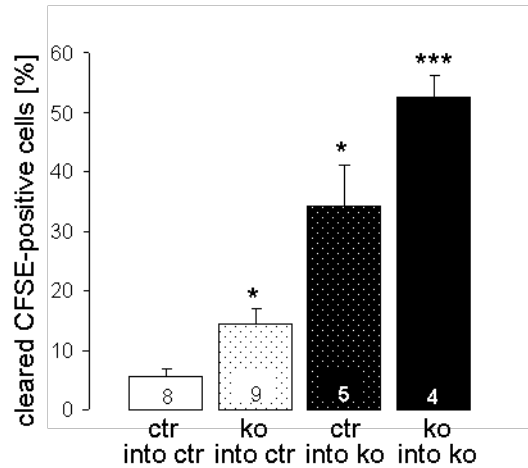


Figure 13. *In vivo* clearance of CFSE-labeled erythrocytes. Erythrocytes were isolated from and injected into 10-week-old cGKI knockout mice (ko) or their litter-matched controls (ctr). The configuration of each transfer experiment is indicated below each bar and the number of injected animals (n) is indicated inside each bar. The percentage of cleared CFSE-labeled cells was determined two days after injection (*, $p < 0.05$ vs ctr; ***, $p < 0.001$ vs ctr). The genotypes of the ctr mice were cGKI^{+/+} or cGKI^{+/-}.

Together, these data indicated that anemia of cGKI-deficient mice was not only due to an erythrocyte-autonomous component, *i.e.* increased eryptosis, but was potentiated by the development of enlarged spleens retaining more erythrocytes than normal spleens. Along those lines, anemia but not splenomegaly was detectable in 3- to 4-week-old cGKI ko mice (Figure 14A), whereas 10-week-old knockout mice were both anemic and had enlarged spleens (Figs. 6A and 7A-C). Note that MCV was not increased in 3- to 4-week-old cGKI ko mice (data not shown), although they were already anemic. Cause and effect of the observed phenotypes were further resolved in a time course study with cohorts of cGKI SM rescue and litter-matched control mice. Animals were monitored from 4 to 10 weeks of age for RBC count and by magnetic resonance imaging (MRI) for spleen volume. As shown in Figure 14B, by 5 weeks of age, cGKI SM rescue mice became anemic, but still had a normal spleen size. Thus, anemia appeared to precede splenomegaly in cGKI-deficient mice.

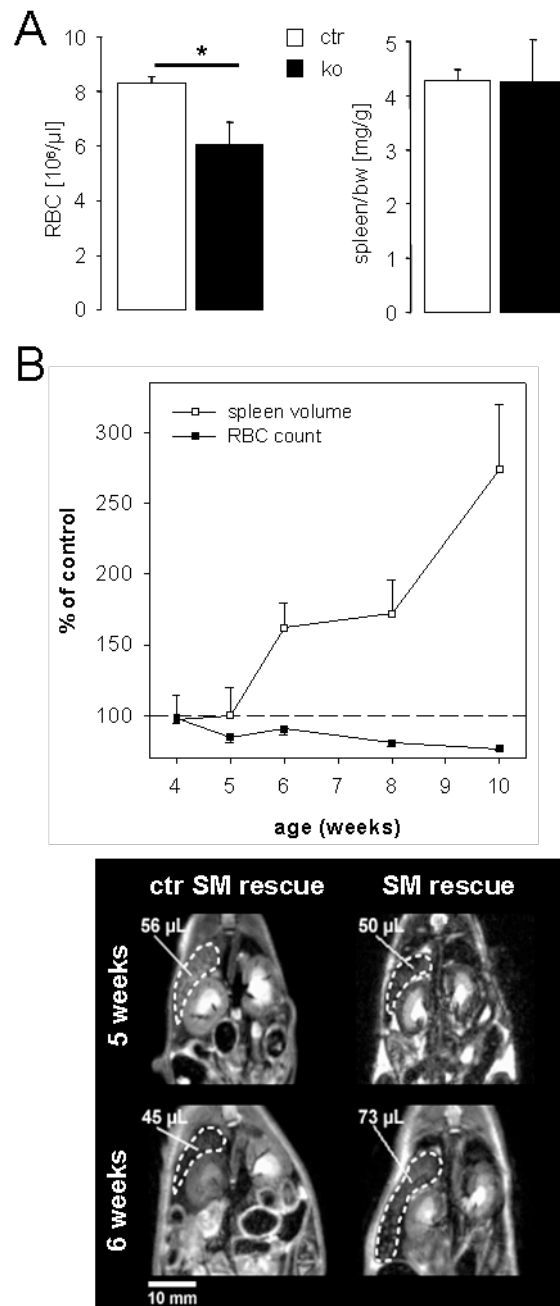


Figure 14. Anemia precedes splenomegaly in cGKI-deficient mice. (A) The number of red blood cells (RBC, $n=5$) and the spleen/body weight (bw) ratio ($n=10$) were determined in 3- to 4-week-old control (ctr, open bars) and cGKI ko (ko, black bars) mice (*, $P<0.05$). The genotypes of ctr mice were cGKI^{+/+} or cGKI^{+/-}. (B) Time course of the development of anemia and splenomegaly in cGKI SM rescue mice. Spleen volume was determined by non-invasive MRI. RBC count (black boxes) and spleen volume (open boxes) were longitudinally monitored from 4 to 10 weeks of age in 4 cGKI SM rescue mice and 5 litter-matched control mice (ctr SM rescue). For each experimental day, RBC counts and spleen volumes of the SM rescue mice were normalized to the respective mean values of the control animals, which were set to 100%. Note that 5-week-old SM rescue mice have already had a significantly lower RBC count than control mice ($P<0.05$) but a normal spleen volume. The lower panel shows representative MR images (coronal sections, top view) of individual control and SM rescue mice at 5 and 6 weeks of age. Spleens (broken lines) and corresponding volumes are indicated. The genotypes of the ctr SM rescue mice were cGKI^{+/-};SM-1 α ^{+/-} or cGKI^{+/-};SM-1 β ^{+/-}. The experiments presented in this figure have been performed by members of Robert Feil's group, Interfakultäres Institut für Biochemie, University of Tübingen.

4.3 Study of PDK1-mediated regulation of suicidal death of erythrocytes

First, hematological parameters of the mice were determined. The erythrocyte count was similar in PDK1 hypomorphic mice (*pdkl^{hm}*) and their wild type littermates (*pdkl^{wt}*). MCV and MCHC were significantly smaller in *pdkl^{hm}* than in *pdkl^{wt}* mice (Table 3).

Table 3. Erythrocyte parameters of *pdkl^{wt}* and *pdkl^{hm}* mice.

	<i>pdkl^{wt}</i> (n=4-8)	<i>pdkl^{hm}</i> (n=4-8)	<i>p</i>
RBC count [$10^6/\mu\text{l}$]	10.0 ± 0.4	10.9 ± 0.2	n.s.
HCT [%]	52.2 ± 1.4	53.4 ± 0.7	n.s.
MCV [fl]	52.2 ± 1.1	49.2 ± 0.6	< 0.05
HGB [g/dl]	15.7 ± 0.5	15.4 ± 0.3	n.s.
MCH [pg]	15.7 ± 0.3	14.2 ± 0.0	< 0.001
MCHC [g/dl]	30.1 ± 0.2	28.8 ± 0.2	< 0.01
Reticulocyte number [%]	4.5 ± 0.4	5.0 ± 0.2	n.s.

The erythrocyte forward scatter was again slightly but significantly smaller (by 6.1 ± 0.1%, n =10) in *pdkl^{hm}* mice than in *pdkl^{wt}* mice after 6 hours of incubation in Ringer solution at 37°C, pointing to decreased volume of *pdkl^{hm}* erythrocytes. The reticulocyte number tended to be higher in *pdkl^{hm}* mice (Table 3), a difference, however, not reaching statistical significance.

The Ca²⁺-permeable erythrocyte cation channels are activated by oxidative stress, which triggers Ca²⁺ entry, erythrocyte shrinkage, and phospholipids scrambling (Lang *et al.*, 2005a). To explore whether PDK1 deficiency affects the sensitivity of erythrocytes to oxidative stress, *pdkl^{hm}* and *pdkl^{wt}* erythrocytes were exposed for 30 minutes to 100 μM *tert*-Butyl hydroperoxide (t-BOOH). As illustrated in Figure 15, oxidative stress significantly decreased the forward scatter in both genotypes. Following treatment with 100 μM t-BOOH, the forward scatter was similarly low in *pdkl^{hm}* and *pdkl^{wt}* erythrocytes.

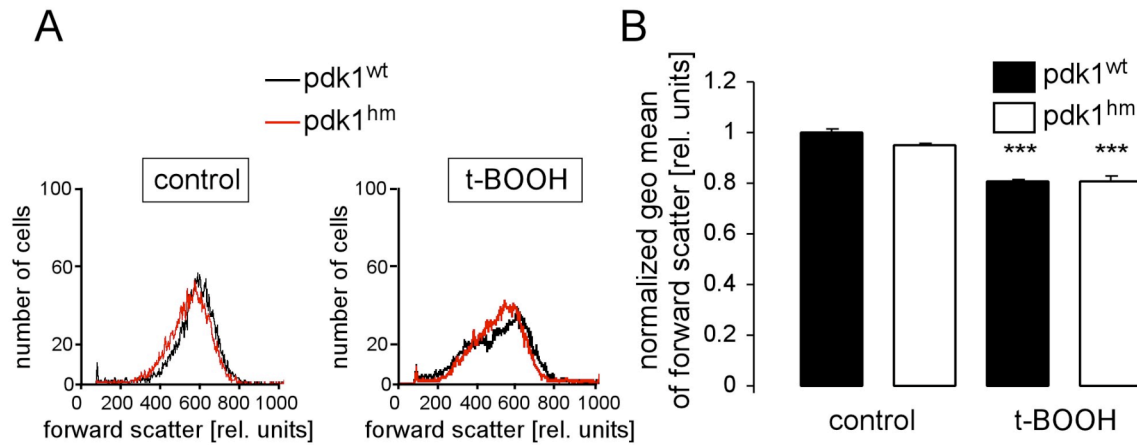


Figure 15. Effect of oxidative stress on forward scatter of *pdk1*^{hm} and *pdk1*^{wt} erythrocytes. Forward scatter determined by FACS analysis of erythrocytes from PDK1 hypomorphic mice (*pdk1*^{hm}) and their wild type littermates (*pdk1*^{wt}) following a 30 min incubation in the presence or absence of 100 μ M tert-Butyl hydroperoxide (t-BOOH). (A) Original histograms of forward scatter. (B) Arithmetic means \pm SEM (n=8) of forward scatter of *pdk1*^{hm} (white bars) and *pdk1*^{wt} (black bars) erythrocytes incubated in the absence (control) or presence (t-BOOH) of t-BOOH. *** indicates significant difference ($p < 0.001$) between control and t-BOOH.

Oxidative stress further increased phosphatidylserine exposure, as evident from annexin V-binding (Figure 16). The increase in annexin V-binding was, however, significantly smaller in *pdk1*^{hm} than in *pdk1*^{wt} erythrocytes.

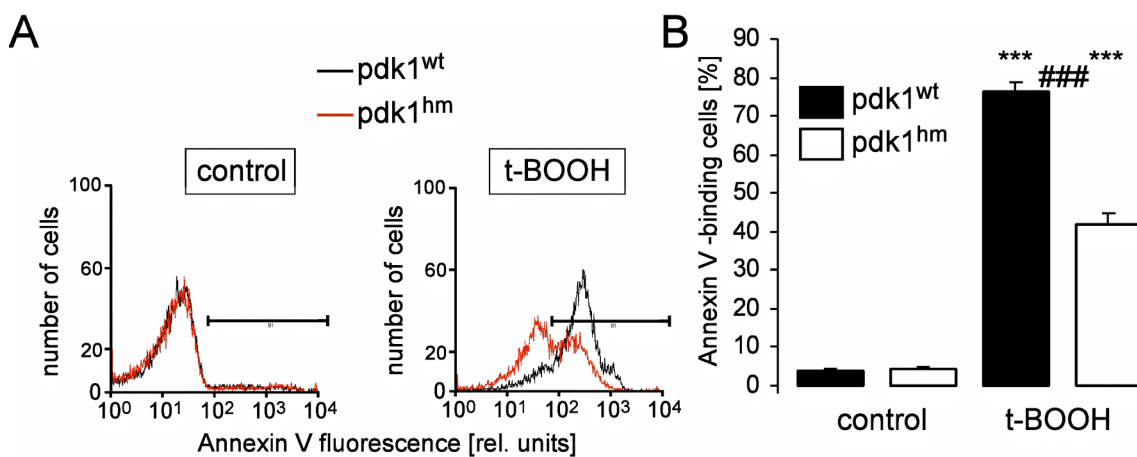


Figure 16. Effect of oxidative stress on annexin V-binding of *pdk1*^{hm} and *pdk1*^{wt} erythrocytes. Annexin V-binding determined by FACS analysis of erythrocytes from PDK1 hypomorphic mice (*pdk1*^{hm}) and their wild type littermates (*pdk1*^{wt}) following a 30 min incubation in the presence or absence of 100 μ M tert-Butyl hydroperoxide (t-BOOH). (A) Original histograms of annexin V-binding. (B) Arithmetic means \pm SEM (n = 12) of the percentage of annexin V-binding of *pdk1*^{hm} (white bars) and *pdk1*^{wt} (black bars) erythrocytes incubated in the absence (control) or presence (t-BOOH) of t-BOOH. *** indicates significant difference ($p < 0.001$) between control and t-BOOH; ### indicates significant difference ($p < 0.001$) between the genotypes.

Another activator of the Ca^{2+} -permeable erythrocyte cation channels is hyperosmotic shock, which similarly increases Ca^{2+} entry, erythrocyte shrinkage, and phospholipid scrambling (Lang *et al.*, 2005a). To explore whether PDK1 deficiency affects the sensitivity of erythrocytes to osmotic shock, *pdk1^{hm}* and *pdk1^{wt}* erythrocytes were exposed to hyperosmotic Ringer (300 mM sucrose added to isotonic Ringer). Hypertonic shock led to the expected decrease of forward scatter in both, *pdk1^{hm}* and *pdk1^{wt}* erythrocytes (Figure 17).

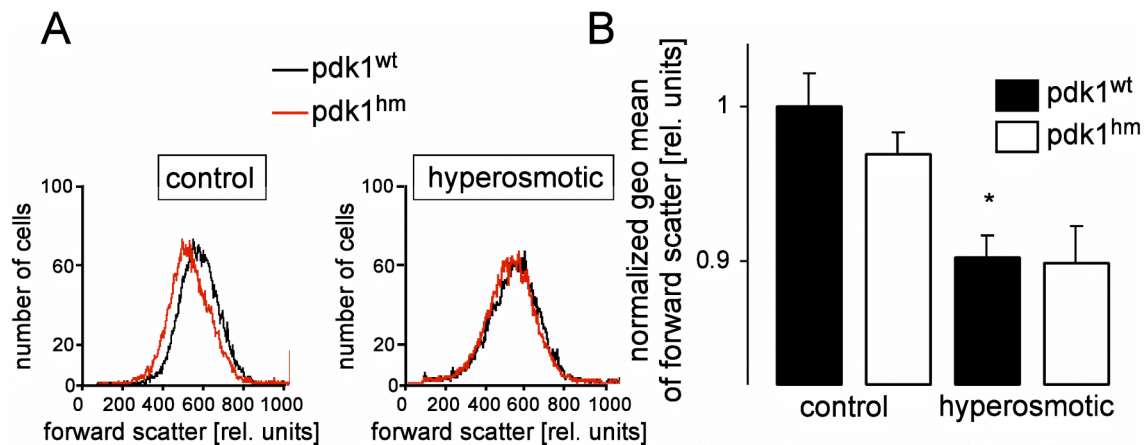


Figure 17. Effect of osmotic shock on forward scatter of *pdk1^{hm}* and *pdk1^{wt}* erythrocytes. Forward scatter determined by FACS analysis of erythrocytes from PDK1 hypomorphic mice (*pdk1^{hm}*) and their wild type littermates (*pdk1^{wt}*) following a 120 min incubation in the presence or absence of additional 300 mM sucrose. (A) Original histograms of forward scatter. (B) Arithmetic means \pm SEM ($n=6$) of forward scatter of *pdk1^{hm}* (white bars) and *pdk1^{wt}* (black bars) erythrocytes incubated in the absence (control) or presence (hyperosmotic) of sucrose. * indicates significant difference ($p < 0.05$) between isotonic and hypertonic fluid.

In hypertonic solution, the forward scatter was similarly low in *pdk1^{hm}* and *pdk1^{wt}* erythrocytes. Osmotic shock further increased annexin V-binding (Figure 18). The increase in annexin V-binding was, however, significantly smaller in *pdk1^{hm}* than in *pdk1^{wt}* erythrocytes.

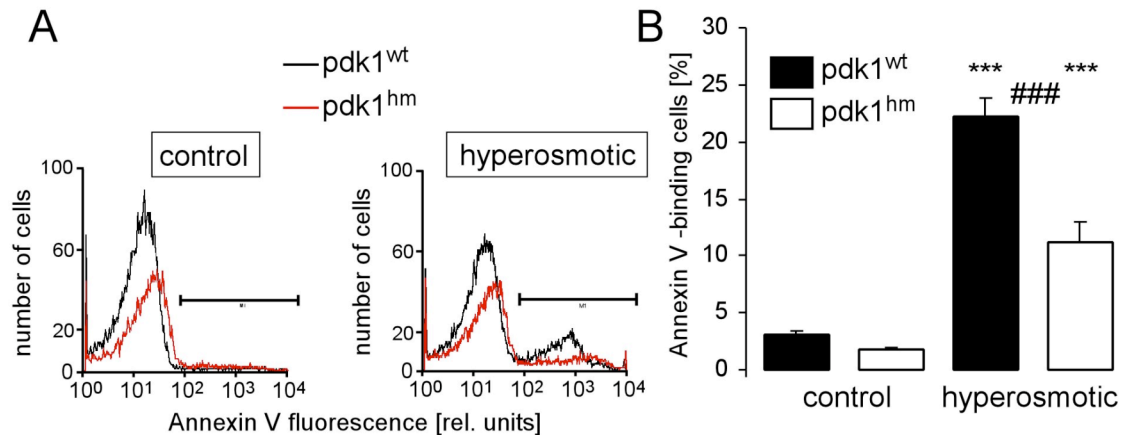


Figure 18. Effect of osmotic shock on annexin V-binding of *pdk1^{hm}* and *pdk1^{wt}* erythrocytes. Annexin V-binding determined by FACS analysis of erythrocytes from PDK1 hypomorphic mice (*pdk1^{hm}*) and their wild type littermates (*pdk1^{wt}*) following a 120 min incubation in the presence or absence of additional 300 mM sucrose. (A) Original histograms of annexin V-binding. (B) Arithmetic means \pm SEM ($n = 10$) of the percentage of annexin V-binding *pdk1^{hm}* (white bars) and *pdk1^{wt}* (black bars) erythrocytes incubated in the absence (control) or presence (hyperosmotic) of sucrose. *** indicates significant difference ($p < 0.001$) between isotonic and hypertonic fluid, ### indicates significant difference ($p < 0.001$) between genotypes.

The Ca^{2+} -permeable erythrocyte cation channels are inhibited by Cl^- and activated by Cl^- removal (Lang *et al.*, 2005a). Accordingly, replacement of extracellular Cl^- with gluconate decreased the forward scatter in both, *pdk1^{hm}* and *pdk1^{wt}* erythrocytes (Figure 19). In the absence of Cl^- , the forward scatter was again similarly low in *pdk1^{hm}* and *pdk1^{wt}* erythrocytes.

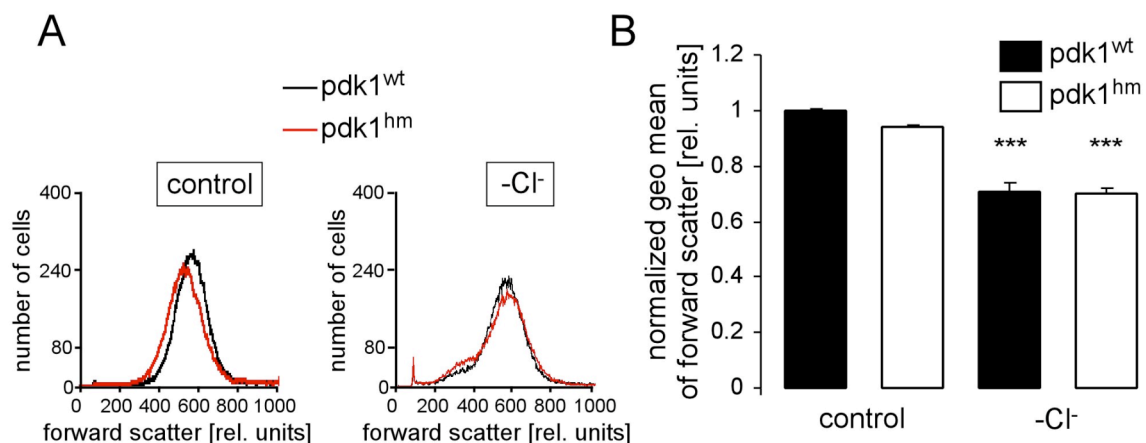


Figure 19. Effect of Cl^- removal on forward scatter of *pdk1^{hm}* and *pdk1^{wt}* erythrocytes. Forward scatter determined by FACS analysis of erythrocytes from PDK1 hypomorphic mice (*pdk1^{hm}*) and their wild type littermates (*pdk1^{wt}*) following a 6 h incubation in the presence or absence of extracellular Cl^- (Cl^- replaced by gluconate). (A) Original histograms of forward scatter. (B) Arithmetic means \pm SEM ($n = 10$) of the forward scatter of *pdk1^{hm}* (white bars) and *pdk1^{wt}* (black bars) erythrocytes incubated in the presence (control) or absence ($-\text{Cl}^-$) of chloride. *** indicates significant difference ($p < 0.001$) between the presence and absence of Cl^- .

Similar to the observations following oxidative stress and osmotic shock, Cl^- removal increased annexin V-binding, an effect significantly smaller in $pdk1^{hm}$ than in $pdk1^{wt}$ erythrocytes (Figure 20).

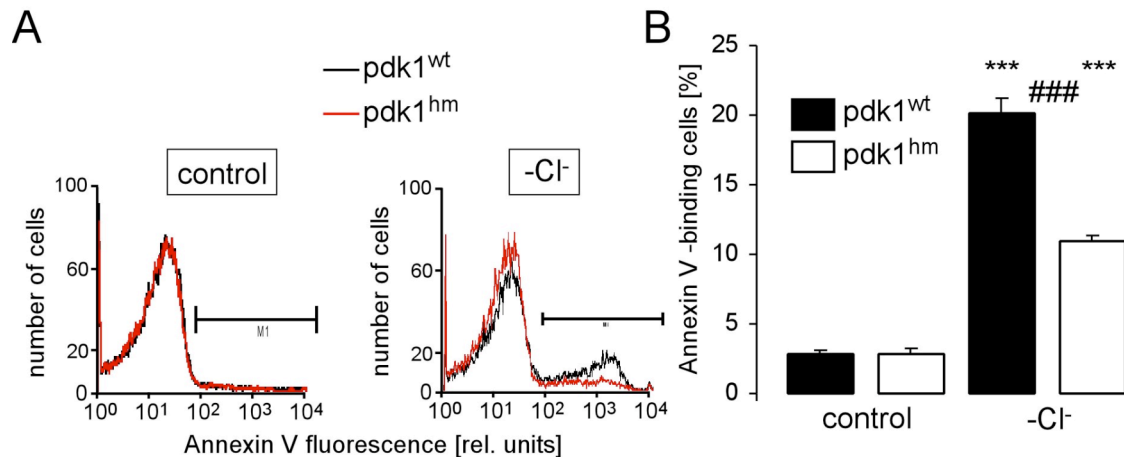


Figure 20. Effect of Cl^- removal on annexin V-binding of $pdk1^{hm}$ and $pdk1^{wt}$ erythrocytes. Annexin V-binding determined by FACS analysis of erythrocytes from PDK1 hypomorphic mice ($pdk1^{hm}$) and their wild type littermates ($pdk1^{wt}$) following a 24 h incubation in the presence or absence of extracellular Cl^- (Cl^- replaced by gluconate). (A) Original histograms of annexin V-binding. (B) Arithmetic means \pm SEM (n = 8) of the percentage of annexin V-binding $pdk1^{hm}$ (white bars) and $pdk1^{wt}$ (black bars) erythrocytes incubated in the presence (control) or absence (- Cl^-) of chloride. *** indicates significant difference ($p < 0.001$) between presence and absence of Cl^- , ### indicates significant difference ($p < 0.001$) between genotypes.

The decreased sensitivity of PDK1-deficient erythrocytes to oxidative stress, osmotic shock, or Cl^- removal could result from decreased Ca^{2+} entry or decreased Ca^{2+} sensitivity of cellular phospholipid scrambling. In order to discriminate between those two possibilities, fluo3 fluorescence was employed as an indicator of intracellular Ca^{2+} activity. As illustrated in Figure 21, fluo3 fluorescence reflecting cytosolic Ca^{2+} activity was significantly lower in $pdk1^{hm}$ than in $pdk1^{wt}$ erythrocytes. Cl^- removal increased fluo3 fluorescence in erythrocytes from both genotypes. In the absence of extracellular Cl^- , fluo3 fluorescence was, however, again significantly lower in $pdk1^{hm}$ than in $pdk1^{wt}$ erythrocytes.

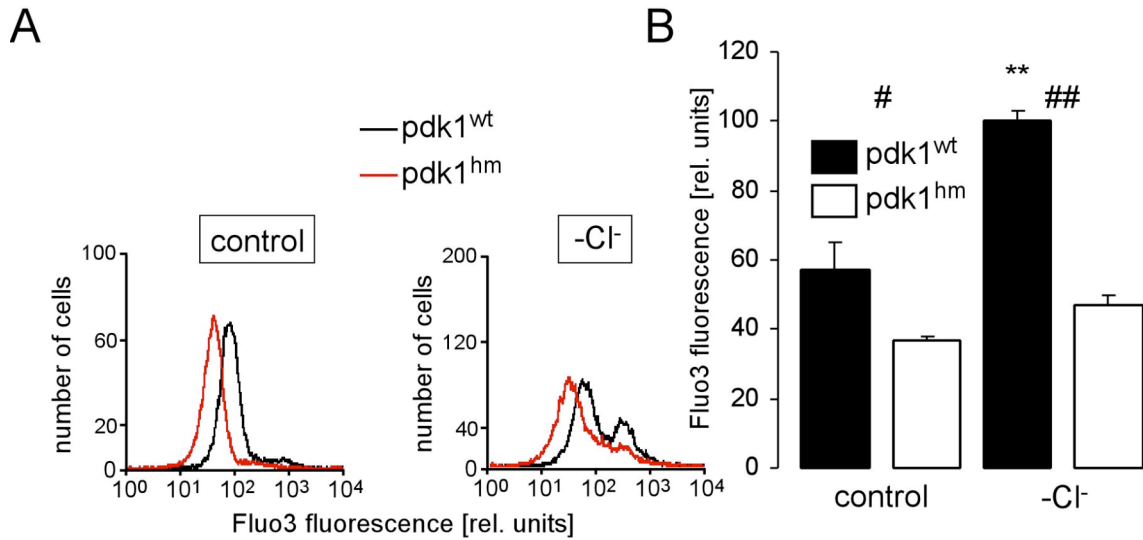


Figure 21. Erythrocyte Ca²⁺ concentration of pdk1^{hm} and pdk1^{wt} erythrocytes, effect of Cl⁻ removal. (A) Ca²⁺-sensitive fluorescence of fluo3-loaded erythrocytes determined by FACS analysis of erythrocytes from PDK1 hypomorphic mice (pdk1^{hm}) and their wild type littermates (pdk1^{wt}) following a 6 h incubation in the presence or absence of extracellular Cl⁻ (Cl⁻ replaced by gluconate). (B) Arithmetic means ± SEM (n = 4-13) of the Ca²⁺-sensitive fluorescence of fluo3-loaded pdk1^{hm} (white bars) and pdk1^{wt} (black bars) erythrocytes incubated in the presence (control) or absence (-Cl⁻) of chloride ** indicates significant difference (p < 0.01) between the presence and absence of Cl⁻, #, ## indicate significant difference (p < 0.05, p < 0.01) between genotypes.

To quantify the intracellular Ca²⁺ concentrations of *pdk1^{hm}* and *pdk1^{wt}* erythrocytes, the dependence of fluo3 fluorescence on the intracellular Ca²⁺ concentration was analysed. To this end, fluo3 fluorescence of erythrocytes in solutions of defined free Ca²⁺ concentrations was measured after exposure to the Ca²⁺ ionophore ionomycin adjusting the intracellular Ca²⁺ concentrations to the levels of the respective solutions (data not shown). By graphical deduction from the linear fits (*pdk1^{hm}*: R² = 0.98; *pdk1^{wt}*: R² = 0.98) of the graphs illustrating the dependence of fluo3 fluorescence on intracellular Ca²⁺ concentration, the intracellular Ca²⁺ concentrations of *pdk1^{hm}* and *pdk1^{wt}* erythrocytes were estimated to be approximately 29 nM (*pdk1^{hm}*; n=4) and 54 nM (*pdk1^{wt}*; n=4) after 6 hours of incubation in Ringer solution at 37°C.

If the decreased sensitivity of PDK1-deficient erythrocytes to oxidative stress, osmotic shock, and Cl⁻ removal was exclusively due to blunted Ca²⁺ entry, then treatment with the Ca²⁺ ionophore ionomycin should have similar effects on forward scatter and phosphatidylserine exposure. To explore whether PDK1 deficiency affects the sensitivity of erythrocytes to enhanced cytosolic Ca²⁺ activity, *pdk1^{hm}* and *pdk1^{wt}* erythrocytes were exposed to 1 μM ionomycin for 30 min. As illustrated in Figure 22, ionomycin decreased forward scatter in both, *pdk1^{hm}* and *pdk1^{wt}* erythrocytes to a similar extent.

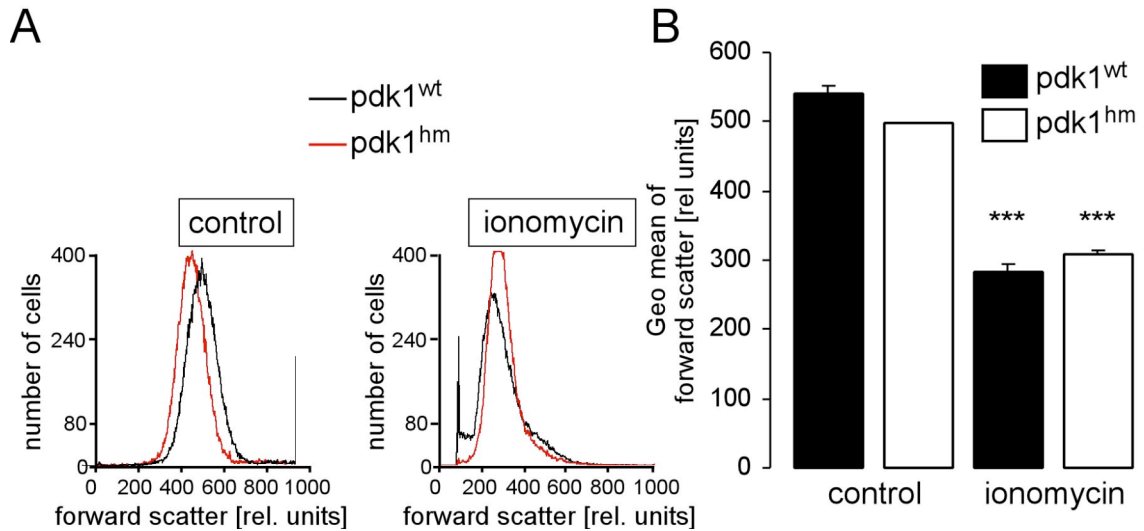


Figure 22. Effect of the Ca²⁺ ionophore ionomycin on forward scatter of pdk1^{hm} and pdk1^{wt} erythrocytes. Forward scatter determined by FACS analysis of erythrocytes from PDK1 hypomorphic mice (pdk1^{hm}) and their wild type littermates (pdk1^{wt}) following a 30 minute incubation in the absence and presence of 1 μ M Ca²⁺ ionophore ionomycin. (A) Original histograms of forward scatter. (B) Arithmetic means \pm SEM (n = 3-9) of forward scatter of pdk1^{hm} (white bars) and pdk1^{wt} (black bars) erythrocytes incubated in the absence (control) or presence (ionomycin) of ionomycin. *** indicates significant difference (p < 0.001) between control and ionomycin treatment.

Most importantly, ionomycin increased the percentage of annexin V-binding erythrocytes in both genotypes to the same levels (Figure 23). Thus, Ca²⁺ sensitivity of erythrocyte phospholipids scrambling is not different in pdk1^{hm} and pdk1^{wt} erythrocytes.

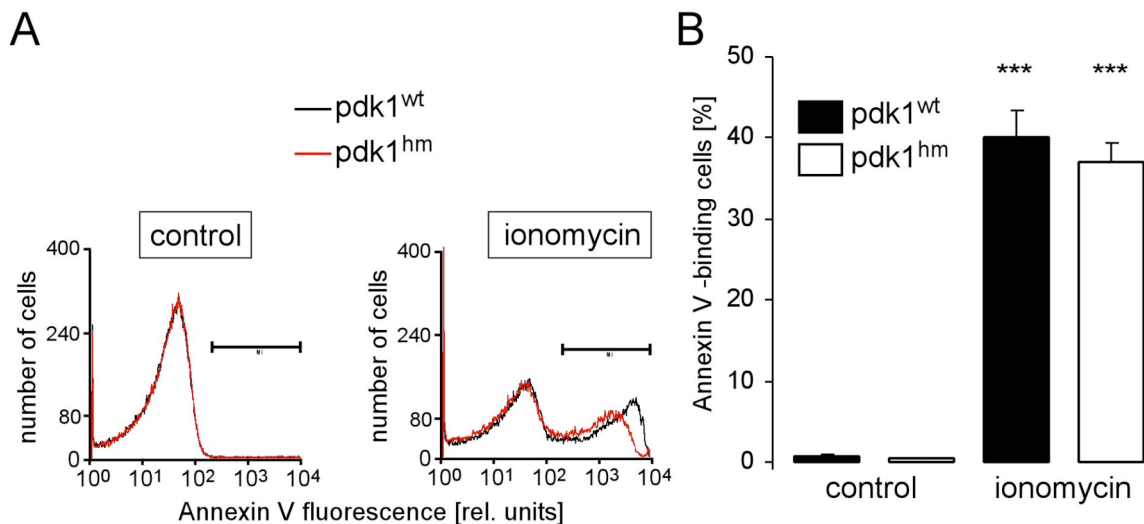


Figure 23. Effect of the Ca²⁺ ionophore ionomycin on annexin V-binding of pdk1^{hm} and pdk1^{wt} erythrocytes. Annexin V-binding determined by FACS analysis of erythrocytes from PDK1 hypomorphic mice (pdk1^{hm}) and their wild type littermates (pdk1^{wt}) following a 30 minute incubation in the absence and presence of 1 μ M Ca²⁺-ionophore ionomycin (Ionomycin). (A) Original histograms of annexin V-binding. (B) Arithmetic means \pm SEM (n = 3-8) of the percentage of annexin V-binding pdk1^{hm} (white bars) and pdk1^{wt} (black bars) erythrocytes incubated in the absence (control) or presence (ionomycin) of ionomycin. *** indicates significant difference (p < 0.001) between control and ionomycin treatment.

Additional experiments were performed to explore the *in vivo* significance of the reduced susceptibility of *pdk1^{hm}* erythrocytes to triggers of eryptosis. To this end, erythrocytes were drawn and labeled with CFSE and subsequently reinjected into the mice. As illustrated in Figure 24, the clearance of labeled erythrocytes was significantly enhanced by treatment with 0.4 mM tBOOH for 30 minutes. A comparison between *pdk1^{hm}* and *pdk1^{wt}* erythrocytes revealed that partial lack of PDK1 significantly blunted the clearance of oxidized erythrocytes.

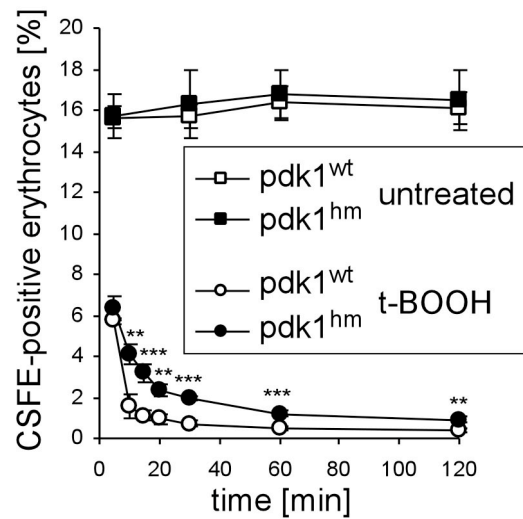


Figure 24. Clearance of erythrocytes from *pdk1^{hm}* and *pdk1^{wt}* mice. Time-dependent decay of CFSE-labeled circulating erythrocytes originally taken from PDK1 hypomorphic mice (*pdk1^{hm}*, closed symbols) and their wild type littermates (*pdk1^{wt}*, open symbols) and reinjected into the same mouse. The erythrocytes were left untreated (squares) or treated for 30 minutes with 0.4 mM tBOOH (circles). The percentage of CFSE-labeled cells is plotted against time after injection. Values are arithmetic means \pm SEM (n=5-10). **, *** indicate significant difference between genotypes in case of oxidized erythrocytes (p < 0.01, p < 0.001).

4.4 Bacterial peptidoglycan induces cell death of erythrocytes

Phosphatidylserine exposure at the surface of erythrocytes was determined from binding of fluorescent annexin V. As demonstrated by fluorescence microscopy, erythrocytes bathed in Ringer solution did not expose appreciable amounts of annexin V at their surface (Figure 25B). In contrast, treatment with *S. aureus* soluble PGN (100 $\mu\text{g/ml}$ for 48 hours) increased annexin V-binding of otherwise intact erythrocytes thus pointing to stimulation of phosphatidylserine exposure (Figure 25B).

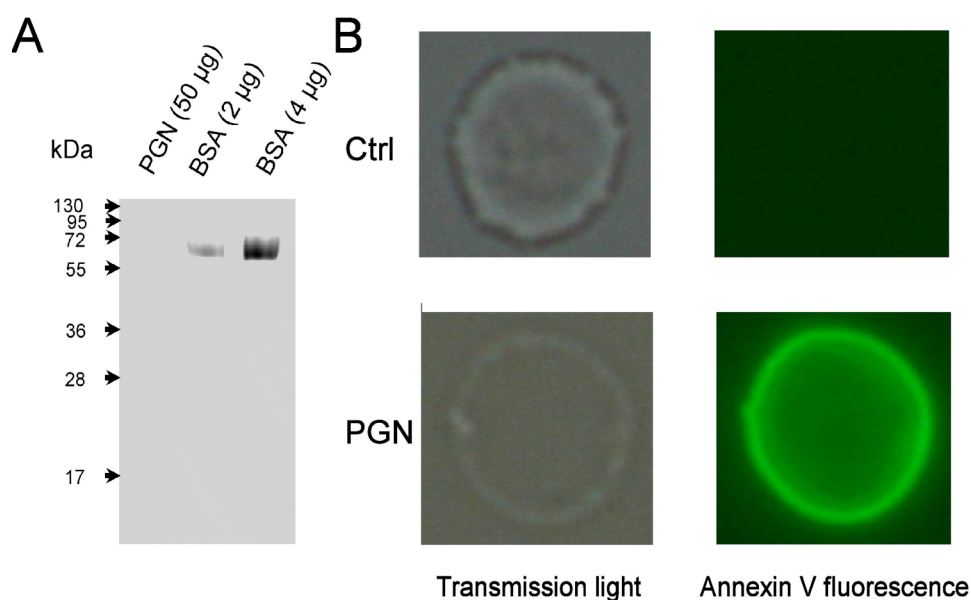


Figure 25. Purity of soluble peptidoglycans. Light transmission and fluorescence microphotographs of erythrocytes exposed to peptidoglycans. (A) Soluble peptidoglycan (PGN) was used in this study. 1 μg of the preparation was loaded on a 10% SDS-PAGE and subsequently stained with Coomassie Blue to examine for purity of the sample used. (B) The left panels depict transmission microphotographs and the right panels show fluorescence microphotographs of erythrocytes stained with fluorescent annexin V. Prior to microscopy, the erythrocytes were exposed for 48 h to Ringer (upper panels), or for 48 h to 100 $\mu\text{g/ml}$ PGN in Ringer solution (lower panels).

After 48 hours of incubation at 37°C, no appreciable rate of hemolysis was determined. More importantly, the rate of hemolysis did not differ between samples of erythrocytes treated without or with PGN at concentrations of 50 $\mu\text{g/ml}$ or 100 $\mu\text{g/ml}$ (data not shown).

FACS analysis was subsequently performed to quantify annexin V-binding following PGN treatment. Incubation of erythrocytes in Ringer solution for 48 hours

(control) resulted in an average percentage of annexin V-exposing erythrocytes of $7.4 \pm 1.0\%$ ($n = 16$). The addition of soluble PGN from *S. aureus* at concentrations of $50 \mu\text{g/ml}$ and $100 \mu\text{g/ml}$ significantly increased the percentage of annexin V-binding cells to $25.2 \pm 2.3\%$ ($n = 12$) and $48.0 \pm 2.6\%$ ($n = 16$), respectively (Figure 26A,B). Since the control values were dependent on the erythrocytes used, annexin V-binding of erythrocytes exposed to $5 \mu\text{g/ml}$ PGN was normalized to the respective control values in addition. As illustrated in Figure 26C, upon normalisation, the increase in the percentage of annexin V-binding erythrocytes reached statistical significance even at exposure to $5 \mu\text{g/ml}$ PGN. The results revealed that peptidoglycan led to breakdown of phosphatidylserine asymmetry of the erythrocyte cell membrane.

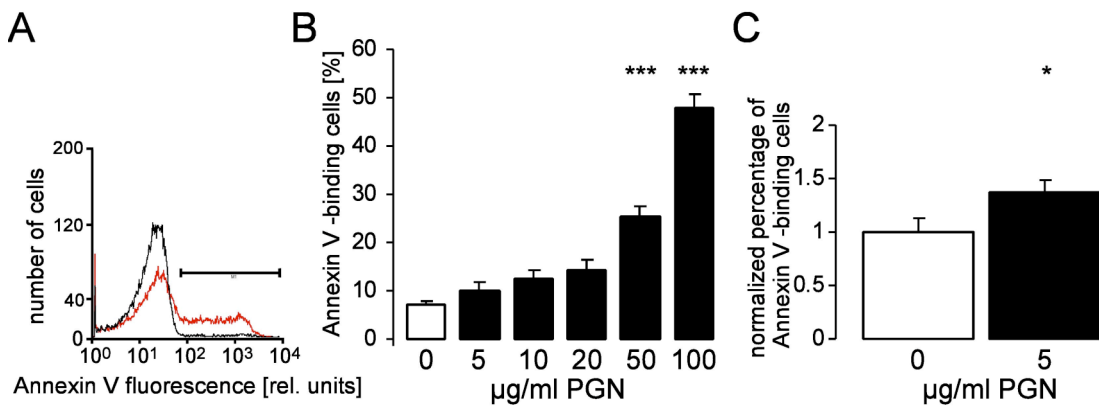


Figure 26. Stimulation of phosphatidylserine exposure by peptidoglycans. (A) Histogram of annexin V-binding in a representative experiment of erythrocytes from healthy volunteers exposed for 48 hours to Ringer solution without (black line) or with $50 \mu\text{g/ml}$ pure soluble peptidoglycan (red line). (B) Dose dependence of the peptidoglycan effect on phosphatidylserine exposure. Arithmetic means \pm SEM ($n = 8-16$) of the percentage of annexin V-binding erythrocytes exposed for 48 hours to Ringer solution without (white bar) or with (black bars) peptidoglycan at the indicated concentrations. *** ($p < 0.001$) indicates significant difference from values in control Ringer solution (ANOVA). (C) Arithmetic means \pm SEM ($n = 8$) of the normalized percentage of annexin V-binding erythrocytes exposed for 48 hours to Ringer solution without (white bar) or with (black bar) $5 \mu\text{g/ml}$ peptidoglycan. * ($p < 0.05$) indicates significant difference from values in control Ringer solution (t-test).

To test for specificity of the effect of soluble PGN, erythrocytes were exposed to muramyl dipeptide (MDP), a component of PGN, and lipopolysaccharides (LPS), the major endotoxin of gram-negative bacteria, for 48 hours. Subsequently, annexin V-binding of these erythrocytes was determined. As shown in Figure 27A,B, neither MDP nor LPS significantly influenced erythrocyte annexin V-binding pointing to a PGN-specific process.

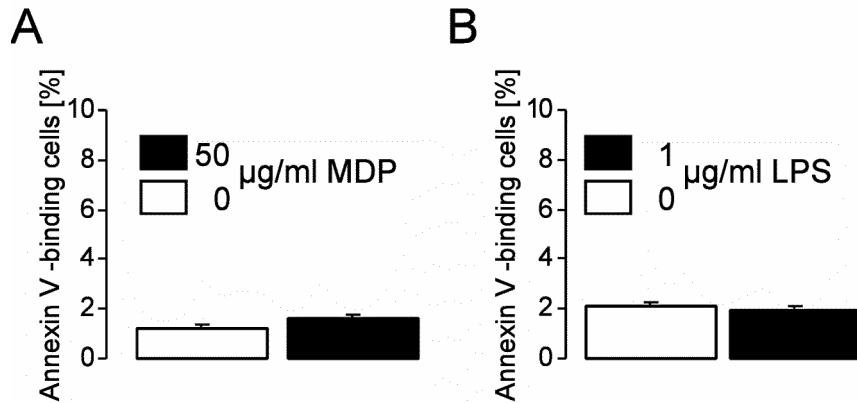


Figure 27. Effects of muramyl dipeptide (MDP) and lipopolysaccharide (LPS) on erythrocyte phosphatidylserine exposure. (A) Arithmetic means \pm SEM ($n = 8$) of the percentage of annexin V-binding erythrocytes exposed for 48 hours to Ringer solution without (white bar) or with (black bar) 50 $\mu\text{g/ml}$ MDP (B) Arithmetic means \pm SEM ($n = 4$) of the percentage of annexin V-binding erythrocytes exposed for 48 hours to Ringer solution without (white bar) or with (black bar) 1 $\mu\text{g/ml}$ LPS.

A further hallmark of eryptosis is cell shrinkage (Lang *et al.*, 2003b), which is reflected by a decrease of the forward scatter in FACS analysis. Thus, the effect of PGN on erythrocyte forward scatter was determined. Incubation of erythrocytes in Ringer solution containing PGN for 48 hours resulted in a significant decrease of the forward scatter (Figure 28A,B). Thus, peptidoglycan decreased erythrocyte volume.

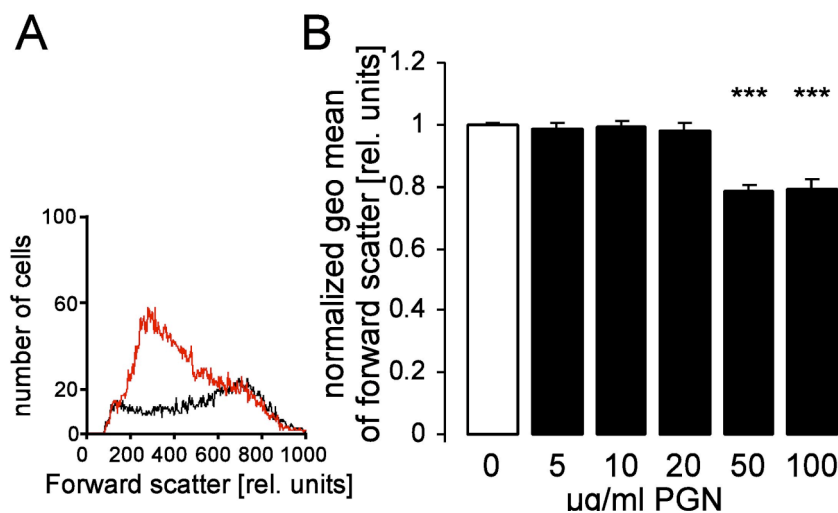


Figure 28. Effects of peptidoglycans on erythrocyte forward scatter. (A) Histogram of forward scatter in a representative experiment of erythrocytes from healthy volunteers exposed for 48 hours to Ringer solution without (black line) or with 50 $\mu\text{g/ml}$ pure soluble peptidoglycan (red line). (B) Dose dependence of the peptidoglycan effect on forward scatter. Arithmetic means \pm SEM ($n = 7-12$) of the normalized forward scatter of erythrocytes exposed for 48 hours to Ringer solution without (white bar) or with (black bars) peptidoglycan at the indicated concentrations. *** ($p < 0.001$) indicates significant difference from values in control Ringer solution (ANOVA).

Additional experiments were performed to elucidate the underlying mechanisms. Both, phosphatidylserine scrambling and cell shrinkage could be triggered by an increase in the cytosolic Ca^{2+} concentration (Lang *et al.*, 2003b). Thus, fluo3 fluorescence was employed to determine whether PGN affected cytosolic Ca^{2+} activity in erythrocytes. As illustrated in Figure 29, PGN indeed increased fluo3 fluorescence pointing to an increase in the cytosolic Ca^{2+} concentration. As a positive control, the samples were incubated for 2 minutes with the Ca^{2+} ionophore ionomycin (1 μM). Exposure to ionomycin led to the expected increase in fluo3 fluorescence to similar values in the absence and presence of 50 $\mu\text{g/ml}$ PGN (Figure 29A, right panel).

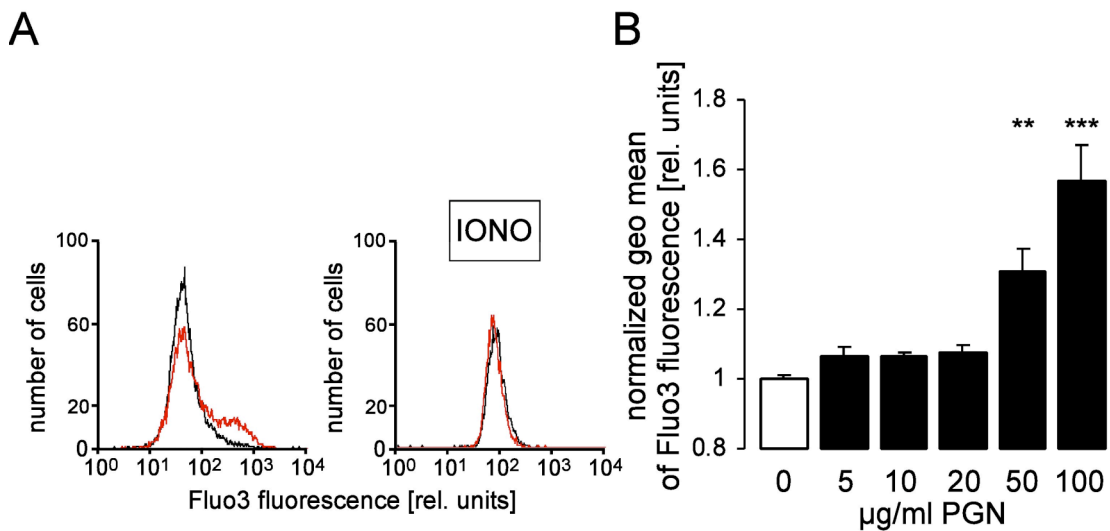


Figure 29. Effects of peptidoglycans on cytosolic Ca^{2+} activity. (A) Histogram of fluo3 fluorescence in a representative experiment of erythrocytes from healthy volunteers exposed for 48 hours to Ringer solution without (black line) or with 50 $\mu\text{g/ml}$ pure soluble peptidoglycan (red line; left panel). As a positive control, the erythrocytes were exposed subsequently to 1 μM ionomycin for 2 min (IONO, right panel). (B) Dose dependence of the peptidoglycan effect on fluo3 fluorescence. Arithmetic means \pm SEM ($n = 9-15$) of the normalized fluo3 fluorescence of erythrocytes exposed for 48 hours to Ringer solution without (white bar) or with (black bars) peptidoglycan at the indicated concentrations. ** ($p < 0.01$), *** ($p < 0.001$) indicate significant difference from values in control Ringer solution (ANOVA).

To determine the significance of cytosolic Ca^{2+} for the increase in phospholipid scrambling, experiments were performed in the presence and absence of extracellular Ca^{2+} . Removal of extracellular Ca^{2+} indeed significantly blunted the stimulation of annexin V-binding (Figure 30).

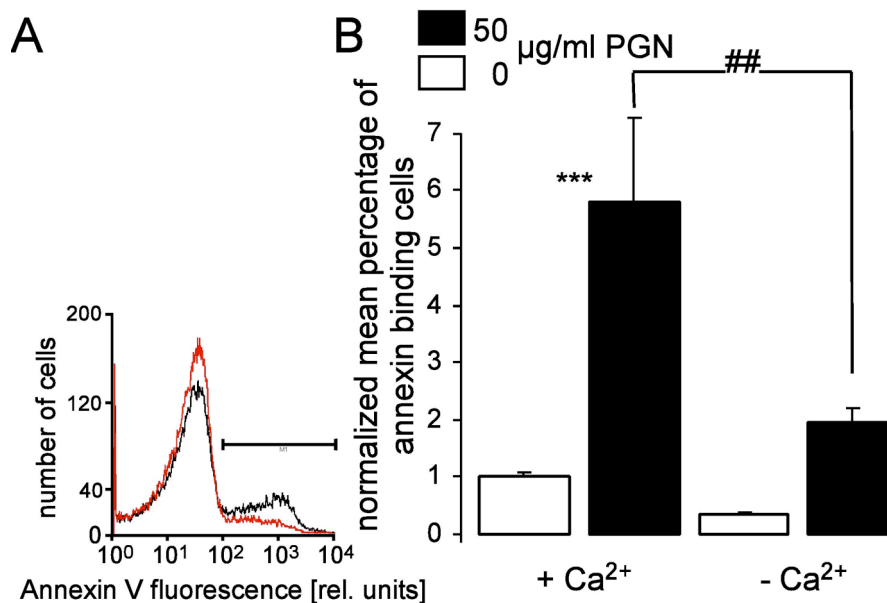


Figure 30. Role of Ca²⁺ in the stimulation of phosphatidylserine exposure by peptidoglycans. (A) Histogram of annexin V-binding in a representative experiment of erythrocytes from healthy volunteers exposed for 48 hours to 50 µg/ml peptidoglycan in Ringer solution in the absence (red line) and presence (black line) of 1 mM Ca²⁺. (B) Arithmetic means ± SEM (n = 8-12) of the normalized percentage of annexin V-binding erythrocytes exposed for 48 hours to 0 µg/ml (white bars) or 50 µg/ml (black bars) peptidoglycan in Ringer solution in the presence (left bars) and absence (right bars) of Ca²⁺ in extracellular fluid. *** (p < 0.001) indicates significant difference from values in control Ringer solution, ## (p < 0.01) indicates significant difference from respective values in the presence of Ca²⁺ (ANOVA).

Nevertheless, annexin V-binding tended to be slightly enhanced following exposure to 50 µg/ml PGN even in the absence of extracellular Ca²⁺. Thus, Ca²⁺ entry largely but not fully accounted for the stimulation of phospholipid scrambling following exposure to PGN.

Phospholipid scrambling is further stimulated by ceramide (Lang *et al.*, 2004a). Therefore, additional experiments were performed to elucidate the effect of PGN on ceramide formation. As illustrated in Figure 31A,B, a 48 hours exposure to 50 µg/ml PGN led to a slight but significant increase in ceramide formation. Thus, ceramide may contribute to the stimulation of phospholipid scrambling by PGN.

In a further series of experiments, ATP concentrations were determined to explore, whether PGN affects the energy status of the erythrocytes. As illustrated in Figure 31C, 100 µg/ml PGN within 48 h indeed significantly decreased the ATP content of the erythrocytes.

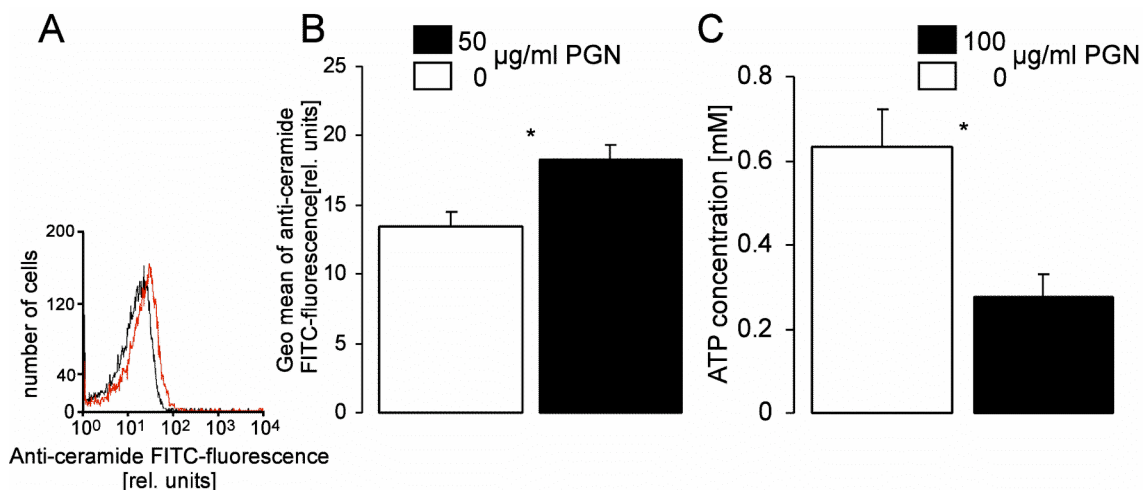


Figure 31. Stimulation of ceramide formation and lowering of the erythrocyte ATP concentration by peptidoglycans. (A) Histogram of ceramide abundance in a representative experiment of erythrocytes from healthy volunteers exposed for 48 hours to Ringer solution without (black line) or with (red line) 50 μg/ml peptidoglycan. (B) Arithmetic means ± SEM (n = 4) of ceramide abundance in erythrocytes exposed for 48 hours to Ringer solution without (white bar) or with 50 μg/ml (black bar) peptidoglycan. * (p < 0.05) indicates significant difference from values in control Ringer solution (t-test). (C) Arithmetic means ± SEM (n = 4) of the ATP concentration in erythrocytes from healthy volunteers incubated for 48 h in Ringer solution without (open bar) or with 100 μg/ml peptidoglycan (closed bar). * (p < 0.05) indicates significant difference from values in control Ringer solution (t-test).

Additional experiments were performed to elucidate the *in vivo* significance of PGN-induced eryptosis. To this end, erythrocytes were drawn, labeled with the fluorescent dye CFSE, and subsequently reinjected into the mice. As illustrated in Figure 32, the disappearance of labeled erythrocytes was significantly more rapid following treatment with 100 μg/ml PGN for 24 hours compared to nontreated erythrocytes. Therefore, exposure to PGN accelerates the clearance of erythrocytes from circulating blood *in vivo*.

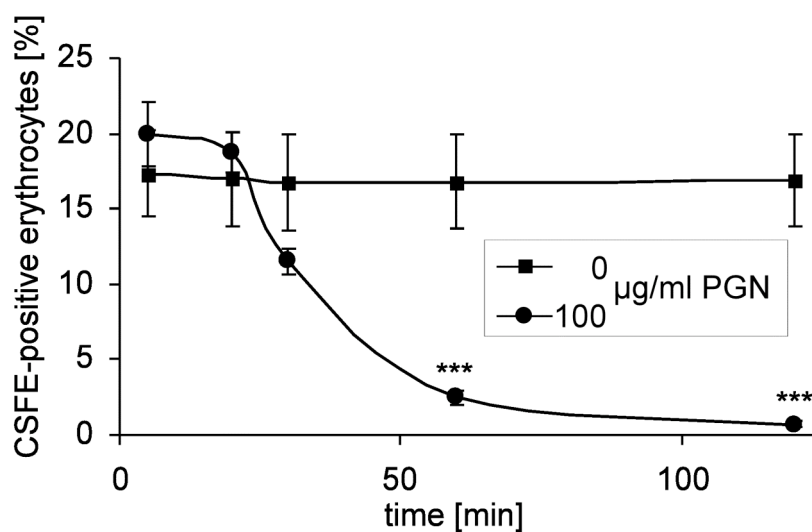


Figure 32. Clearance of erythrocytes treated with peptidoglycans. Time-dependent decay of CFSE-labeled circulating erythrocytes originally taken from wildtype mice and reinjected into the same mouse. Before injection, the erythrocytes had been incubated for 24 hours in the absence (squares) or presence of 100 µg/ml peptidoglycan (circles). The percentage of CFSE-labeled cells is plotted against time after injection. Values are arithmetic means ± SEM (n=4). *** (P < 0.001) indicates significant difference from values in control Ringer solution (t-test).

5 Discussion

5.1 Investigation of the impact of the Gardos channel on survival of erythrocytes

The present study demonstrates that $K_{Ca3.1}$ represents the Gardos channel in murine erythrocytes. Since $K_{Ca3.1}$ -deficient erythrocytes lacked Ca^{2+} -activated K^+ channel activity and erythrocyte shrinkage, $K_{Ca3.1}$ seems to be the only Ca^{2+} -activated K^+ channel type in murine erythrocytes. This is consistent with a previous study demonstrating almost absent Ca^{2+} -stimulated clotrimazole-sensitive ^{86}Rb uptake by erythrocytes from $K_{Ca3.1}$ -deficient mice (Begenisich *et al.*, 2004). Similarly, human reticulocytes as well as those differentiated *in vitro* from erythroid progenitor cells contain $K_{Ca3.1}$ mRNA, but not the mRNA of small conductance Ca^{2+} -activated K^+ channels (Hoffman *et al.*, 2003). Ca^{2+} -permeabilized human erythrocytes reportedly exhibit a mean open probability of the Gardos channel of $nPo = 3$ (Lew *et al.*, 2005). In the present study, nPo of the Gardos channel in Ca^{2+} -permeabilized mouse erythrocytes was highly variable between individual cells. On average, however, nPo was very similar to that reported in human erythrocytes suggesting similar Gardos channel expression in human and mouse erythrocytes.

The present observations further reveal that blood parameters do not differ between wildtype and $K_{Ca3.1}^{-/-}$ mice. Since $K_{Ca3.1}$ -deficient erythrocytes apparently do not up-regulate other Ca^{2+} -activated K^+ channel types, this observation strongly suggests that under unstressed conditions mature murine erythrocytes do not require Gardos K^+ channel activity. Mature erythrocytes of other species such as sheep or donkey even completely lack Ca^{2+} -activated K^+ channels (Brown *et al.*, 1978) indicating that function of mature mammalian erythrocytes does not depend on Gardos channel activity.

Mature human erythrocytes maintain high intracellular K^+ concentrations. Unlike many nucleated cells, the membrane potential of un-stimulated human erythrocytes, however, is not close to the electrochemical equilibrium of K^+ . Instead, it ranges between -5 mV and -8 mV (Hoffman & Laris, 1974). In contrast to human erythrocytes, sheep erythrocytes owing the L-antigen have low (15 mM) K^+ and high

Na⁺ (84 mM) concentrations (Dunham & Blostein, 1997). Taken together, this suggests that high chemical gradients across the erythrocyte membrane are not required for mature erythrocyte function and survival. Why do then human erythrocytes afford the costly luxury of maintaining high intracellular K⁺ concentrations throughout most of their 120 days of life (only a very small fraction of human erythrocytes belonging to the oldest population has low cytosolic K⁺ concentrations (Lew *et al.*, 2007))? One possibility is that the Gardos effect confers some protection against hemolysis and subsequent release of hemoglobin into the extracellular fluid leading to organ damage. Such a protection has been demonstrated against spherocytosis-associated hemolytic anemia in protein 4.1R-, 4.2-, or band 3-deficient mice (de Franceschi *et al.*, 2005).

The present study suggests a further protective role of the Gardos effect, namely against blood infections with hemolytic bacteria. *S. aureus* is one of the most common causes of bacterial infections in humans, producing a broad spectrum of diseases. Among those are life-threatening septicemias. α -toxin from *S. aureus* belongs to the cytolytins which similarly to hemolysins of other bacteria perforate the plasma membrane of erythrocytes and other cells. It is widely used as biological tool to study the controlled permeabilization of cell membranes due to advantages over most other permeabilizing agents (Grant *et al.*, 1987; de Franceschi *et al.*, 2005; Bhakdi & Tranum-Jensen, 1991; Bader *et al.*, 1986). Besides its valuable role *in vitro*, α -toxin is known to be a major pathogenetic factor during *S. aureus* infections (Bhakdi & Tranum-Jensen, 1991). In intraperitoneal abscesses of mice infected with *S. aureus*, a hemolytic activity of about 100 to 1,000 HU/ml of α -toxin was determined (Kapral *et al.*, 1980). Target cells vary in their susceptibility to α -toxin (Bhakdi & Tranum-Jensen, 1991). Particularly highly sensitive to α -toxin are rabbit erythrocytes while human erythrocytes are less susceptible. Murine erythrocytes have intermediate sensitivity towards α -toxin (Bhakdi & Tranum-Jensen, 1991). Since effects of α -toxin observed at concentrations below 50 HU/ml are considered to be due to high-affinity binding sites on target cells (Bhakdi & Tranum-Jensen, 1991), the concentrations applied in this study (10 HU/ml) are well in the range to have *in vivo* relevance.

Cells permeabilized by α -toxin swell and lyse colloid osmotically (Bhakdi & Tranum-Jensen, 1991). In the present study, α -toxin-treated K_{Ca}3.1^{-/-} mice showed typical features of acute renal failure, a frequent complication of septicemias, while

wildtype mice did not. Because of the hemolytic activity of α -toxin it is suggestive that glomerularly filtrated hemoglobin caused a form of acute renal failure in $K_{Ca3.1}^{-/-}$ mice by precipitating within the acid lumen of the renal tubular system (Sillix & McDonald, 1987).

The Gardos effect transiently delays hemolysis of α -toxin-perforated erythrocytes as evident from *in vitro* hemolysis (Figure 5) of the present study. Moreover, Gardos K^+ channel-mediated hyperpolarization of the erythrocyte membrane increases the intracellularly directed driving force for Ca^{2+} . In parallel, increased intracellular cytosolic $[Ca^{2+}]_i$ (Lew *et al.*, 2007) and erythrocyte shrinkage (Huber *et al.*, 2001; Lang *et al.*, 2003a) reportedly increase the cation conductance of the erythrocyte membrane resulting in an elevated Ca^{2+} leak and elevated $[Ca^{2+}]_i$. In the present study, oxidized wildtype erythrocytes indeed exhibited a higher $[Ca^{2+}]_i$ than $K_{Ca3.1}^{-/-}$ erythrocytes (Figure 4). Elevated $[Ca^{2+}]_i$ together with erythrocyte shrinkage stimulate break-down of the phospholipid asymmetry and exposure of phosphatidylserine exposure at the erythrocyte surface (Lang *et al.*, 2006c). The functional significance of the Gardos effect for this process is clearly shown by almost absent phosphatidylserine exposure in oxidized $K_{Ca3.1}^{-/-}$ erythrocytes (Figure 4). Phosphatidylserine exposure has been demonstrated to be an “eat-me” signal and to foster recognition and clearance of injured erythrocytes by macrophages (Tanaka & Schroit, 1983; Schroit *et al.*, 1985; Bratosin *et al.*, 2001; Boas *et al.*, 1998). Therefore, the present results strongly suggest that Gardos-mediated short extension of erythrocyte survival in concert with Gardos-dependent exposure of phosphatidylserine facilitated the *in vivo* clearance of α -toxin-perforated erythrocytes prior to their hemolysis.

Activation of the Gardos channel is detrimental in sickle cell disease (Lew & Bookchin, 2005) or beta thalassemia (de Franceschi *et al.*, 1996) where it promotes erythrocyte deformation and limits erythrocyte survival, respectively. However, activation of the Gardos channel may be advantageous in several conditions affecting the integrity of erythrocytes, such as Hemolytic Uremic Syndrome (Lang *et al.*, 2006b), sepsis (Kempe *et al.*, 2007) and exposure to hemolysin (Lang *et al.*, 2004b), listeriolysin (Foller *et al.*, 2007b), lead (Kempe *et al.*, 2005) or certain drugs such as paclitaxel (Lang *et al.*, 2006c), or cyclosporine (Niemoeller *et al.*, 2006b). Most importantly, in view of the high incidence and mortality of septicemias (Sessler *et al.*, 2004) and their

frequently occurring complication of acute renal failure, advantages appear to prevail the disadvantages of Gardos channel expression in human erythrocytes.

In conclusion, $K_{Ca3.1}$ is expressed in murine erythrocytes and mediates Ca^{2+} -stimulated shrinkage and phosphatidylserine exposure. In normal un-stressed erythrocyte life, $K_{Ca3.1}$ remains inactive. Under pathophysiological conditions, however, $K_{Ca3.1}$ activity delays hemolysis and promotes recognition and clearance of the dying erythrocyte.

5.2 Regulation of erythrocyte survival by cGKI signaling

The experiments on the cGKI-deficient mouse model reveal that lack of functional cGKI results in anemia and splenomegaly. Most likely, the anemia is not due to impaired formation but rather due to shortened survival of erythrocytes. Increased levels of plasma erythropoietin and reticulocytes indicate that erythropoiesis is indeed activated in cGKI-deficient mice, but eventually cannot compensate for the loss of erythrocytes resulting in anemia. Ter119⁺ erythroid cells with an increased level of PS-exposure accumulate in the spleens of the mutant animals explaining the enlarged spleens and supporting a role of cGKI signaling in erythrocyte survival. Indeed, cGKI-deficient erythrocytes show a decreased survival both *in vitro* and *in vivo*. Mechanistically, the decreased survival of cGKI-deficient erythrocytes might result from an increased intracellular Ca^{2+} concentration triggering the exposure of PS at the erythrocyte surface followed by engulfment by splenic macrophages.

The cytosolic Ca^{2+} concentration is higher in circulating erythrocytes from cGKI-deficient mice as compared to control mice. It is well known that the NO/cGMP/cGKI pathway inhibits agonist-induced increases in cytosolic Ca^{2+} in vascular smooth muscle cells (Pfeifer *et al.*, 1998; Feil *et al.*, 2002). Many studies have suggested that this pathway decreases the cytosolic Ca^{2+} concentration also in a variety of other cell types and that the Ca^{2+} -lowering effect might, at least in part, be due to inhibition of Ca^{2+} entry through Ca^{2+} -permeable channels (Ay *et al.*, 2006; Kwan *et al.*, 2006; Gomes *et al.*, 2006) or stimulation of the Ca^{2+} -ATPase (Dedkova & Blatter, 2002; Rashatwar *et al.*, 1987). In line with their increased cytosolic Ca^{2+} concentration, a

well-known trigger of phospholipid scrambling (Lang *et al.*, 2003b), cGKI-deficient erythrocytes show increased surface exposure of PS, a hallmark of eryptosis (Woon *et al.*, 1999; Bratosin *et al.*, 2001). The exposure of PS at the erythrocyte surface mediates binding to PS receptors of macrophages (Fadok *et al.*, 2000) followed by engulfment (Boas *et al.*, 1998) and clearance from circulating blood (Kempe *et al.*, 2007). Indeed, cGKI-deficient erythrocytes disappear faster from the circulation than control erythrocytes. The mechanical properties of cGKI-deficient erythrocytes are not affected adversely and, therefore, can not contribute to their accumulation in the spleen.

Erythrocytes from cGKI knockout animals are more rapidly cleared from circulating blood than erythrocytes from control mice following injection into either knockout or control animals. These results disclose that the anemia is at least in part due to a property of knockout erythrocytes. The accelerated death of the erythrocytes presumably leads to enlargement of the spleen, which in turn is expected to enhance the sequestration of circulating erythrocytes. Accordingly, erythrocytes from both knockout and control animals are more rapidly cleared after injection into knockout animals than into control animals. It is important to note that anemia is observed in cGKI mutant mice prior to development of splenomegaly (Figure 14). Thus, anemia cannot be explained by splenomegaly alone, even though it presumably contributes to anemia in older animals. Beyond enhanced susceptibility to eryptosis and splenomegaly, vitamin B12 insufficiency could also contribute to the development of anemia in conventional cGKI ko mice. Their vitamin B12 deficiency most likely results from deranged intestinal motility and contributes to their increased erythrocyte volume. Interestingly, the cGKI SM rescue mice do also develop anemia and splenomegaly, but have normal vitamin B12 levels and only slightly increased cell volumes, which could result from decreased activation of KCl symport in the absence of cGKI. KCl symport is normally stimulated by cGK leading to cellular KCl loss and cell shrinkage (Adragna *et al.*, 2002).

The present results disclose a novel role of cGKI in the regulation of erythrocyte survival. Cyclic GMP and cGKI have previously been shown to counteract apoptosis of nucleated cells (Nagai-Kusuhara *et al.*, 2007). The mechanism that suppresses eryptosis via cGKI and lowering of the cytosolic Ca^{2+} concentration may be similarly effective in the regulation of apoptotic death of nucleated cells. Although indirect effects, *e.g.* resulting

from altered erythropoiesis or defects in nonerythroid cells of the cGKI mutants, cannot be completely ruled out, several findings suggest a direct effect of cGKI on the survival of mature erythrocytes. First, the eryptotic phenotype is observed in isolated mature erythrocytes, and knockout erythrocytes are cleared faster from the circulation than control cells. Second, anemia and splenomegaly are similarly present in “sick” conventional cGKI knockout mice and in relatively “healthy” cGKI SM rescue mice. Third, anemia appears to precede splenomegaly excluding the possibility that development of a large spleen and the associated increased clearance of erythrocytes are the primary cause of anemia. Thus, we propose that the primary defect leading to anemia in cGKI-deficient mice is a higher susceptibility of mature erythrocytes to eryptosis, which results in accumulation of the apoptotic cells in the spleen and, thereby, in its enlargement and further retention of erythrocytes. In this way, a vicious cycle is generated in which anemia and splenomegaly potentiate each other to reach the level observed in the adult cGKI mouse mutants. Clearly, to unequivocally establish a causal relationship between erythrocytic cGKI, anemia, and splenomegaly, an erythrocyte-specific cGKI knockout would be needed.

A major stimulator of cGKI is NO (Nagai-Kusuhara *et al.*, 2007; Das *et al.*, 2006; Li & Billiar, 1999), which can be released or removed by erythrocytes (Crawford *et al.*, 2006; Grubina *et al.*, 2007; McMahon *et al.*, 2002). Oxygenated hemoglobin takes up NO, whereas desoxygenated hemoglobin releases NO (Power *et al.*, 2007). Most recently, NO donors have been shown to counteract eryptosis, an effect partially mimicked by dibutyryl-cGMP (Nicolay *et al.*, 2007). Similar to what has been shown in nucleated cells (Benhar & Stamler, 2005; Diesen & Stamler, 2007), NO may further be effective in erythrocytes through nitrosylation of enzymes necessary for the induction of cell membrane scrambling (Nicolay *et al.*, 2007). As NO is released from desoxygenated erythrocytes (Angelo *et al.*, 2006; Reynolds *et al.*, 2007), the anti-eryptotic effect of NO would be particularly important in hypoxic tissue. Impaired NO formation in erythrocytes has been implicated in the vasoconstriction and ischemia following transfusion (Reynolds *et al.*, 2007), pulmonary hypertension (McMahon *et al.*, 2002), and deranged microcirculation in sickle cell anemia (Pawloski *et al.*, 2005). A decrease of NO-dependent activation of cGKI could participate in the pathophysiology of those conditions. Moreover, accelerated eryptosis participates in the pathophysiology of several diseases such as iron deficiency, hemolytic uremic syndrome (Lang *et al.*, 2006b),

sepsis (Kempe *et al.*, 2007) , malaria (Brand *et al.*, 2003), Wilson's disease (Lang *et al.*, 2007), thalassemia (Lang *et al.*, 2002), glucose-phosphate dehydrogenase deficiency (Lang *et al.*, 2002), and diabetes (Nicolay *et al.*, 2006). At least in theory, stimulation of cGKI could reverse accelerated eryptosis in those diseases.

In conclusion, the present study demonstrates that lack of cGKI leads to an increased cytosolic Ca^{2+} concentration with subsequent breakdown of PS asymmetry, accelerated clearance of circulating erythrocytes, and anemia despite counterregulation by erythropoietin release. These observations identify a novel function of cGKI signaling in the regulation of erythrocyte survival and support the emerging concept that pathways via NO, cGMP, and cGKI stimulate growth and survival in a number of cell types *in vivo* (Feil *et al.*, 2005a; Wolfsgruber *et al.*, 2003; Guo *et al.*, 2007).

5.3 Study of PDK1-mediated regulation of suicidal death of erythrocytes

The present observations disclose that PDK1 deficiency confers partial protection against suicidal erythrocyte death or eryptosis. Accordingly, phosphatidylserine exposure is significantly smaller in PDK1 hypomorphic mice (*pdkl^{hm}*) than in their wild type littermates (*pdkl^{wt}*). The difference holds for oxidative stress, osmotic shock, and Cl^- removal. The different susceptibility of *pdkl^{hm}* and *pdkl^{wt}* erythrocytes leads to significantly different clearance of oxidized erythrocytes *in vivo*. Notably, in the absence of oxidative stress, both, *pdkl^{hm}* and *pdkl^{wt}* erythrocytes are cleared very slowly from circulating blood, indicating that the observed difference is of little relevance for the survival of non-stressed erythrocytes. Small differences of erythrocyte clearance could easily be compensated by increased erythrocyte formation. However, the difference may become biologically significant under conditions of erythrocytic stress by oxidation or gross cell volume changes.

As mentioned, oxidative stress, osmotic shock, and Cl^- removal trigger eryptosis by activating Ca^{2+} -permeable cation channels with subsequent Ca^{2+} entry (Andrews *et al.*, 2002; Duranton *et al.*, 2003; Duranton *et al.*, 2002; Huber *et al.*, 2001). The decreased eryptosis of PDK1-deficient erythrocytes is at least in part due to decreased cytosolic Ca^{2+} concentration. Hitherto nothing is known about the regulation of Ca^{2+} channels by PDK1.

PDK1 is, however, known to participate in the PI3-kinase dependent stimulation of SGK1 (Lang & Cohen, 2001), which in turn has been shown to stimulate the Ca²⁺ channel TRPV5 (Palmada *et al.*, 2005). The Ca²⁺-permeable cation channel in erythrocytes presumably involves TRPC6 (Föller *et al.*, 2007). Possibly, TRPC6 is similarly a target for SGK1, its isoforms SGK2 and SGK3, and/or the related kinases PKB/Akt. However, the effect of SGK1 and its related kinases on TRP channels other than TRPV5 has never been tested.

PDK1 is known to activate voltage-gated K⁺ channels, thus mimicking the effect of SGK1 (Gamper *et al.*, 2002). Activation of K⁺ channels and/or subsequent K⁺ loss could stimulate suicidal death of erythrocytes (Lang *et al.*, 2003d) and contributes to apoptosis of nucleated cells (Bortner & Cidlowski, 1999; Dallaporta *et al.*, 1998; Okada *et al.*, 2001; Maeno *et al.*, 2000; Wang, 2004; Yu *et al.*, 1997) following treatment with TNF α (Gantner *et al.*, 1995), activating CD95 antibodies (Gomez-Angelats *et al.*, 2000; Storey *et al.*, 2003), glucocorticoids (Benson *et al.*, 1996; Yurinskaya *et al.*, 2005a; Yurinskaya *et al.*, 2005b), GABA (Erdo *et al.*, 1991), dopamine (Offen *et al.*, 1995), sulfonylureas (Bankers-Fulbright *et al.*, 1998), etoposide (Salido *et al.*, 2001), sphingosine (Dangel *et al.*, 2005), amyloid (Colom *et al.*, 1998), staurosporine (Prehn *et al.*, 1997), urea (Michea *et al.*, 2000), oxidative stress (Bergamo *et al.*, 2004; Pal *et al.*, 2004), hypoxia (Liu *et al.*, 2005), and radiation (Rosette & Karin, 1996). K⁺ loss may further participate in the regulation of apoptosis by Cl⁻ channel blockers (Takahashi *et al.*, 2005), K⁺ channel blockers (Chin *et al.*, 1997), growth factor depletion (Sturm *et al.*, 2004), thyroid status (Alisi *et al.*, 2005), transformation (Wenzel & Daniel, 2004), choline deficiency (Albright *et al.*, 2005), and glutamine depletion (Rotoli *et al.*, 2005). However, under control conditions, K⁺ channel activity is low in erythrocytes and presumably not decisive for the triggering of Ca²⁺ entry and eryptosis (Lang *et al.*, 2005a). Nevertheless, the Ca²⁺ and K⁺ channel-regulating capacity of PDK1 may well impact on apoptosis of nucleated cells.

As described, erythrocytes exposing phosphatidylserine at their surface are rapidly cleared from circulating blood (Kempe *et al.*, 2006). Thus, enhanced eryptosis contributes to the development of anemia (Lang *et al.*, 2005a). Under unstressed conditions, the difference between *pdkl^{hm}* and *pdkl^{wt}* erythrocytes is, however, presumably too small to

appreciably affect the *in vivo* clearance of erythrocytes. Thus, no significant differences were observed in blood parameters between *pdk1^{hm}* and *pdk1^{wt}* mice.

In conclusion, PDK1 deficient erythrocytes are more resistant to eryptosis than erythrocytes from wild type animals. The effect is at least partially due to reduced Ca^{2+} entry into *pdk1^{hm}* erythrocytes. The observations disclose a novel function of PDK1, i.e. an influence on cellular Ca^{2+} entry, which may well influence the function and survival not only of erythrocytes but as well of nucleated cells.

5.4 Bacterial peptidoglycan induces cell death of erythrocytes

The present study discloses a novel effect of peptidoglycan (PGN), i.e. the triggering of eryptosis. The concentrations required are similar to those previously reported to be effective on monocytes (Hadley *et al.*, 2005), mononuclear cells (Weidemann *et al.*, 1994), B lymphocytes (Babu & Zeiger, 1983), muscle cells (Ishii *et al.*, 2007), and alveolar type II cells (Cheon *et al.*, 2007). Whether or not those concentrations are approached *in vivo*, remains, however, uncertain. To our knowledge, no local PGN concentrations during sepsis with *S. aureus* have been reported so far.

The presented experiments further provide insight into the mechanisms mediating the phospholipid scrambling-effect of PGN. As evident from fluo3 fluorescence, PGN stimulates Ca^{2+} entry. The channels are activated by prostaglandin E_2 , which is formed from arachidonic acid (Lang *et al.*, 2005b). In polymorphonuclear leukocytes, PGN has been shown to trigger the arachidonic acid cascade with subsequent formation of prostaglandin E_2 (Valera *et al.*, 2007). Removal of extracellular Ca^{2+} blunts the effect of PGN (50 $\mu\text{g}/\text{ml}$).

As PGN increases the intracellular Ca^{2+} concentration, it indirectly activates the Ca^{2+} -dependent K^+ channel (Gardos channel) thereby fostering cell shrinkage. In macrophages, PGN has been shown to activate MaxiK K^+ channels (Scheel *et al.*, 2006). The rather abrupt transition from normal to reduced forward scatter may reflect steep Ca^{2+} sensitivity of the Ca^{2+} -sensitive K^+ channels.

The experiments further disclose a slight, but statistically significant effect of PGN (50 $\mu\text{g}/\text{ml}$) on ceramide formation. Ceramide has previously been shown to sensitize the cells to the scrambling effect of Ca^{2+} (Lang *et al.*, 2004a). Thus, ceramide formation

could contribute to the scrambling effect of PGN. Moreover, PGN led to a significant decrease of the cytosolic ATP concentration. Thus, treatment with PGN compromises the energy expenditure of erythrocytes. Previous experiments revealed that energy depletion stimulates eryptosis (Klarl *et al.*, 2006).

The present study did not attempt to define the PGN receptors involved. To our knowledge, no PGN receptor has been identified in erythrocytes so far. Among the known PGN receptors, PGRP-S has been shown to require an increase in the intracellular Ca^{2+} concentration for its effect (Lee *et al.*, 2004).

Phosphatidylserine-exposing cells are subjected to phagocytosis by phagocytes, which are equipped with phosphatidylserine receptors (Fadok *et al.*, 2000) and thus eliminate phosphatidylserine-exposing cells (Boas *et al.*, 1998). Accordingly, treatment of erythrocytes with PGN indeed accelerated the elimination of circulating erythrocytes. At least in theory, peptidoglycan induced eryptosis could contribute to the anemia of sepsis. As reported earlier (Kempe *et al.*, 2007), accelerated eryptosis is indeed observed in sepsis, an effect, however, partially due to the release of sphingomyelinase from the pathogen.

In conclusion, PGN stimulates Ca^{2+} entry into erythrocytes, which in turn triggers phosphatidylserine exposure and cell shrinkage. The phosphatidylserine exposure is expected to accelerate the clearance of affected erythrocytes and thus presumably contributes to anemia during bacterial infection.

6 References

Reference List

Aderem, A. & Ulevitch, R. J. (2000). Toll-like receptors in the induction of the innate immune response. *Nature* **406**, 782-787.

Adragna, N. C., Di Fulvio, M., & Lauf, P. K. (2004). Regulation of K-Cl cotransport: from function to genes. *J.Membr.Biol.* **201**, 109-137.

Adragna, N. C., Ferrell, C. M., Zhang, J., Di Fulvio, M., Temprana, C. F., Sharma, A., Fyffe, R. E., Cool, D. R., & Lauf, P. K. (2006). Signal transduction mechanisms of K⁺-Cl⁻ cotransport regulation and relationship to disease. *Acta Physiol (Oxf)* **187**, 125-139.

Adragna, N. C., White, R. E., Orlov, S. N., & Lauf, P. K. (2000). K-Cl cotransport in vascular smooth muscle and erythrocytes: possible implication in vasodilation. *Am.J.Physiol Cell Physiol* **278**, C381-C390.

Adragna, N. C., Zhang, J., Di Fulvio, M., Lincoln, T. M., & Lauf, P. K. (2002). KCl cotransport regulation and protein kinase G in cultured vascular smooth muscle cells. *J.Membr.Biol.* **187**, 157-165.

Ahnert-Hilger, G., Bhakdi, S., & Gratzl, M. (1985). Minimal requirements for exocytosis. A study using PC 12 cells permeabilized with staphylococcal alpha-toxin. *J.Biol.Chem.* **260**, 12730-12734.

Albright, C. D., da Costa, K. A., Craciunescu, C. N., Klem, E., Mar, M. H., & Zeisel, S. H. (2005). Regulation of choline deficiency apoptosis by epidermal growth factor in CWSV-1 rat hepatocytes. *Cell Physiol Biochem* **15**, 59-68.

Alessi, D. R., Deak, M., Casamayor, A., Caudwell, F. B., Morrice, N., Norman, D. G., Gaffney, P., Reese, C. B., MacDougall, C. N., Harbison, D., Ashworth, A., & Bownes, M. (1997a). 3-Phosphoinositide-dependent protein kinase-1 (PDK1): structural and functional homology with the Drosophila DSTPK61 kinase. *Curr.Biol.* **7**, 776-789.

Alessi, D. R., James, S. R., Downes, C. P., Holmes, A. B., Gaffney, P. R., Reese, C. B., & Cohen, P. (1997b). Characterization of a 3-phosphoinositide-dependent protein kinase which phosphorylates and activates protein kinase Balpha. *Curr.Biol.* **7**, 261-269.

Alisi, A., Demori, I., Spagnuolo, S., Pierantozzi, E., Fugassa, E., & Leoni, S. (2005). Thyroid status affects rat liver regeneration after partial hepatectomy by regulating cell cycle and apoptosis. *Cell Physiol Biochem* **15**, 69-76.

Alvarez, J. & Garcia-Sancho, J. (1987). An estimate of the number of Ca²⁺-dependent K⁺ channels in the human red cell. *Biochim.Biophys.Acta* **903**, 543-546.

Anderson, K. E., Coadwell, J., Stephens, L. R., & Hawkins, P. T. (1998). Translocation of PDK-1 to the plasma membrane is important in allowing PDK-1 to activate protein kinase B. *Curr.Biol.* **8**, 684-691.

Andjelkovic, M., Alessi, D. R., Meier, R., Fernandez, A., Lamb, N. J., Frech, M., Cron, P., Cohen, P., Lucocq, J. M., & Hemmings, B. A. (1997). Role of translocation in the activation and function of protein kinase B. *J.Biol.Chem.* **272**, 31515-31524.

Andrews, D. A., Yang, L., & Low, P. S. (2002). Phorbol ester stimulates a protein kinase C-mediated agatoxin-TK-sensitive calcium permeability pathway in human red blood cells. *Blood* **100**, 3392-3399.

Angelo, M., Singel, D. J., & Stamler, J. S. (2006). An S-nitrosothiol (SNO) synthase function of hemoglobin that utilizes nitrite as a substrate. *Proc.Natl.Acad.Sci.U.S.A* **103**, 8366-8371.

Artunc, F., Rexhepaj, R., Volkl, H., Grahammer, F., Remy, C., Sandulache, D., Nasir, O., Wagner, C. A., Alessi, D. R., & Lang, F. (2006). Impaired intestinal and renal glucose transport in PDK-1 hypomorphic mice. *Am J Physiol Regul.Integr.Comp Physiol* **291**, R1533-R1538.

Ay, B., Iyanoye, A., Sieck, G. C., Prakash, Y. S., & Pabelick, C. M. (2006). Cyclic nucleotide regulation of store-operated Ca²⁺ influx in airway smooth muscle. *Am.J.Physiol Lung Cell Mol.Physiol* **290**, L278-L283.

Babu, U. M. & Zeiger, A. R. (1983). Soluble peptidoglycan from *Staphylococcus aureus* is a murine B-lymphocyte mitogen. *Infect.Immun.* **42**, 1013-1016.

Bader, M. F., Thierse, D., Aunis, D., Ahnert-Hilger, G., & Gratzl, M. (1986). Characterization of hormone and protein release from alpha-toxin-permeabilized chromaffin cells in primary culture. *J.Biol.Chem.* **261**, 5777-5783.

- Bankers-Fulbright, J. L., Kephart, G. M., Loegering, D. A., Bradford, A. L., Okada, S., Kita, H., & Gleich, G. J. (1998). Sulfonyleureas inhibit cytokine-induced eosinophil survival and activation. *J Immunol.* **160**, 5546-5553.
- Barrett, J. F. & Shockman, G. D. (1984). Isolation and characterization of soluble peptidoglycan from several strains of *Streptococcus faecium*. *J Bacteriol.* **159**, 511-519.
- Barry, P. H. & Lynch, J. W. (1991). Liquid junction potentials and small cell effects in patch-clamp analysis. *J.Membr.Biol.* **121**, 101-117.
- Begenisich, T., Nakamoto, T., Ovitt, C. E., Nehrke, K., Brugnara, C., Alper, S. L., & Melvin, J. E. (2004). Physiological roles of the intermediate conductance, Ca²⁺-activated potassium channel Kcnn4. *J.Biol.Chem.* **279**, 47681-47687.
- Belmonte, G., Cescatti, L., Ferrari, B., Nicolussi, T., Ropele, M., & Menestrina, G. (1987). Pore formation by *Staphylococcus aureus* alpha-toxin in lipid bilayers. Dependence upon temperature and toxin concentration. *Eur.Biophys.J.* **14**, 349-358.
- Benhar, M. & Stamler, J. S. (2005). A central role for S-nitrosylation in apoptosis. *Nat.Cell Biol.* **7**, 645-646.
- Bennekou, P., De Franceschi, L., Pedersen, O., Lian, L., Asakura, T., Evans, G., Brugnara, C., & Christophersen, P. (2001). Treatment with NS3623, a novel Cl⁻ conductance blocker, ameliorates erythrocyte dehydration in transgenic SAD mice: a possible new therapeutic approach for sickle cell disease. *Blood* **97**, 1451-1457.
- Bennekou, P., Pedersen, O., Moller, A., & Christophersen, P. (2000). Volume control in sickle cells is facilitated by the novel anion conductance inhibitor NS1652. *Blood* **95**, 1842-1848.
- Benson, R. S., Heer, S., Dive, C., & Watson, A. J. (1996). Characterization of cell volume loss in CEM-C7A cells during dexamethasone-induced apoptosis. *Am J Physiol* **270**, C1190-C1203.
- Berg, C. P., Engels, I. H., Rothbart, A., Lauber, K., Renz, A., Schlosser, S. F., Schulze-Osthoff, K., & Wesselborg, S. (2001). Human mature red blood cells express caspase-3 and caspase-8, but are devoid of mitochondrial regulators of apoptosis. *Cell Death.Differ.* **8**, 1197-1206.

- Bergamo, P., Luongo, D., & Rossi, M. (2004). Conjugated linoleic acid--mediated apoptosis in Jurkat T cells involves the production of reactive oxygen species. *Cell Physiol Biochem* **14**, 57-64.
- Bernheimer, A. W. & Rudy, B. (1986). Interactions between membranes and cytolytic peptides. *Biochim.Biophys.Acta* **864**, 123-141.
- Bhakdi, S., Muhly, M., Korom, S., & Hugo, F. (1989). Release of interleukin-1 beta associated with potent cytotoxic action of staphylococcal alpha-toxin on human monocytes. *Infect.Immun.* **57**, 3512-3519.
- Bhakdi, S. & Tranum-Jensen, J. (1991). Alpha-toxin of *Staphylococcus aureus*. *Microbiol.Rev.* **55**, 733-751.
- Bieberich, E., MacKinnon, S., Silva, J., Noggle, S., & Condie, B. G. (2003). Regulation of cell death in mitotic neural progenitor cells by asymmetric distribution of prostate apoptosis response 4 (PAR-4) and simultaneous elevation of endogenous ceramide. *J Cell Biol* **162**, 469-479.
- Bluml, S., Kirchberger, S., Bochkov, V. N., Kronke, G., Stuhlmeier, K., Majdic, O., Zlabinger, G. J., Knapp, W., Binder, B. R., Stockl, J., & Leitinger, N. (2005). Oxidized phospholipids negatively regulate dendritic cell maturation induced by TLRs and CD40. *J Immunol.* **175**, 501-508.
- Boas, F. E., Forman, L., & Beutler, E. (1998). Phosphatidylserine exposure and red cell viability in red cell aging and in hemolytic anemia. *Proc.Natl.Acad.Sci.U.S.A* **95**, 3077-3081.
- Bookchin, R. M. & Lew, V. L. (1980). Progressive inhibition of the Ca pump and Ca:Ca exchange in sickle red cells. *Nature* **284**, 561-563.
- Bortner, C. D. & Cidlowski, J. A. (1999). Caspase independent/dependent regulation of K(+), cell shrinkage, and mitochondrial membrane potential during lymphocyte apoptosis. *J.Biol.Chem.* **274**, 21953-21962.
- Brand, V. B., Sandu, C. D., Durantou, C., Tanneur, V., Lang, K. S., Huber, S. M., & Lang, F. (2003). Dependence of *Plasmodium falciparum* in vitro growth on the cation permeability of the human host erythrocyte. *Cell Physiol Biochem.* **13**, 347-356.
- Branton, D., Cohen, C. M., & Tyler, J. (1981). Interaction of cytoskeletal proteins on the human erythrocyte membrane. *Cell* **24**, 24-32.

Bratosin, D., Estaquier, J., Petit, F., Arnoult, D., Quatannens, B., Tissier, J. P., Slomianny, C., Sartiaux, C., Alonso, C., Huart, J. J., Montreuil, J., & Ameisen, J. C. (2001). Programmed cell death in mature erythrocytes: a model for investigating death effector pathways operating in the absence of mitochondria. *Cell Death.Differ.* **8**, 1143-1156.

Brown, A. M., Ellory, J. C., Young, J. D., & Lew, V. L. (1978). A calcium-activated potassium channel present in foetal red cells of the sheep but absent from reticulocytes and mature red cells. *Biochim.Biophys.Acta* **511**, 163-175.

Brown, D. R. & Pattee, P. A. (1980). Identification of a chromosomal determinant of alpha-toxin production in *Staphylococcus aureus*. *Infect.Immun.* **30**, 36-42.

Brugnara, C., Bunn, H. F., & Tosteson, D. C. (1986). Regulation of erythrocyte cation and water content in sickle cell anemia. *Science* **232**, 388-390.

Brugnara, C., de Franceschi, L., & Alper, S. L. (1993). Ca(2+)-activated K⁺ transport in erythrocytes. Comparison of binding and transport inhibition by scorpion toxins. *J.Biol.Chem.* **268**, 8760-8768.

Brugnara, C. & Tosteson, D. C. (1987). Inhibition of K transport by divalent cations in sickle erythrocytes. *Blood* **70**, 1810-1815.

Brune, B. (2003). Nitric oxide: NO apoptosis or turning it ON? *Cell Death.Differ.* **10**, 864-869.

Caldwell, K. K. & Harris, R. A. (1985). Effects of anesthetic and anticonvulsant drugs on calcium-dependent efflux of potassium from human erythrocytes. *Eur.J.Pharmacol.* **107**, 119-125.

Cassidy, P. & Harshman, S. (1976a). Purification of staphylococcal alpha-toxin by adsorption chromatography on glass. *Infect.Immun.* **13**, 982-986.

Cassidy, P. & Harshman, S. (1976b). Studies on the binding of staphylococcal 125I-labeled alpha-toxin to rabbit erythrocytes. *Biochemistry* **15**, 2348-2355.

Chasis, J. A. & Mohandas, N. (1986). Erythrocyte membrane deformability and stability: two distinct membrane properties that are independently regulated by skeletal protein associations. *J.Cell Biol.* **103**, 343-350.

Chasis, J. A., Prenant, M., Leung, A., & Mohandas, N. (1989). Membrane assembly and remodeling during reticulocyte maturation. *Blood* **74**, 1112-1120.

Chen, D., Texada, D. E., Duggan, C., Liang, C., Reden, T. B., Kooragayala, L. M., & Langford, M. P. (2005). Surface calreticulin mediates muramyl dipeptide-induced apoptosis in RK13 cells. *J Biol Chem.* **280**, 22425-22436.

Chen, L. Y. & Mehta, J. L. (1998). Evidence for the presence of L-arginine-nitric oxide pathway in human red blood cells: relevance in the effects of red blood cells on platelet function. *J.Cardiovasc.Pharmacol.* **32**, 57-61.

Cheon, I. S., Woo, S. S., Kang, S. S., Im, J., Yun, C. H., Chung, D. K., Park, D. K., & Han, S. H. (2007). Peptidoglycan-mediated IL-8 expression in human alveolar type II epithelial cells requires lipid raft formation and MAPK activation. *Mol.Immunol.*

Chin, L. S., Park, C. C., Zitnay, K. M., Sinha, M., DiPatri, A. J., Jr., Perillan, P., & Simard, J. M. (1997). 4-Aminopyridine causes apoptosis and blocks an outward rectifier K⁺ channel in malignant astrocytoma cell lines. *J Neurosci.Res* **48**, 122-127.

Clark, M. R., Guatelli, J. C., White, A. T., & Shohet, S. B. (1981). Study on the dehydrating effect of the red cell Na⁺/K⁺-pump in nystatin-treated cells with varying Na⁺ and water contents. *Biochim.Biophys.Acta* **646**, 422-432.

Coccia, M. A., Cooke, K., Stoney, G., Pistillo, J., Del Castillo, J., Duryea, D., Tarpley, J. E., & Molineux, G. (2001). Novel erythropoiesis stimulating protein (darbepoetin alfa) alleviates anemia associated with chronic inflammatory disease in a rodent model. *Exp Hematol.* **29**, 1201-1209.

Colino, J. & Snapper, C. M. (2003). Two distinct mechanisms for induction of dendritic cell apoptosis in response to intact *Streptococcus pneumoniae*. *J Immunol.* **171**, 2354-2365.

Colom, L. V., Diaz, M. E., Beers, D. R., Neely, A., Xie, W. J., & Appel, S. H. (1998). Role of potassium channels in amyloid-induced cell death. *J Neurochem* **70**, 1925-1934.

Crawford, J. H., Isbell, T. S., Huang, Z., Shiva, S., Chacko, B. K., Schechter, A. N., Darley-Usmar, V. M., Kerby, J. D., Lang, J. D., Jr., Kraus, D., Ho, C., Gladwin, M. T., & Patel, R. P. (2006). Hypoxia, red blood cells, and nitrite regulate NO-dependent hypoxic vasodilation. *Blood* **107**, 566-574.

- Currie, R. A., Walker, K. S., Gray, A., Deak, M., Casamayor, A., Downes, C. P., Cohen, P., Alessi, D. R., & Lucocq, J. (1999). Role of phosphatidylinositol 3,4,5-trisphosphate in regulating the activity and localization of 3-phosphoinositide-dependent protein kinase-1. *Biochem.J.* **337** (Pt 3), 575-583.
- Dallaporta, B., Hirsch, T., Susin, S. A., Zamzami, N., Larochette, N., Brenner, C., Marzo, I., & Kroemer, G. (1998). Potassium leakage during the apoptotic degradation phase. *J Immunol.* **160**, 5605-5615.
- Dangel, G. R., Lang, F., & Lepple-Wienhues, A. (2005). Effect of sphingosine on Ca²⁺ entry and mitochondrial potential of Jurkat T cells--interaction with Bcl2. *Cell Physiol Biochem* **16**, 9-14.
- Das, A., Smolenski, A., Lohmann, S. M., & Kukreja, R. C. (2006). Cyclic GMP-dependent protein kinase Ialpha attenuates necrosis and apoptosis following ischemia/reoxygenation in adult cardiomyocyte. *J.Biol.Chem.* **281**, 38644-38652.
- Daugas, E., Cande, C., & Kroemer, G. (2001). Erythrocytes: death of a mummy. *Cell Death.Differ.* **8**, 1131-1133.
- de Franceschi, L., Rivera, A., Fleming, M. D., Honczarenko, M., Peters, L. L., Gascard, P., Mohandas, N., & Brugnara, C. (2005). Evidence for a protective role of the Gardos channel against hemolysis in murine spherocytosis. *Blood* **106**, 1454-1459.
- de Franceschi, L., Rouyer-Fessard, P., Alper, S. L., Jouault, H., Brugnara, C., & Beuzard, Y. (1996). Combination therapy of erythropoietin, hydroxyurea, and clotrimazole in a beta thalassemic mouse: a model for human therapy. *Blood* **87**, 1188-1195.
- Dedkova, E. N. & Blatter, L. A. (2002). Nitric oxide inhibits capacitative Ca²⁺ entry and enhances endoplasmic reticulum Ca²⁺ uptake in bovine vascular endothelial cells. *J.Physiol* **539**, 77-91.
- Desai, S. A., Schlesinger, P. H., & Krogstad, D. J. (1991). Physiologic rate of carrier-mediated Ca²⁺ entry matches active extrusion in human erythrocytes. *J.Gen.Physiol* **98**, 349-364.
- Diesen, D. & Stamler, J. S. (2007). S-nitrosylation and PEGylation of hemoglobin: toward a blood substitute that recapitulates blood. *J.Mol.Cell Cardiol.* **42**, 921-923.

- Dimmeler, S., Haendeler, J., & Zeiher, A. M. (2002). Regulation of endothelial cell apoptosis in atherothrombosis. *Curr.Opin.Lipidol.* **13**, 531-536.
- Domek-Lopacinska, K. & Strosznajder, J. B. (2005). Cyclic GMP metabolism and its role in brain physiology. *J.Physiol Pharmacol.* **56 Suppl 2**, 15-34.
- Doyle, D. A., Morais, C. J., Pfuetzner, R. A., Kuo, A., Gulbis, J. M., Cohen, S. L., Chait, B. T., & MacKinnon, R. (1998). The structure of the potassium channel: molecular basis of K⁺ conduction and selectivity. *Science* **280**, 69-77.
- Dunham, P. B. & Blostein, R. (1997). L antigens of sheep red blood cell membranes and modulation of ion transport. *Am.J.Physiol* **272**, C357-C368.
- Dunham, P. B. & Hoffman, J. F. (1970). Partial purification of the ouabain-binding component and of Na,K-ATPase from human red cell membranes. *Proc.Natl.Acad.Sci.U.S.A* **66**, 936-943.
- Durantón, C., Huber, S., Tanneur, V., Lang, K., Brand, V., Sandu, C., & Lang, F. (2003). Electrophysiological properties of the Plasmodium Falciparum-induced cation conductance of human erythrocytes. *Cell Physiol Biochem* **13**, 189-198.
- Durantón, C., Huber, S. M., & Lang, F. (2002). Oxidation induces a Cl⁻-dependent cation conductance in human red blood cells. *J.Physiol* **539**, 847-855.
- Dziarski, R. (1991). Demonstration of peptidoglycan-binding sites on lymphocytes and macrophages by photoaffinity cross-linking. *J Biol Chem.* **266**, 4713-4718.
- Dziarski, R. (2003). Recognition of bacterial peptidoglycan by the innate immune system. *Cell Mol.Life Sci.* **60**, 1793-1804.
- Dziarski, R., Wang, Q., Miyake, K., Kirschning, C. J., & Gupta, D. (2001). MD-2 enables Toll-like receptor 2 (TLR2)-mediated responses to lipopolysaccharide and enhances TLR2-mediated responses to Gram-positive and Gram-negative bacteria and their cell wall components. *J.Immunol.* **166**, 1938-1944.
- Eda, S. & Sherman, I. W. (2002). Cytoadherence of malaria-infected red blood cells involves exposure of phosphatidylserine. *Cell Physiol Biochem.* **12**, 373-384.

El Husseini, A. E., Bladen, C., & Vincent, S. R. (1995). Molecular characterization of a type II cyclic GMP-dependent protein kinase expressed in the rat brain. *J.Neurochem.* **64**, 2814-2817.

El Husseini, A. E., Williams, J., Reiner, P. B., Pelech, S., & Vincent, S. R. (1999). Localization of the cGMP-dependent protein kinases in relation to nitric oxide synthase in the brain. *J.Chem.Neuroanat.* **17**, 45-55.

Engelmann, B. & Duhm, J. (1987). Intracellular calcium content of human erythrocytes: relation to sodium transport systems. *J.Membr.Biol.* **98**, 79-87.

Erdo, S., Michler, A., & Wolff, J. R. (1991). GABA accelerates excitotoxic cell death in cortical cultures: protection by blockers of GABA-gated chloride channels. *Brain Res* **542**, 254-258.

Evora, P. R. & Viaro, F. (2006). The guanylyl cyclase inhibition by MB as vasoplegic circulatory shock therapeutical target. *Curr.Drug Targets.* **7**, 1195-1204.

Fadok, V. A., Bratton, D. L., Rose, D. M., Pearson, A., Ezekewitz, R. A., & Henson, P. M. (2000). A receptor for phosphatidylserine-specific clearance of apoptotic cells. *Nature* **405**, 85-90.

Feil, R., Feil, S., & Hofmann, F. (2005a). A heretical view on the role of NO and cGMP in vascular proliferative diseases. *Trends Mol.Med.* **11**, 71-75.

Feil, R., Gappa, N., Rutz, M., Schlossmann, J., Rose, C. R., Konnerth, A., Brummer, S., Kuhbandner, S., & Hofmann, F. (2002). Functional reconstitution of vascular smooth muscle cells with cGMP-dependent protein kinase I isoforms. *Circ.Res.* **90**, 1080-1086.

Feil, R., Lohmann, S. M., de Jonge, H., Walter, U., & Hofmann, F. (2003). Cyclic GMP-dependent protein kinases and the cardiovascular system: insights from genetically modified mice. *Circ.Res.* **93**, 907-916.

Feil, S., Zimmermann, P., Knorn, A., Brummer, S., Schlossmann, J., Hofmann, F., & Feil, R. (2005b). Distribution of cGMP-dependent protein kinase type I and its isoforms in the mouse brain and retina. *Neuroscience* **135**, 863-868.

Ferreira, H. G. & Lew, V. L. (1976). Use of ionophore A23187 to measure cytoplasmic Ca buffering and activation of the Ca pump by internal Ca. *Nature* **259**, 47-49.

Fischer, H. & Tomasz, A. (1984). Production and release of peptidoglycan and wall teichoic acid polymers in pneumococci treated with beta-lactam antibiotics. *J Bacteriol.* **157**, 507-513.

Föller, M., Kasinathan, R. S., Koka, S., Lang, C., Shumilina, E., Birnbaumer, L., Lang, F., & Huber, S. M. (2007). TRPC6 contributes to the Ca²⁺ leak of human erythrocytes. *Cell Physiol Biochem* -in press.

Foller, M., Geiger, C., Mahmud, H., Nicolay, J., & Lang, F. (2007a). Stimulation of suicidal erythrocyte death by amantadine. *Eur.J.Pharmacol.*

Foller, M., Kasinathan, R. S., Koka, S., Lang, C., Shumilina, E., Birnbaumer, L., Lang, F., & Huber, S. M. (2008). TRPC6 Contributes to the Ca Leak of Human Erythrocytes. *Cell Physiol Biochem.* **21**, 183-192.

Foller, M., Shumilina, E., Lam, R., Mohamed, W., Kasinathan, R., Huber, S., Chakraborty, T., & Lang, F. (2007b). Induction of suicidal erythrocyte death by listeriolysin from *Listeria monocytogenes*. *Cell Physiol Biochem.* **20**, 1051-1060.

Forti, S. & Menestrina, G. (1989). Staphylococcal alpha-toxin increases the permeability of lipid vesicles by cholesterol- and pH-dependent assembly of oligomeric channels. *Eur.J.Biochem.* **181**, 767-773.

Fournier, B. & Philpott, D. J. (2005). Recognition of *Staphylococcus aureus* by the innate immune system. *Clin.Microbiol.Rev.* **18**, 521-540.

Franco, R. S., Palascak, M., Thompson, H., & Joiner, C. H. (1995). KCl cotransport activity in light versus dense transferrin receptor-positive sickle reticulocytes. *J.Clin.Invest* **95**, 2573-2580.

Franco, R. S., Palascak, M., Thompson, H., Rucknagel, D. L., & Joiner, C. H. (1996). Dehydration of transferrin receptor-positive sickle reticulocytes during continuous or cyclic deoxygenation: role of KCl cotransport and extracellular calcium. *Blood* **88**, 4359-4365.

Freedman, J. C. & Hoffman, J. F. (1979). Ionic and osmotic equilibria of human red blood cells treated with nystatin. *J.Gen.Physiol* **74**, 157-185.

Freeman, C. J., Bookchin, R. M., Ortiz, O. E., & Lew, V. L. (1987). K-permeabilized human red cells lose an alkaline, hypertonic fluid containing excess K over diffusible anions. *J.Membr.Biol.* **96**, 235-241.

Freer, J. H., Arbuthnott, J. P., & Bernheimer, A. W. (1968). Interaction of staphylococcal alpha-toxin with artificial and natural membranes. *J.Bacteriol.* **95**, 1153-1168.

Friebe, A. & Koesling, D. (2003). Regulation of nitric oxide-sensitive guanylyl cyclase. *Circ.Res.* **93**, 96-105.

Gamm, D. M., Francis, S. H., Angelotti, T. P., Corbin, J. D., & Uhler, M. D. (1995). The type II isoform of cGMP-dependent protein kinase is dimeric and possesses regulatory and catalytic properties distinct from the type I isoforms. *J.Biol.Chem.* **270**, 27380-27388.

Gamper, N., Fillon, S., Huber, S. M., Feng, Y., Kobayashi, T., Cohen, P., & Lang, F. (2002). IGF-1 up-regulates K⁺ channels via PI3-kinase, PDK1 and SGK1. *Pflugers Arch* **443**, 625-634.

Gantner, F., Uhlig, S., & Wendel, A. (1995). Quinine inhibits release of tumor necrosis factor, apoptosis, necrosis and mortality in a murine model of septic liver failure. *Eur J Pharmacol* **294**, 353-355.

Garcia-Sancho, J. & Lew, V. L. (1988). Detection and separation of human red cells with different calcium contents following uniform calcium permeabilization. *J.Physiol* **407**, 505-522.

Gardos, G. (1959). The role of calcium in the potassium permeability of human erythrocytes. *Acta Physiol Hung.* **15**, 121-125.

Garrahan, P. J. & Glynn, I. M. (1967). The stoichiometry of the sodium pump. *J.Physiol* **192**, 217-235.

Gillen, C. M., Brill, S., Payne, J. A., & Forbush, B., III (1996). Molecular cloning and functional expression of the K-Cl cotransporter from rabbit, rat, and human. A new member of the cation-chloride cotransporter family. *J.Biol.Chem.* **271**, 16237-16244.

Glader, B. E. & Nathan, D. G. (1978). Cation permeability alterations during sickling: relationship to cation composition and cellular hydration of irreversibly sickled cells. *Blood* **51**, 983-989.

Glynn, I. M. & Karlish, S. J. (1975). The sodium pump. *Annu.Rev.Physiol* **37**, 13-55.

- Gomes, B., Savignac, M., Cabral, M. D., Paulet, P., Moreau, M., Leclerc, C., Feil, R., Hofmann, F., Guery, J. C., Dietrich, G., & Pelletier, L. (2006). The cGMP/protein kinase G pathway contributes to dihydropyridine-sensitive calcium response and cytokine production in TH2 lymphocytes. *J.Biol.Chem.* **281**, 12421-12427.
- Gomez-Angelats, M., Bortner, C. D., & Cidlowski, J. A. (2000). Protein kinase C (PKC) inhibits fas receptor-induced apoptosis through modulation of the loss of K⁺ and cell shrinkage. A role for PKC upstream of caspases. *J Biol Chem.* **275**, 19609-19619.
- Grant, N. J., Aunis, D., & Bader, M. F. (1987). Morphology and secretory activity of digitonin- and alpha-toxin-permeabilized chromaffin cells. *Neuroscience* **23**, 1143-1155.
- Grassme, H., Jendrossek, V., Bock, J., Riehle, A., & Gulbins, E. (2002). Ceramide-rich membrane rafts mediate CD40 clustering. *J Immunol.* **168**, 298-307.
- Green, D. R. & Reed, J. C. (1998). Mitochondria and apoptosis. *Science* **281**, 1309-1312.
- Grubina, R., Huang, Z., Shiva, S., Joshi, M. S., Azarov, I., Basu, S., Ringwood, L. A., Jiang, A., Hogg, N., Kim-Shapiro, D. B., & Gladwin, M. T. (2007). Concerted nitric oxide formation and release from the simultaneous reactions of nitrite with deoxy- and oxyhemoglobin. *J.Biol.Chem.* **282**, 12916-12927.
- Grygorczyk, R. (1987). Temperature dependence of Ca²⁺-activated K⁺ currents in the membrane of human erythrocytes. *Biochim.Biophys.Acta* **902**, 159-168.
- Grygorczyk, R. & Schwarz, W. (1983). Properties of the CA²⁺-activated K⁺ conductance of human red cells as revealed by the patch-clamp technique. *Cell Calcium* **4**, 499-510.
- Grygorczyk, R., Schwarz, W., & Passow, H. (1984). Ca²⁺-activated K⁺ channels in human red cells. Comparison of single-channel currents with ion fluxes. *Biophys.J.* **45**, 693-698.
- Gulbins, E., Jekle, A., Ferlinz, K., Grassme, H., & Lang, F. (2000). Physiology of apoptosis. *Am.J.Physiol Renal Physiol* **279**, F605-F615.
- Gulbins, E., Szabo, I., Baltzer, K., & Lang, F. (1997). Ceramide-induced inhibition of T lymphocyte voltage-gated potassium channel is mediated by tyrosine kinases. *Proc.Natl.Acad.Sci.U.S.A* **94**, 7661-7666.

Guo, D., Tan, Y. C., Wang, D., Madhusoodanan, K. S., Zheng, Y., Maack, T., Zhang, J. J., & Huang, X. Y. (2007). A Rac-cGMP signaling pathway. *Cell* **128**, 341-355.

Hadley, J. S., Wang, J. E., Foster, S. J., Thiemermann, C., & Hinds, C. J. (2005). Peptidoglycan of *Staphylococcus aureus* upregulates monocyte expression of CD14, Toll-like receptor 2 (TLR2), and TLR4 in human blood: possible implications for priming of lipopolysaccharide signaling. *Infect.Immun.* **73**, 7613-7619.

Hall, A. C. & Ellory, J. C. (1986). Evidence for the presence of volume-sensitive KCl transport in 'young' human red cells. *Biochim.Biophys.Acta* **858**, 317-320.

Harrison, D. G. & Long, C. (1968). The calcium content of human erythrocytes. *J.Physiol* **199**, 367-381.

Haslinger-Loffler, B., Kahl, B. C., Grundmeier, M., Strangfeld, K., Wagner, B., Fischer, U., Cheung, A. L., Peters, G., Schulze-Osthoff, K., & Sinha, B. (2005). Multiple virulence factors are required for *Staphylococcus aureus*-induced apoptosis in endothelial cells. *Cell Microbiol.* **7**, 1087-1097.

Haslinger-Loffler, B., Wagner, B., Bruck, M., Strangfeld, K., Grundmeier, M., Fischer, U., Volker, W., Peters, G., Schulze-Osthoff, K., & Sinha, B. (2006). *Staphylococcus aureus* induces caspase-independent cell death in human peritoneal mesothelial cells. *Kidney Int.* **70**, 1089-1098.

Heinz, A. & Hoffman, J. F. (1990). Membrane sidedness and the interaction of H⁺ and K⁺ on Ca²⁺(+)-activated K⁺ transport in human red blood cells. *Proc.Natl.Acad.Sci.U.S.A* **87**, 1998-2002.

Heinz, A. & Passow, H. (1980). Role of external potassium in the calcium-induced potassium efflux from human red blood cell ghosts. *J.Membr.Biol.* **57**, 119-131.

Hoffman, J. F., Joiner, W., Nehrke, K., Potapova, O., Foye, K., & Wickrema, A. (2003). The hSK4 (KCNN4) isoform is the Ca²⁺-activated K⁺ channel (Gardos channel) in human red blood cells. *Proc.Natl.Acad.Sci.U.S.A* **100**, 7366-7371.

Hoffman, J. F. & Laris, P. C. (1974). Determination of membrane potentials in human and *Amphiuma* red blood cells by means of fluorescent probe. *J.Physiol* **239**, 519-552.

Hoffman, J. F. & Laris, P. C. (1984). Membrane electrical parameters of normal human red blood cells. *Soc.Gen.Physiol Ser.* **38**, 287-293.

- Hofmann, F. (2005). The biology of cyclic GMP-dependent protein kinases. *J.Biol.Chem.* **280**, 1-4.
- Hofmann, F., Feil, R., Kleppisch, T., & Schlossmann, J. (2006). Function of cGMP-dependent protein kinases as revealed by gene deletion. *Physiol Rev.* **86**, 1-23.
- Hofmann, F., Gensheimer, H. P., & Gobel, C. (1985). cGMP-dependent protein kinase. Autophosphorylation changes the characteristics of binding site 1. *Eur.J.Biochem.* **147**, 361-365.
- Hohman, R. J., Hultsch, T., & Talbot, E. (1990). IgE receptor-mediated phosphatidylinositol hydrolysis and exocytosis from rat basophilic leukemia cells are independent of extracellular Ca²⁺ in a hypotonic buffer containing a high concentration of K⁺. *J.Immunol.* **145**, 3876-3882.
- Huber, S. M., Gamper, N., & Lang, F. (2001). Chloride conductance and volume-regulatory nonselective cation conductance in human red blood cell ghosts. *Pflugers Arch.* **441**, 551-558.
- Ikuta, T., Ausenda, S., & Cappellini, M. D. (2001). Mechanism for fetal globin gene expression: role of the soluble guanylate cyclase-cGMP-dependent protein kinase pathway. *Proc.Natl.Acad.Sci.U.S.A* **98**, 1847-1852.
- Inohara, N., Ogura, Y., & Nunez, G. (2002). Nods: a family of cytosolic proteins that regulate the host response to pathogens. *Curr.Opin.Microbiol.* **5**, 76-80.
- Ishii, K., Hamamoto, H., Kamimura, M., & Sekimizu, K. (2007). Activation of the silkworm cytokine by bacterial and fungal cell wall components via a reactive oxygen species-triggered mechanism. *J Biol Chem.*
- Iwaki, D., Mitsuzawa, H., Murakami, S., Sano, H., Konishi, M., Akino, T., & Kuroki, Y. (2002). The extracellular toll-like receptor 2 domain directly binds peptidoglycan derived from *Staphylococcus aureus*. *J.Biol.Chem.* **277**, 24315-24320.
- Jacobs, W. A. & Craig, L. C. (1935). THE ERGOT ALKALOIDS. SYNTHESIS OF 4-CARBOLINE CARBONIC ACIDS. *Science* **82**, 421-422.
- James, S. R., Downes, C. P., Gigg, R., Grove, S. J., Holmes, A. B., & Alessi, D. R. (1996). Specific binding of the Akt-1 protein kinase to phosphatidylinositol 3,4,5-trisphosphate without subsequent activation. *Biochem.J.* **315 (Pt 3)**, 709-713.

Janeway, C. A., Jr. & Medzhitov, R. (2002). Innate immune recognition. *Annu.Rev.Immunol.* **20**, 197-216.

Jennings, M. L. (1999). Volume-sensitive K(+)/Cl(-) cotransport in rabbit erythrocytes. Analysis of the rate-limiting activation and inactivation events. *J.Gen.Physiol* **114**, 743-758.

Jennings, M. L. & Adame, M. F. (2001). Direct estimate of 1:1 stoichiometry of K(+)-Cl(-) cotransport in rabbit erythrocytes. *Am.J.Physiol Cell Physiol* **281**, C825-C832.

Jennings, M. L. & al Rohil, N. (1990). Kinetics of activation and inactivation of swelling-stimulated K+/Cl- transport. The volume-sensitive parameter is the rate constant for inactivation. *J.Gen.Physiol* **95**, 1021-1040.

Johnstone, R. M., Adam, M., Hammond, J. R., Orr, L., & Turbide, C. (1987). Vesicle formation during reticulocyte maturation. Association of plasma membrane activities with released vesicles (exosomes). *J.Biol.Chem.* **262**, 9412-9420.

Johnstone, R. M. & Ahn, J. (1990). A common mechanism may be involved in the selective loss of plasma membrane functions during reticulocyte maturation. *Biomed.Biochim.Acta* **49**, S70-S75.

Johnstone, R. M., Bianchini, A., & Teng, K. (1989). Reticulocyte maturation and exosome release: transferrin receptor containing exosomes shows multiple plasma membrane functions. *Blood* **74**, 1844-1851.

Johnstone, R. M., Mathew, A., Mason, A. B., & Teng, K. (1991). Exosome formation during maturation of mammalian and avian reticulocytes: evidence that exosome release is a major route for externalization of obsolete membrane proteins. *J.Cell Physiol* **147**, 27-36.

Joiner, C. H., Jiang, M., Fathallah, H., Giraud, F., & Franco, R. S. (1998). Deoxygenation of sickle red blood cells stimulates KCl cotransport without affecting Na⁺/H⁺ exchange. *Am.J.Physiol* **274**, C1466-C1475.

Joiner, C. H. & Lauf, P. K. (1978). The correlation between ouabain binding and potassium pump inhibition in human and sheep erythrocytes. *J.Physiol* **283**, 155-175.

Joiner, C. H., Platt, O. S., & Lux, S. E. (1986). Cation depletion by the sodium pump in red cells with pathologic cation leaks. Sick cells and xerocytes. *J.Clin.Invest* **78**, 1487-1496.

Kaestner, L., Christophersen, P., Bernhardt, I., & Bennekou, P. (2000). The non-selective voltage-activated cation channel in the human red blood cell membrane: reconciliation between two conflicting reports and further characterisation. *Bioelectrochemistry*. **52**, 117-125.

Kang, D., Liu, G., Lundstrom, A., Gelius, E., & Steiner, H. (1998). A peptidoglycan recognition protein in innate immunity conserved from insects to humans. *Proc.Natl.Acad.Sci.U.S.A* **95**, 10078-10082.

Kapral, F. A., Godwin, J. R., & Dye, E. S. (1980). Formation of intraperitoneal abscesses by *Staphylococcus aureus*. *Infect.Immun.* **30**, 204-211.

Keglevic, D., Ladesic, B., Hadzija, O., Tomasic, J., Valinger, Z., Pokorny, M., & Naumski, R. (1974). Isolation and study of the composition of a peptidoglycan complex excreted by the biotin-requiring mutant of *Brevibacterium divaricatum* NRRL-2311 in the presence of penicillin. *Eur J Biochem* **42**, 389-400.

Kempe, D. S., Akel, A., Lang, P. A., Hermle, T., Biswas, R., Muresanu, J., Friedrich, B., Dreischer, P., Wolz, C., Schumacher, U., Peschel, A., Gotz, F., Doring, G., Wieder, T., Gulbins, E., & Lang, F. (2007). Suicidal erythrocyte death in sepsis. *J.Mol.Med.* **85**, 273-281.

Kempe, D. S., Lang, P. A., Duranton, C., Akel, A., Lang, K. S., Huber, S. M., Wieder, T., & Lang, F. (2006). Enhanced programmed cell death of iron-deficient erythrocytes. *FASEB J.* **20**, 368-370.

Kempe, D. S., Lang, P. A., Eisele, K., Klarl, B. A., Wieder, T., Huber, S. M., Duranton, C., & Lang, F. (2005). Stimulation of erythrocyte phosphatidylserine exposure by lead ions. *Am.J.Physiol Cell Physiol* **288**, C396-C402.

Kepler, T. B. & Chan, C. (2007). Spatiotemporal programming of a simple inflammatory process. *Immunol.Rev.* **216**, 153-163.

Kiefer, C. R. & Snyder, L. M. (2000). Oxidation and erythrocyte senescence. *Curr.Opin.Hematol.* **7**, 113-116.

Kina, T., Ikuta, K., Takayama, E., Wada, K., Majumdar, A. S., Weissman, I. L., & Katsura, Y. (2000). The monoclonal antibody TER-119 recognizes a molecule associated with glycophorin A and specifically marks the late stages of murine erythroid lineage. *Br.J.Haematol.* **109**, 280-287.

Klainer, A. S., Chang, T. W., & Weinstein, L. (1972). Effects of purified staphylococcal alpha toxin on the ultrastructure of human and rabbit erythrocytes. *Infect.Immun.* **5**, 808-813.

Klarl, B. A., Lang, P. A., Kempe, D. S., Niemoeller, O. M., Akel, A., Sobiesiak, M., Eisele, K., Podolski, M., Huber, S. M., Wieder, T., & Lang, F. (2006). Protein kinase C mediates erythrocyte "programmed cell death" following glucose depletion. *Am.J.Physiol Cell Physiol* **290**, C244-C253.

Kleinbongard, P., Schulz, R., Rassaf, T., Lauer, T., Dejam, A., Jax, T., Kumara, I., Gharini, P., Kabanova, S., Ozuyaman, B., Schnurch, H. G., Godecke, A., Weber, A. A., Robenek, M., Robenek, H., Bloch, W., Rosen, P., & Kelm, M. (2006). Red blood cells express a functional endothelial nitric oxide synthase. *Blood* **107**, 2943-2951.

Kluytmans, J., van Belkum, A., & Verbrugh, H. (1997). Nasal carriage of *Staphylococcus aureus*: epidemiology, underlying mechanisms, and associated risks. *Clin.Microbiol.Rev.* **10**, 505-520.

Kwan, H. Y., Huang, Y., & Yao, X. (2006). Protein kinase C can inhibit TRPC3 channels indirectly via stimulating protein kinase G. *J.Cell Physiol* **207**, 315-321.

Lang, F., Bohmer, C., Palmada, M., Seebohm, G., Strutz-Seebohm, N., & Vallon, V. (2006a). (Patho)physiological significance of the serum- and glucocorticoid-inducible kinase isoforms. *Physiol Rev* **86**, 1151-1178.

Lang, F., Busch, G. L., Ritter, M., Volkl, H., Waldegger, S., Gulbins, E., & Haussinger, D. (1998a). Functional significance of cell volume regulatory mechanisms. *Physiol Rev.* **78**, 247-306.

Lang, F. & Cohen, P. (2001). Regulation and physiological roles of serum- and glucocorticoid-induced protein kinase isoforms. *Sci STKE.* **2001**, RE17.

Lang, F., Lang, K. S., Wieder, T., Myssina, S., Birka, C., Lang, P. A., Kaiser, S., Kempe, D., Duranton, C., & Huber, S. M. (2003a). Cation channels, cell volume and the death of an erythrocyte. *Pflugers Arch.* **447**, 121-125.

Lang, F., Madlung, J., Bock, J., Lukewille, U., Kaltenbach, S., Lang, K. S., Belka, C., Wagner, C. A., Lang, H. J., Gulbins, E., & Lepple-Wienhues, A. (2000). Inhibition of Jurkat-T-lymphocyte Na⁺/H⁺-exchanger by CD95(Fas/Apo-1)-receptor stimulation. *Pflugers Arch.* **440**, 902-907.

- Lang, F., Madlung, J., Uhlemann, A. C., Risler, T., & Gulbins, E. (1998b). Cellular taurine release triggered by stimulation of the Fas(CD95) receptor in Jurkat lymphocytes. *Pflugers Arch.* **436**, 377-383.
- Lang, K. S., Durantou, C., Poehlmann, H., Myssina, S., Bauer, C., Lang, F., Wieder, T., & Huber, S. M. (2003b). Cation channels trigger apoptotic death of erythrocytes. *Cell Death.Differ.* **10**, 249-256.
- Lang, K. S., Lang, P. A., Bauer, C., Durantou, C., Wieder, T., Huber, S. M., & Lang, F. (2005a). Mechanisms of suicidal erythrocyte death. *Cell Physiol Biochem.* **15**, 195-202.
- Lang, K. S., Myssina, S., Brand, V., Sandu, C., Lang, P. A., Berchtold, S., Huber, S. M., Lang, F., & Wieder, T. (2004a). Involvement of ceramide in hyperosmotic shock-induced death of erythrocytes. *Cell Death.Differ.* **11**, 231-243.
- Lang, K. S., Myssina, S., Tanneur, V., Wieder, T., Huber, S. M., Lang, F., & Durantou, C. (2003c). Inhibition of erythrocyte cation channels and apoptosis by ethylisopropylamiloride. *Naunyn Schmiedebergs Arch.Pharmacol.* **367**, 391-396.
- Lang, K. S., Roll, B., Myssina, S., Schittenhelm, M., Scheel-Walter, H. G., Kanz, L., Fritz, J., Lang, F., Huber, S. M., & Wieder, T. (2002). Enhanced erythrocyte apoptosis in sickle cell anemia, thalassemia and glucose-6-phosphate dehydrogenase deficiency. *Cell Physiol Biochem.* **12**, 365-372.
- Lang, P. A., Beringer, O., Nicolay, J. P., Amon, O., Kempe, D. S., Hermle, T., Attanasio, P., Akel, A., Schafer, R., Friedrich, B., Risler, T., Baur, M., Olbricht, C. J., Zimmerhackl, L. B., Zipfel, P. F., Wieder, T., & Lang, F. (2006b). Suicidal death of erythrocytes in recurrent hemolytic uremic syndrome. *J.Mol.Med.* **84**, 378-388.
- Lang, P. A., Huober, J., Bachmann, C., Kempe, D. S., Sobiesiak, M., Akel, A., Niemoeller, O. M., Dreischer, P., Eisele, K., Klarl, B. A., Gulbins, E., Lang, F., & Wieder, T. (2006c). Stimulation of erythrocyte phosphatidylserine exposure by paclitaxel. *Cell Physiol Biochem.* **18**, 151-164.
- Lang, P. A., Kaiser, S., Myssina, S., Birka, C., Weinstock, C., Northoff, H., Wieder, T., Lang, F., & Huber, S. M. (2004b). Effect of *Vibrio parahaemolyticus* haemolysin on human erythrocytes. *Cell Microbiol.* **6**, 391-400.
- Lang, P. A., Kaiser, S., Myssina, S., Wieder, T., Lang, F., & Huber, S. M. (2003d). Role of Ca²⁺-activated K⁺ channels in human erythrocyte apoptosis. *Am.J.Physiol Cell Physiol* **285**, C1553-C1560.

Lang, P. A., Kempe, D. S., Myssina, S., Tanneur, V., Birka, C., Laufer, S., Lang, F., Wieder, T., & Huber, S. M. (2005b). PGE(2) in the regulation of programmed erythrocyte death. *Cell Death Differ* **12**, 415-428.

Lang, P. A., Schenck, M., Nicolay, J. P., Becker, J. U., Kempe, D. S., Lupescu, A., Koka, S., Eisele, K., Klarl, B. A., Rubben, H., Schmid, K. W., Mann, K., Hildenbrand, S., Hefter, H., Huber, S. M., Wieder, T., Erhardt, A., Haussinger, D., Gulbins, E., & Lang, F. (2007). Liver cell death and anemia in Wilson disease involve acid sphingomyelinase and ceramide. *Nat.Med.* **13**, 164-170.

Laris, P. C. & Hoffman, J. F. (1986). Optical determination of electrical properties of red blood cell and Ehrlich ascites tumor cell membranes with fluorescent dyes. *Soc.Gen.Physiol Ser.* **40**, 199-210.

Lauf, P. K. (1985). K⁺:Cl⁻ cotransport: sulfhydryls, divalent cations, and the mechanism of volume activation in a red cell. *J.Membr.Biol.* **88**, 1-13.

Lauf, P. K., Bauer, J., Adragna, N. C., Fujise, H., Zade-Oppen, A. M., Ryu, K. H., & Delpire, E. (1992). Erythrocyte K-Cl cotransport: properties and regulation. *Am.J.Physiol* **263**, C917-C932.

Lauf, P. K. & Theg, B. E. (1980). A chloride dependent K⁺ flux induced by N-ethylmaleimide in genetically low K⁺ sheep and goat erythrocytes. *Biochem.Biophys.Res.Commun.* **92**, 1422-1428.

Lawlor, M. A., Mora, A., Ashby, P. R., Williams, M. R., Murray-Tait, V., Malone, L., Prescott, A. R., Lucocq, J. M., & Alessi, D. R. (2002). Essential role of PDK1 in regulating cell size and development in mice. *EMBO J.* **21**, 3728-3738.

Lee, M. H., Osaki, T., Lee, J. Y., Baek, M. J., Zhang, R., Park, J. W., Kawabata, S., Soderhall, K., & Lee, B. L. (2004). Peptidoglycan recognition proteins involved in 1,3-beta-D-glucan-dependent prophenoloxidase activation system of insect. *J Biol Chem.* **279**, 3218-3227.

Leinders, T., van Kleef, R. G., & Vijverberg, H. P. (1992). Single Ca(2⁺)-activated K⁺ channels in human erythrocytes: Ca²⁺ dependence of opening frequency but not of open lifetimes. *Biochim.Biophys.Acta* **1112**, 67-74.

Lepple-Wienhues, A., Belka, C., Laun, T., Jekle, A., Walter, B., Wieland, U., Welz, M., Heil, L., Kun, J., Busch, G., Weller, M., Bamberg, M., Gulbins, E., & Lang, F. (1999). Stimulation of CD95 (Fas) blocks T lymphocyte calcium channels through sphingomyelinase and sphingolipids. *Proc.Natl.Acad.Sci.U.S.A* **96**, 13795-13800.

Lew, V. L. & Bookchin, R. M. (1986). Volume, pH, and ion-content regulation in human red cells: analysis of transient behavior with an integrated model. *J.Membr.Biol.* **92**, 57-74.

Lew, V. L. & Bookchin, R. M. (2005). Ion transport pathology in the mechanism of sickle cell dehydration. *Physiol Rev.* **85**, 179-200.

Lew, V. L., Daw, N., Etzion, Z., Tiffert, T., Muoma, A., Vanagas, L., & Bookchin, R. M. (2007). Effects of age-dependent membrane transport changes on the homeostasis of senescent human red blood cells. *Blood* **110**, 1334-1342.

Lew, V. L., Daw, N., Perdomo, D., Etzion, Z., Bookchin, R. M., & Tiffert, T. (2003). Distribution of plasma membrane Ca²⁺ pump activity in normal human red blood cells. *Blood* **102**, 4206-4213.

Lew, V. L. & Ferreira, H. G. (1976). Variable Ca sensitivity of a K-selective channel in intact red-cell membranes. *Nature* **263**, 336-338.

Lew, V. L., Muallem, S., & Seymour, C. A. (1982a). Properties of the Ca²⁺-activated K⁺ channel in one-step inside-out vesicles from human red cell membranes. *Nature* **296**, 742-744.

Lew, V. L., Ortiz, O. E., & Bookchin, R. M. (1997). Stochastic nature and red cell population distribution of the sickling-induced Ca²⁺ permeability. *J.Clin.Invest* **99**, 2727-2735.

Lew, V. L., Tiffert, T., Etzion, Z., Perdomo, D., Daw, N., Macdonald, L., & Bookchin, R. M. (2005). Distribution of dehydration rates generated by maximal Gardos-channel activation in normal and sickle red blood cells. *Blood* **105**, 361-367.

Lew, V. L., Tsien, R. Y., Miner, C., & Bookchin, R. M. (1982b). Physiological [Ca²⁺]_i level and pump-leak turnover in intact red cells measured using an incorporated Ca chelator. *Nature* **298**, 478-481.

Li, J. & Billiar, T. R. (1999). The anti-apoptotic actions of nitric oxide in hepatocytes. *Cell Death.Differ.* **6**, 952-955.

Liu, C., Xu, Z., Gupta, D., & Dziarski, R. (2001). Peptidoglycan recognition proteins: a novel family of four human innate immunity pattern recognition molecules. *J.Biol.Chem.* **276**, 34686-34694.

Liu, L. & Stamler, J. S. (1999). NO: an inhibitor of cell death. *Cell Death.Differ.* **6**, 937-942.

Liu, X. H., Kirschenbaum, A., Yu, K., Yao, S., & Levine, A. C. (2005). Cyclooxygenase-2 suppresses hypoxia-induced apoptosis via a combination of direct and indirect inhibition of p53 activity in a human prostate cancer cell line. *J Biol Chem.* **280**, 3817-3823.

Lux, S. E. (1979). Spectrin-actin membrane skeleton of normal and abnormal red blood cells. *Semin.Hematol.* **16**, 21-51.

Maeno, E., Ishizaki, Y., Kanaseki, T., Hazama, A., & Okada, Y. (2000). Normotonic cell shrinkage because of disordered volume regulation is an early prerequisite to apoptosis. *Proc.Natl.Acad.Sci.U.S.A* **97**, 9487-9492.

Maher, A. D. & Kuchel, P. W. (2003). The Gardos channel: a review of the Ca²⁺-activated K⁺ channel in human erythrocytes. *Int.J.Biochem.Cell Biol.* **35**, 1182-1197.

McMahon, T. J., Moon, R. E., Lusching, B. P., Carraway, M. S., Stone, A. E., Stolp, B. W., Gow, A. J., Pawloski, J. R., Watke, P., Singel, D. J., Piantadosi, C. A., & Stamler, J. S. (2002). Nitric oxide in the human respiratory cycle. *Nat.Med.* **8**, 711-717.

Medzhitov, R. (2001). Toll-like receptors and innate immunity. *Nat.Rev.Immunol.* **1**, 135-145.

Michea, L., Ferguson, D. R., Peters, E. M., Andrews, P. M., Kirby, M. R., & Burg, M. B. (2000). Cell cycle delay and apoptosis are induced by high salt and urea in renal medullary cells. *Am J Physiol Renal Physiol* **278**, F209-F218.

Mirelman, D., Bracha, R., & Sharon, N. (1974). Penicillin-induced secretion of soluble, uncross-linked peptidoglycan by *Micrococcus luteus* cells. *Biochemistry* **13**, 5045-5053.

Mitsuzawa, H., Wada, I., Sano, H., Iwaki, D., Murakami, S., Himi, T., Matsushima, N., & Kuroki, Y. (2001). Extracellular Toll-like receptor 2 region containing Ser40-Ile64 but not Cys30-Ser39 is critical for the recognition of *Staphylococcus aureus* peptidoglycan. *J.Biol.Chem.* **276**, 41350-41356.

Moran, J., Hernandez-Pech, X., Merchant-Larios, H., & Pasantes-Morales, H. (2000). Release of taurine in apoptotic cerebellar granule neurons in culture. *Pflugers Arch.* **439**, 271-277.

- Munzel, T., Feil, R., Mulsch, A., Lohmann, S. M., Hofmann, F., & Walter, U. (2003). Physiology and pathophysiology of vascular signaling controlled by guanosine 3',5'-cyclic monophosphate-dependent protein kinase [corrected]. *Circulation* **108**, 2172-2183.
- Nagai-Kusuhara, A., Nakamura, M., Mukuno, H., Kanamori, A., Negi, A., & Seigel, G. M. (2007). cAMP-responsive element binding protein mediates a cGMP/protein kinase G-dependent anti-apoptotic signal induced by nitric oxide in retinal neuro-glial progenitor cells. *Exp. Eye Res.* **84**, 152-162.
- Nagy, A., Rossant, J., Nagy, R., Abramow-Newerly, W., & Roder, J. C. (1993). Derivation of completely cell culture-derived mice from early-passage embryonic stem cells. *Proc. Natl. Acad. Sci. U.S.A* **90**, 8424-8428.
- Namba, T., Ishii, T. M., Ikeda, M., Hisano, T., Itoh, T., Hirota, K., Adelman, J. P., & Fukuda, K. (2000). Inhibition of the human intermediate conductance Ca(2+)-activated K(+) channel, hIK1, by volatile anesthetics. *Eur. J. Pharmacol.* **395**, 95-101.
- Nicolay, J. P., Liebig, G., Niemoeller, O. M., Koka, S., Ghashghaieinia, M., Wieder, T., Haendeler, J., Busse, R., & Lang, F. (2007). Inhibition of suicidal erythrocyte death by nitric oxide. *Pflugers Arch.*
- Nicolay, J. P., Schneider, J., Niemoeller, O. M., Artunc, F., Portero-Otin, M., Haik, G., Jr., Thornalley, P. J., Schleicher, E., Wieder, T., & Lang, F. (2006). Stimulation of suicidal erythrocyte death by methylglyoxal. *Cell Physiol Biochem.* **18**, 223-232.
- Niemoeller, O. M., Akel, A., Lang, P. A., Attanasio, P., Kempe, D. S., Hermle, T., Sobiesiak, M., Wieder, T., & Lang, F. (2006b). Induction of eryptosis by cyclosporine. *Naunyn Schmiedebergs Arch. Pharmacol.* **374**, 41-49.
- Niemoeller, O. M., Akel, A., Lang, P. A., Attanasio, P., Kempe, D. S., Hermle, T., Sobiesiak, M., Wieder, T., & Lang, F. (2006a). Induction of eryptosis by cyclosporine. *Naunyn Schmiedebergs Arch. Pharmacol.* **374**, 41-49.
- Niemoeller, O. M., Kiedaisch, V., Dreischer, P., Wieder, T., & Lang, F. (2006c). Stimulation of eryptosis by aluminium ions. *Toxicol. Appl. Pharmacol.* **217**, 168-175.
- Offen, D., Ziv, I., Gorodin, S., Barzilai, A., Malik, Z., & Melamed, E. (1995). Dopamine-induced programmed cell death in mouse thymocytes. *Biochim. Biophys Acta* **1268**, 171-177.

Okada, Y., Maeno, E., Shimizu, T., Dezaki, K., Wang, J., & Morishima, S. (2001). Receptor-mediated control of regulatory volume decrease (RVD) and apoptotic volume decrease (AVD). *J Physiol* **532**, 3-16.

Pal, S., He, K., & Aizenman, E. (2004). Nitrosative stress and potassium channel-mediated neuronal apoptosis: is zinc the link? *Pflugers Arch* **448**, 296-303.

Palek, J. & Lambert, S. (1990). Genetics of the red cell membrane skeleton. *Semin.Hematol.* **27**, 290-332.

Palek, J. & Liu, S. C. (1979). Membrane protein organization in ATP-depleted and irreversibly sickled red cells. *J.Supramol.Struct.* **10**, 79-96.

Palmada, M., Poppendieck, S., Embark, H. M., van de Graaf, S. F., Boehmer, C., Bindels, R. J., & Lang, F. (2005). Requirement of PDZ domains for the stimulation of the epithelial Ca²⁺ channel TRPV5 by the NHE regulating factor NHERF2 and the serum and glucocorticoid inducible kinase SGK1. *Cell Physiol Biochem* **15**, 175-182.

Pattee, P. A. (1986). Chromosomal map location of the alpha-hemolysin structural gene in *Staphylococcus aureus* NCTC 8325. *Infect.Immun.* **54**, 593-596.

Pawloski, J. R., Hess, D. T., & Stamler, J. S. (2005). Impaired vasodilation by red blood cells in sickle cell disease. *Proc.Natl.Acad.Sci.U.S.A* **102**, 2531-2536.

Pellegrino, M. & Pellegrini, M. (1998). Modulation of Ca²⁺-activated K⁺ channels of human erythrocytes by endogenous cAMP-dependent protein kinase. *Pflugers Arch.* **436**, 749-756.

Petersen, O. H. & Maruyama, Y. (1984). Calcium-activated potassium channels and their role in secretion. *Nature* **307**, 693-696.

Pfeifer, A., Klatt, P., Massberg, S., Ny, L., Sausbier, M., Hirneiss, C., Wang, G. X., Korth, M., Aszodi, A., Andersson, K. E., Krombach, F., Mayerhofer, A., Ruth, P., Fassler, R., & Hofmann, F. (1998). Defective smooth muscle regulation in cGMP kinase I-deficient mice. *EMBO J.* **17**, 3045-3051.

Pfeifer, A., Ruth, P., Dostmann, W., Sausbier, M., Klatt, P., & Hofmann, F. (1999). Structure and function of cGMP-dependent protein kinases. *Rev.Physiol Biochem.Pharmacol.* **135**, 105-149.

Post, R. L. (1974). A reminiscence about sodium, potassium-ATPase. *Ann.N.Y.Acad.Sci.* **242**, 6-11.

Post, R. L., Albright, C. D., & Dayani, K. (1967). Resolution of pump and leak components of sodium and potassium ion transport in human erythrocytes. *J.Gen.Physiol* **50**, 1201-1220.

Power, G. G., Bragg, S. L., Oshiro, B. T., Dejam, A., Hunter, C. J., & Blood, A. B. (2007). A novel method of measuring reduction of nitrite-induced methemoglobin applied to fetal and adult blood of humans and sheep. *J.Appl.Physiol* **103**, 1359-1365.

Prehn, J. H., Jordan, J., Ghadge, G. D., Preis, E., Galindo, M. F., Roos, R. P., Krieglstein, J., & Miller, R. J. (1997). Ca²⁺ and reactive oxygen species in staurosporine-induced neuronal apoptosis. *J Neurochem* **68**, 1679-1685.

Pullen, N., Dennis, P. B., Andjelkovic, M., Dufner, A., Kozma, S. C., Hemmings, B. A., & Thomas, G. (1998). Phosphorylation and activation of p70s6k by PDK1. *Science* **279**, 707-710.

Rashatwar, S. S., Cornwell, T. L., & Lincoln, T. M. (1987). Effects of 8-bromo-cGMP on Ca²⁺ levels in vascular smooth muscle cells: possible regulation of Ca²⁺-ATPase by cGMP-dependent protein kinase. *Proc.Natl.Acad.Sci.U.S.A* **84**, 5685-5689.

Reichwein, J., Hugo, F., Roth, M., Sinner, A., & Bhakdi, S. (1987). Quantitative analysis of the binding and oligomerization of staphylococcal alpha-toxin in target erythrocyte membranes. *Infect.Immun.* **55**, 2940-2944.

Rexhepaj, R., Grahammer, F., Volkl, H., Remy, C., Wagner, C. A., Sandulache, D., Artunc, F., Henke, G., Nammi, S., Capasso, G., Alessi, D. R., & Lang, F. (2006). Reduced intestinal and renal amino acid transport in PDK1 hypomorphic mice. *FASEB J* **20**, 2214-2222.

Reynolds, J. D., Ahearn, G. S., Angelo, M., Zhang, J., Cobb, F., & Stamler, J. S. (2007). S-nitrosohemoglobin deficiency: a mechanism for loss of physiological activity in banked blood. *Proc.Natl.Acad.Sci.U.S.A* **104**, 17058-17062.

Rogolsky, M. (1979). Nonenteric toxins of *Staphylococcus aureus*. *Microbiol.Rev.* **43**, 320-360.

Romero, P. J. & Rojas, L. (1992). The effect of ATP on Ca(2+)-dependent K⁺ channels of human red cells. *Acta Cient.Venez.* **43**, 19-25.

Romero, P. J. & Romero, E. A. (1999). Effect of cell ageing on Ca²⁺ influx into human red cells. *Cell Calcium* **26**, 131-137.

Rosenthal, R. S. & Dziarski, R. (1994a). Isolation of peptidoglycan and soluble peptidoglycan fragments. *Methods Enzymol.* **235**, 253-285.

Rosenthal, R. S. & Dziarski, R. (1994b). Isolation of peptidoglycan and soluble peptidoglycan fragments. *Methods Enzymol.* **235**, 253-285.

Rosette, C. & Karin, M. (1996). Ultraviolet light and osmotic stress: activation of the JNK cascade through multiple growth factor and cytokine receptors. *Science* **274**, 1194-1197.

Rotoli, B. M., Uggeri, J., Dall'Asta, V., Visigalli, R., Barilli, A., Gatti, R., Orlandini, G., Gazzola, G. C., & Bussolati, O. (2005). Inhibition of glutamine synthetase triggers apoptosis in asparaginase-resistant cells. *Cell Physiol Biochem* **15**, 281-292.

Ruth, P., Pfeifer, A., Kamm, S., Klatt, P., Dostmann, W. R., & Hofmann, F. (1997). Identification of the amino acid sequences responsible for high affinity activation of cGMP kinase Ialpha. *J.Biol.Chem.* **272**, 10522-10528.

Salido, M., Vilches, J., Lopez, A., & Roomans, G. M. (2001). X-ray microanalysis of etoposide-induced apoptosis in the PC-3 prostatic cancer cell line. *Cell Biol Int* **25**, 499-508.

Sandu, C., Artunc, F., Palmada, M., Rexhepaj, R., Grahammer, F., Hussain, A., Yun, C., Alessi, D. R., & Lang, F. (2006). Impaired intestinal NHE3 activity in the PDK1 hypomorphic mouse. *Am J Physiol Gastrointest.Liver Physiol* **291**, G868-G876.

Sausbier, M., Matos, J. E., Sausbier, U., Beranek, G., Arntz, C., Neuhuber, W., Ruth, P., & Leipziger, J. (2006). Distal colonic K(+) secretion occurs via BK channels. *J.Am.Soc.Nephrol.* **17**, 1275-1282.

Scharff, O. & Foder, B. (1989). Halothane inhibits hyperpolarization and potassium channels in human red blood cells. *Eur.J.Pharmacol.* **159**, 165-173.

Scheel, O., Papavlassopoulos, M., Blunck, R., Gebert, A., Hartung, T., Zahringer, U., Seydel, U., & Schromm, A. B. (2006). Cell activation by ligands of the toll-like receptor and interleukin-1 receptor family depends on the function of the large-conductance potassium channel MaxiK in human macrophages. *Infect.Immun.* **74**, 4354-4356.

Schleifer, K. H. & Kandler, O. (1972). Peptidoglycan types of bacterial cell walls and their taxonomic implications. *Bacteriol.Rev.* **36**, 407-477.

Schneider, J., Nicolay, J. P., Foller, M., Wieder, T., & Lang, F. (2007). Suicidal erythrocyte death following cellular K⁺ loss. *Cell Physiol Biochem.* **20**, 35-44.

Schroit, A. J., Madsen, J. W., & Tanaka, Y. (1985). In vivo recognition and clearance of red blood cells containing phosphatidylserine in their plasma membranes. *J.Biol.Chem.* **260**, 5131-5138.

Schwandner, R., Dziarski, R., Wesche, H., Rothe, M., & Kirschning, C. J. (1999). Peptidoglycan- and lipoteichoic acid-induced cell activation is mediated by toll-like receptor 2. *J.Biol.Chem.* **274**, 17406-17409.

Sessler, C. N., Perry, J. C., & Varney, K. L. (2004). Management of severe sepsis and septic shock. *Curr.Opin.Crit Care* **10**, 354-363.

Siegel, I. & COHEN, S. (1964). ACTION OF STAPHYLOCOCCAL TOXIN ON HUMAN PLATELETS. *J.Infect.Dis.* **114**, 488-502.

Sillix, D. H. & McDonald, F. D. (1987). Acute renal failure. *Crit Care Clin.* **3**, 909-925.

Simons, M. P., Moore, J. M., Kemp, T. J., & Griffith, T. S. (2007). Identification of the mycobacterial subcomponents involved in the release of tumor necrosis factor-related apoptosis-inducing ligand from human neutrophils. *Infect.Immun.* **75**, 1265-1271.

Simons, T. J. (1976). Calcium-dependent potassium exchange in human red cell ghosts. *J.Physiol* **256**, 227-244.

Skou, J. C. & Esmann, M. (1992). The Na,K-ATPase. *J.Bioenerg.Biomembr.* **24**, 249-261.

Song, L., Hobaugh, M. R., Shustak, C., Cheley, S., Bayley, H., & Gouaux, J. E. (1996). Structure of staphylococcal alpha-hemolysin, a heptameric transmembrane pore. *Science* **274**, 1859-1866.

Sopjani, M., Foller, M., & Lang, F. (2007). Gold stimulates Ca²⁺ entry into and subsequent suicidal death of erythrocytes. *Toxicology.*

Stampe, P. & Vestergaard-Bogind, B. (1989). Ca²⁺-activated K⁺ conductance of the human red cell membrane: voltage-dependent Na⁺ block of outward-going currents. *J.Membr.Biol.* **112**, 9-14.

Steck, T. L. (1974). The organization of proteins in the human red blood cell membrane. A review. *J.Cell Biol.* **62**, 1-19.

Stephens, L., Anderson, K., Stokoe, D., Erdjument-Bromage, H., Painter, G. F., Holmes, A. B., Gaffney, P. R., Reese, C. B., McCormick, F., Tempst, P., Coadwell, J., & Hawkins, P. T. (1998). Protein kinase B kinases that mediate phosphatidylinositol 3,4,5-trisphosphate-dependent activation of protein kinase B. *Science* **279**, 710-714.

Stephens, L. R., Jackson, T. R., & Hawkins, P. T. (1993). Agonist-stimulated synthesis of phosphatidylinositol(3,4,5)-trisphosphate: a new intracellular signalling system? *Biochim.Biophys.Acta* **1179**, 27-75.

Storey, N. M., Gomez-Angelats, M., Bortner, C. D., Armstrong, D. L., & Cidlowski, J. A. (2003). Stimulation of Kv1.3 potassium channels by death receptors during apoptosis in Jurkat T lymphocytes. *J Biol Chem.* **278**, 33319-33326.

Sturm, J. W., Zhang, H., Magdeburg, R., Hasenberg, T., Bonninghoff, R., Oulmi, J., Keese, M., & McCuskey, R. (2004). Altered apoptotic response and different liver structure during liver regeneration in FGF-2-deficient mice. *Cell Physiol Biochem* **14**, 249-260.

Szabo, I., Lepple-Wienhues, A., Kaba, K. N., Zoratti, M., Gulbins, E., & Lang, F. (1998). Tyrosine kinase-dependent activation of a chloride channel in CD95-induced apoptosis in T lymphocytes. *Proc.Natl.Acad.Sci.U.S.A* **95**, 6169-6174.

Takahashi, N., Wang, X., Tanabe, S., Uramoto, H., Jishage, K., Uchida, S., Sasaki, S., & Okada, Y. (2005). ClC-3-independent sensitivity of apoptosis to Cl⁻ channel blockers in mouse cardiomyocytes. *Cell Physiol Biochem* **15**, 263-270.

Tanaka, Y. & Schroit, A. J. (1983). Insertion of fluorescent phosphatidylserine into the plasma membrane of red blood cells. Recognition by autologous macrophages. *J.Biol.Chem.* **258**, 11335-11343.

Thelestam, M. & Mollby, R. (1975). Determination of toxin-induced leakage of different-size nucleotides through the plasma membrane of human diploid fibroblasts. *Infect.Immun.* **11**, 640-648.

Tiedt, R., Schomber, T., Hao-Shen, H., & Skoda, R. C. (2007). Pf4-Cre transgenic mice allow the generation of lineage-restricted gene knockouts for studying megakaryocyte and platelet function in vivo. *Blood* **109**, 1503-1506.

Tiffert, T., Etzion, Z., Bookchin, R. M., & Lew, V. L. (1993). Effects of deoxygenation on active and passive Ca²⁺ transport and cytoplasmic Ca²⁺ buffering in normal human red cells. *J.Physiol* **464**, 529-544.

Tiffert, T. & Lew, V. L. (1997). Cytoplasmic calcium buffers in intact human red cells. *J.Physiol* **500 (Pt 1)**, 139-154.

Tiffert, T., Spivak, J. L., & Lew, V. L. (1988). Magnitude of calcium influx required to induce dehydration of normal human red cells. *Biochim.Biophys.Acta* **943**, 157-165.

Tynecka, Z. & Ward, J. B. (1975). Peptidoglycan synthesis in *Bacillus licheniformis*. The inhibition of cross-linking by benzylpenicillin and cephaloridine in vivo accompanied by the formation of soluble peptidoglycan. *Biochem J* **146**, 253-267.

Underhill, D. M., Ozinsky, A., Hajjar, A. M., Stevens, A., Wilson, C. B., Bassetti, M., & Aderem, A. (1999). The Toll-like receptor 2 is recruited to macrophage phagosomes and discriminates between pathogens. *Nature* **401**, 811-815.

Vaandrager, A. B., Hogema, B. M., Edixhoven, M., van den Burg, C. M., Bot, A. G., Klatt, P., Ruth, P., Hofmann, F., Van Damme, J., Vandekerckhove, J., & de Jonge, H. R. (2003). Autophosphorylation of cGMP-dependent protein kinase type II. *J.Biol.Chem.* **278**, 28651-28658.

Valera, I., Vigo, A. G., Alonso, S., Barbolla, L., Crespo, M. S., & Fernandez, N. (2007). Peptidoglycan and mannose-based molecular patterns trigger the arachidonic acid cascade in human polymorphonuclear leukocytes. *J Leukoc.Biol* **81**, 925-933.

Vallon, V. (2003). In vivo studies of the genetically modified mouse kidney. *Nephron Physiol* **94**, 1-5.

Vandorpe, D. H., Shmukler, B. E., Jiang, L., Lim, B., Maylie, J., Adelman, J. P., de Franceschi, L., Cappellini, M. D., Brugnara, C., & Alper, S. L. (1998). cDNA cloning and functional characterization of the mouse Ca²⁺-gated K⁺ channel, mIK1. Roles in regulatory volume decrease and erythroid differentiation. *J.Biol.Chem.* **273**, 21542-21553.

Vanhaesebroeck, B. & Alessi, D. R. (2000). The PI3K-PDK1 connection: more than just a road to PKB. *Biochem.J.* **346 Pt 3**, 561-576.

Vanhaesebroeck, B. & Waterfield, M. D. (1999). Signaling by distinct classes of phosphoinositide 3-kinases. *Exp. Cell Res.* **253**, 239-254.

Venugopal, J. (2001). Cardiac natriuretic peptides--hope or hype? *J.Clin.Pharm.Ther.* **26**, 15-31.

Verstak, B., Hertzog, P., & Mansell, A. (2007). Toll-like receptor signalling and the clinical benefits that lie within. *Inflamm.Res.* **56**, 1-10.

Wall, M. E., Francis, S. H., Corbin, J. D., Grimes, K., Richie-Jannetta, R., Kotera, J., Macdonald, B. A., Gibson, R. R., & Trehwella, J. (2003). Mechanisms associated with cGMP binding and activation of cGMP-dependent protein kinase. *Proc.Natl.Acad.Sci.U.S.A* **100**, 2380-2385.

Wang, Z. (2004). Roles of K⁺ channels in regulating tumour cell proliferation and apoptosis. *Pflugers Arch* **448**, 274-286.

Watanabe, M. & Kato, I. (1974). Purification and properties of staphylococcal alpha-toxin. *Jpn.J.Med.Sci.Biol.* **27**, 86-89.

Weber, S., Bernhard, D., Lukowski, R., Weinmeister, P., Worner, R., Wegener, J. W., Valtcheva, N., Feil, S., Schlossmann, J., Hofmann, F., & Feil, R. (2007). Rescue of cGMP kinase I knockout mice by smooth muscle specific expression of either isozyme. *Circ.Res.* **101**, 1096-1103.

Wegener, J. W., Nawrath, H., Wolfsgruber, W., Kuhbandner, S., Werner, C., Hofmann, F., & Feil, R. (2002). cGMP-dependent protein kinase I mediates the negative inotropic effect of cGMP in the murine myocardium. *Circ.Res.* **90**, 18-20.

Weidemann, B., Brade, H., Rietschel, E. T., Dziarski, R., Bazil, V., Kusumoto, S., Flad, H. D., & Ulmer, A. J. (1994). Soluble peptidoglycan-induced monokine production can be blocked by anti-CD14 monoclonal antibodies and by lipid A partial structures. *Infect.Immun.* **62**, 4709-4715.

Welch, H., Eguinoa, A., Stephens, L. R., & Hawkins, P. T. (1998). Protein kinase B and rac are activated in parallel within a phosphatidylinositide 3OH-kinase-controlled signaling pathway. *J.Biol.Chem.* **273**, 11248-11256.

- Wenzel, U. & Daniel, H. (2004). Early and late apoptosis events in human transformed and non-transformed colonocytes are independent on intracellular acidification. *Cell Physiol Biochem* **14**, 65-76.
- Werner, C., Raivich, G., Cowen, M., Strekalova, T., Sillaber, I., Buters, J. T., Spanagel, R., & Hofmann, F. (2004). Importance of NO/cGMP signalling via cGMP-dependent protein kinase II for controlling emotionality and neurobehavioural effects of alcohol. *Eur.J.Neurosci.* **20**, 3498-3506.
- Wiley, J. S. (1981). Increased erythrocyte cation permeability in thalassemia and conditions of marrow stress. *J.Clin.Invest* **67**, 917-922.
- Wiseman, G. M. (1975). The hemolysins of *Staphylococcus aureus*. *Bacteriol.Rev.* **39**, 317-344.
- Wiseman, G. M. & Caird, J. D. (1970). Mode of action of the alpha toxin of *Staphylococcus aureus*. *Can.J.Microbiol.* **16**, 47-50.
- Wiseman, G. M. & Caird, J. D. (1972). Further observations on the mode of action of the alpha toxin of *Staphylococcus aureus* "Wood-46". *Can.J.Microbiol.* **18**, 987-992.
- Wiseman, G. M., Caird, J. D., & Fackrell, H. B. (1975). Trypsin-mediated activation of the alpha-haemolysin of *Staphylococcus aureus*. *J.Med.Microbiol.* **8**, 29-38.
- Wolfsgruber, W., Feil, S., Brummer, S., Kuppinger, O., Hofmann, F., & Feil, R. (2003). A proatherogenic role for cGMP-dependent protein kinase in vascular smooth muscle cells. *Proc.Natl.Acad.Sci.U.S.A* **100**, 13519-13524.
- Woon, L. A., Holland, J. W., Kable, E. P., & Roufogalis, B. D. (1999). Ca²⁺ sensitivity of phospholipid scrambling in human red cell ghosts. *Cell Calcium* **25**, 313-320.
- Woscholski, R. & Parker, P. J. (1997). Inositol lipid 5-phosphatases--traffic signals and signal traffic. *Trends Biochem.Sci.* **22**, 427-431.
- Wymann, M. P. & Pirola, L. (1998). Structure and function of phosphoinositide 3-kinases. *Biochim.Biophys.Acta* **1436**, 127-150.
- Yingst, D. R. & Hoffman, J. F. (1984). Ca-induced K transport in human red blood cell ghosts containing arsenazo III. Transmembrane interactions of Na, K, and Ca and the relationship to the functioning Na-K pump. *J.Gen.Physiol* **83**, 19-45.

Yu, S. P., Yeh, C. H., Sensi, S. L., Gwag, B. J., Canzoniero, L. M., Farhangrazi, Z. S., Ying, H. S., Tian, M., Dugan, L. L., & Choi, D. W. (1997). Mediation of neuronal apoptosis by enhancement of outward potassium current. *Science* **278**, 114-117.

Yurinskaya, V., Goryachaya, T., Guzhova, I., Moshkov, A., Rozanov, Y., Sakuta, G., Shirokova, A., Shumilina, E., Vassilieva, I., Lang, F., & Vereninov, A. (2005a). Potassium and sodium balance in U937 cells during apoptosis with and without cell shrinkage. *Cell Physiol Biochem* **16**, 155-162.

Yurinskaya, V. E., Moshkov, A. V., Rozanov, Y. M., Shirokova, A. V., Vassilieva, I. O., Shumilina, E. V., Lang, F., Volgareva, E. V., & Vereninov, A. A. (2005b). Thymocyte K⁺, Na⁺ and water balance during dexamethasone- and etoposide-induced apoptosis. *Cell Physiol Biochem* **16**, 15-22.

Zeiger, A. R., Wong, W., Chatterjee, A. N., Young, F. E., & Tuazon, C. U. (1982). Evidence for the secretion of soluble peptidoglycans by clinical isolates of *Staphylococcus aureus*. *Infect. Immun.* **37**, 1112-1118.

Zhao, J., Trewhella, J., Corbin, J., Francis, S., Mitchell, R., Brushia, R., & Walsh, D. (1997). Progressive cyclic nucleotide-induced conformational changes in the cGMP-dependent protein kinase studied by small angle X-ray scattering in solution. *J. Biol. Chem.* **272**, 31929-31936.

The experimental work included in this thesis has been carried out in the Institute of Physiology, University of Tübingen, Germany. The results presented in Figures 7, 8, 9, and 14 as well as in Table 2 have been generated by members and/or collaborators of the group of Robert Feil, Interfakultäres Institut für Biochemie, University of Tübingen.

Parts of this thesis have been published:

Foller,M, Mahmud,H, Koka,S, Lang,F: Reduced Ca(2+) entry and suicidal death of erythrocytes in PDK1 hypomorphic mice. *Pflugers Arch.* 455:939-949, 2008

Foller,M, Feil,S, Ghoreschi,K, Koka,S, Gerling,A, Thunemann,M, Hofmann,F, Schuler,B, Vogel,J, Pichler,B, Kasinathan,RS, Nicolay,JP, Huber,SM, Lang,F, Feil,R. Anemia and splenomegaly in cGKI-deficient mice. *Proc Natl Acad Sci U S A* 2008 (in press).

Foller,M, Biswas,R, Mahmud,H, Akel,A, Shumilina,E, Wieder,T, Goetz,F, Lang,F. Effect of Peptidoglycans on Erythrocyte Survival. *Int J Med Microbiol.* (under review)

7 Acknowledgement

I am especially indebted to Prof. Dr. Florian Lang. He gave me the opportunity to study the fascinating death machinery of erythrocytes. Whenever I needed help, advice or discussion, he was willing and prepared to provide most competent support that was necessary to finalize the studies included in this thesis successfully.

My sincere thanks to Privatdozent Dr. Stephan Huber. Throughout my work, he successfully helped to overcome all experimental difficulties.

Furthermore, I would like to thank Prof. Dr. Peter Ruth and Privatdozent Dr. Matthias Sausbier, Pharmaceutical Institute, University of Tübingen, for providing $K_{Ca}3.1$ -deficient mice. In addition, Prof. Dr. Peter Ruth supported me as my second supervisor very kindly.

Prof. Dr. Robert Feil and members of his group (Dr. Susanne Feil, Martin Thunemann, and Andrea Gerling) provided the cGKI-deficient mice models and performed very important experiments on the role of cGKI for erythrocyte survival included in this thesis. Dr. Kamran Ghoreschi similarly contributed important observations to the study on cGKI. Therefore, I would like to express my thanks to all of them.

I would like to thank Prof. Dr. Erwin Schleicher and Dr. Frank Baumgartner, Zentrallabor, University hospital of Tübingen, for the determination of vitamins in mice serum.

My further thanks to Prof. Dr. Dario Alessi, University of Dundee, United Kingdom, for providing the PDK1-hypomorphic mice.

I thank my lab colleagues Mr. Hasan Mahmud, Mrs. Saisudha Koka, Mr. Manuel Braun, Dr. Krishna Boini and Dr. Raja Biswas for their support, suggestions, and encouragement.

Finally, I would like to thank all other colleagues of the Institute of Physiology for their valuable help and support.

8 Complete list of publications

Foller,M, Kasinathan,RS, Duranton,C, Wieder,T, Huber,SM, Lang,F: PGE2-induced apoptotic cell death in K562 human leukaemia cells. *Cell Physiol Biochem.* 17:201-210, 2006

Foller,M, Geiger,C, Mahmud,H, Nicolay,J, Lang,F: Stimulation of suicidal erythrocyte death by amantadine. *Eur.J.Pharmacol.* 2007

Foller,M, Shumilina,E, Lam,R, Mohamed,W, Kasinathan,R, Huber,S, Chakraborty,T, Lang,F: Induction of suicidal erythrocyte death by listeriolysin from *Listeria monocytogenes*. *Cell Physiol Biochem.* 20:1051-1060, 2007

Foller,M, Kasinathan,RS, Koka,S, Huber,SM, Schuler,B, Vogel,J, Gassmann,M, Lang,F: Enhanced susceptibility to suicidal death of erythrocytes from transgenic mice overexpressing erythropoietin. *Am.J.Physiol Regul.Integr.Comp Physiol* 293:R1127-R1134, 2007

Foller,M, Kasinathan,RS, Koka,S, Lang,C, Shumilina,E, Birnbaumer,L, Lang,F, Huber,SM: TRPC6 Contributes to the Ca Leak of Human Erythrocytes. *Cell Physiol Biochem.* 21:183-192, 2008

Foller,M, Mahmud,H, Koka,S, Lang,F: Reduced Ca(2+) entry and suicidal death of erythrocytes in PDK1 hypomorphic mice. *Pflugers Arch.* 455:939-949, 2008

Foller,M, Sopjani,M, Mahmud,H, Lang,F. Vanadate induced suicidal erythrocyte death. *Kidney Blood Press Res* 2008 (in press).

Foller,M, Feil,S, Ghoreschi,K, Koka,S, Gerling,A, Thunemann,M, Hofmann,F, Schuler,B, Vogel,J, Pichler,B, Kasinathan,RS, Nicolay,JP, Huber,SM, Lang,F, Feil,R. Anemia and splenomegaly in cGKI-deficient mice. *Proc Natl Acad Sci U S A* 2008 (in press).

Foller,M, Biswas,R, Mahmud,H, Akel,A, Shumilina,E, Wieder,T, Goetz,F, Lang,F. Effect of Peptidoglycans on Erythrocyte Survival. *Int J Med Microbiol.* (under review)

Geiger,C, Foller,M, Herrlinger,K, Lang,F. Azathioprine induced suicidal erythrocyte death. *Inflamm Bowel Dis.* 2008 (in press).

Hussain A, Wyatt AW, Wang K, Bhandaru M, Biswas R, Avram D, Föller M, Rexhepaj R, Friedrich B, Ulrich S, Müller G, Kuhl D, Risler T, Lang F. SGK1-dependent upregulation of connective tissue factor by angiotensin II. *Kidney Blood Press Res* 2008 (in press).

Kasinathan,RS, Foller,M, Lang,C, Koka,S, Lang,F, Huber,SM: Oxidation induces ClC-3-dependent anion channels in human leukaemia cells. *FEBS Lett.* 581:5407-5412, 2007

- Kasinathan,RS, Foller,M, Koka,S, Huber,SM, Lang,F: Inhibition of eryptosis and intraerythrocytic growth of Plasmodium falciparum by flufenamic acid. Naunyn Schmiedebergs Arch.Pharmacol. 374:255-264, 2007
- Koka,S, Huber,SM, Boini,KM, Lang,C, Foller,M, Lang,F: Lead decreases parasitemia and enhances survival of Plasmodium berghei-infected mice. Biochem.Biophys.Res.Comm. 363:484-489, 2007
- Koka,S, Foller,M, Lamprecht,G, Boini,KM, Lang,C, Huber,SM, Lang,F: Iron deficiency influences the course of malaria in Plasmodium berghei infected mice. Biochem.Biophys.Res.Comm. 357:608-614, 2007
- Kosiek,O, Busque,SM, Foller,M, Shcheynikov,N, Kirchoff,P, Bleich,M, Muallem,S, Geibel,JP: SLC26A7 can function as a chloride-loading mechanism in parietal cells. Pflugers Arch. 454:989-998, 2007
- Lang,F, Foller,M, Lang,KS, Lang,PA, Ritter,M, Gulbins,E, Vereninov,A, Huber,SM: Ion channels in cell proliferation and apoptotic cell death. J.Membr.Biol. 205:147-157, 2005
- Lang,F, Foller,M, Lang,K, Lang,P, Ritter,M, Vereninov,A, Szabo,I, Huber,SM, Gulbins,E: Cell volume regulatory ion channels in cell proliferation and cell death. Methods Enzymol. 428:209-225, 2007
- Niemoeller,OM, Foller,M, Lang,C, Huber,SM, Lang,F: Retinoic Acid induced suicidal erythrocyte death. Cell Physiol Biochem. 21:193-202, 2008
- Schneider,J, Nicolay,JP, Foller,M, Wieder,T, Lang,F: Suicidal erythrocyte death following cellular K⁺ loss. Cell Physiol Biochem. 20:35-44, 2007
- Sopjani,M, Foller,M, Lang,F: Gold stimulates Ca⁽²⁺⁾ entry into and subsequent suicidal death of erythrocytes. Toxicology 2007

9 Academic teachers

The following list contains my academic teachers of biochemistry and this thesis in alphabetical order:

Prof. Dr. Bardehle, Prof. Dr. Bisswanger, Prof. Dr. Bohley, Prof. Dr. Dodt, Prof. Dr. Duszenko, Prof. Dr. Feil, Prof. Dr. Gauglitz, Prof. Dr. Hamprecht, PD. Dr. Huber, Prof. Dr. Kölle, PD Dr. Kun, Prof. Dr. Lang, PD Dr. Maier, Prof. Dr. Meyer, PD Dr. Münzel, Prof. Dr. Oberhammer, Prof. Dr. Probst, Prof. Dr. Ruth, PD Dr. Schmid, Prof. Dr. Schott, Prof. Dr. Schwarz, PD Dr. Stoeva, Prof. Dr. Stehle, Prof. Dr. Stevanovic, Prof. Dr. Dr. Strähle, PD Dr. Verleyesdonk, Prof. Dr. Weser, PD Dr. Wieder